NASA Contractor Report 187060

The High Temperature Creep Behavior of Oxides and Oxide Fibers

Linda E. Jones and Richard E. Tressler
The Pennsylvania State University
University Park, Pennsylvania

January 1991

Prepared for
Lewis Research Center
Under Grant NAGW-1381

National Aeronautics and
Space Administration

TABLE OF CONTENTS

FIGURES

FIGURES

TABLES

1.0 INTRODUCTION

High modulus fibers and composites developed for use in lightweight, stiff structures for space applications are of particular interest today; however, in order to incorporate these materials into the structures of tomorrow considerable research needs to be directed towards understanding strengthening mechanisms, factors which control ductility, environmental effects and interactions between fiber and matrix. This review focuses primarily on fibers for reinforcement of metal and ceramic matrix composites which will operate in oxidative environments at high temperatures, specifically, on the creep behavior of oxide fibers expected to be useful in high-temperature applications.

Continuous fiber reinforced composite materials possess numerous structural advantages over their monolithic counterparts; however, the role of the fiber on these improvements is dependent upon the matrix material.

The advantage of using metal-matrices is their high strength-to-weight ratio, fabricability of thin plies, high thermal conductivity, damage tolerance and toughness. For these reasons, intermetallic matrix composite (IMC) and metal matrix composite (MMC) materials are intended for application as structural components in high-temperature, high-efficiency, high-performance aircraft engines. Currently, there are a wide variety of matrices of interest for such applications which include FeAl, Ti_3Al , TiAl, Ni_3Al, NiAl, Nb_3Al, and $NbAl_3$. The creep of these alloys limits their high-temperature utility, and the incorporation of creep resistant filaments into metal matrices is intended to extend the high-temperature application of these metals.

Ceramic-matrix composites (CMC) are also of interest in high-temperature applications because of their potential for use as uncooled lightweight structures that can operate unprotected at very high temperatures. Their inherent high-temperature oxidation resistance is also a key advantage in the use of ceramics. Ceramics and glasses exhibit relatively high-strength and stability at elevated temperatures as well as low density and

high refractoriness; however, these materials are limited due to their brittle behavior. In order to improve strength and toughness, fibers have been added to the ceramic where they aid in resisting crack propagation. Proper design of the fiber/matrix interface in the CMC's can lead to major improvements in toughness, rendering them more forgiving.

The incorporation of continuous fibers into these matrices clearly yields several distinct advantages which utilize the low densities of the matrix while capitalizing on the high strength and high modulus of the fiber. There are several desired properties which the fibers must possess if they are to reinforce and, hence, improve the high-temperature properties of these composites. The following discussion highlights these materials properties in light of their use as high-temperature reinforcements.

As a general rule one expects the highest strength from a material with the highest modulus. Therefore, it is desirable to use high modulus fibers to both carry the load and maintain composite net shape. Simple bonding theories predict the order of magnitude of the modulus quite correctly [Rosenthal, 1964]. The choice of candidate elements and compounds of high specific modulus is based strongly on the first row of the periodic table and certain elements in the second row [Parrat, 1972]. These elements include Li, Be, B, C, N, O, F, Mg, Al, Si, and Ti.

The high strength and failure strain of the fibers are readily exploited if they are incorporated into a ductile matrix (such as a metal matrix). Incorporating high strength ceramic fibers significantly improves the low strength of aluminide matrices at the higher stemperatures [Stephens et al., 1988]. The matrix in this case serves to transfer load to the fiber and provides a barrier to crack propagation. The presence of fibers may also be expected to decrease the time dependent deformation and to effect the shear transfer from the matrix if the fibers exhibit adequate creep resistance and are well-bonded to the matrix.

Many complexities arise when combining a ceramic fiber with a metal matrix, and there are several disadvantages with this composite materials approach. Some of these complexities for composite systems under investigation are the chemical compatibility and

the thermal expansion match between the fiber and matrix. These issues are critical in assuring long-term thermal stability. For instance, metal matrix composites reinforced with ceramic fibers are susceptible to thermal degradation, particularly when thermal cycling, due to the fact that differential fiber-matrix expansion leads to interface failure or fiber fragmentation during service. Therefore, the differential thermal expansion of the components is an important parameter. The thermal expansion coefficients (α) of several materials are listed in Table 1. These values can be compared to the matrices of interest such as NiAl and Nb which have CTE's of 18 and 7.9 x 10^{-6} C^{-1}, respectively.

Beyond the mechanical behavior of the fiber, its resistance to oxidation by the surrounding atmosphere is of interest because of the composite's eventual use in applications such as structural components for aircraft turbine engines. In such environments, at high temperatures, several possible reactive species may exist which could possibly be present at the composite surface in significant enough concentrations as interact with the fiber, hence altering the structural properties for which the composite was originally designed. For this reason, the most likely materials for fibers in this application are the oxides. High oxidation rates of carbides and borides for instance preclude their use as long-term repeated use at temperatures in excess of 1600°C.

Obviously, candidate fiber materials which are expected to maintain design properties and survive repeated thermal cycling must remain a solid under these conditions, as well as maintain chemical neutrality with the surrounding environment. Therefore, the melting point, as well as oxidation behavior of the material becomes a significant consideration in the selection of a high-temperature materials. For the purposes of this discussion only materials having melting points above 1800°C are considered. This temperature is simply a reference point from which to base materials selection. A list of high melting point candidate oxides is given in Table 2.

Table 1. Potential Oxides and Their Thermal Expansion Coefficients

	Thermal Expansion Coefficient [a] x 10^{-6}/°C (≈20 - ≈1500°C)
Al_2O_3 (polycrystalline)	7.2 - 8.6
Al_2O_3 (single crystal)	
- Normal to C-axis	8.3
- Parallel to C-axis	9.0
MgO	14.2 - 14.9
SrO	13.95
CaO	13.6
ZrO_2 (Partially Stabilized)	8.9 - 10.6
ZrO_2 (Fully Stabilized)	13.5
HfO_2	9.9
$MgAl_2O_4$ (Spinel)	9.8
Mullite	5.3
$Y_3Al_5O_{12}$ (Garnet)	8 - 8.9
ThO_2	9.5
BeO (polycrystalline)	9.1

a W. J. Lackey, D. P. Stinton, G. A. Cerny, L. L. Fahrenbacher, and A. C. Schaffhauser, "Ceramic Coatings for Heat Engine Materials - Status and Future Needs," in Proc. of Int. Symposium on Ceramic Components for Heat Engines, Oct. 17-21, 1983, Hakone, JAPAN.

Table 2. Candidate Oxides with Melting Points Above 1800°C

		Melting Point, °C	Density, g/cc
Oxides (single)			
	Al_2O_3	2072	3.96
	BaO	1918	5.72
	BeO	2530	3.01
	CaO	2614	3.25
	CeO_2	2600	7.13
	Cr_2O_3	2266	5.21
	Dy_2O_3	2340	7.21
	Gd_2O_3	2330	7.4
	HfO	2758	9.68
	La_2O_3	2307	6.51
	MgO	2852	3.58
	Nd_2O_3	1900	7.2
	NiO	1984	6.67
	SrO	2430	4.7
	Ta_2O_5	1872	8.2
	ThO_2	3220	9.86
	TiO_2	1830	4.26
	Ti_2O_3	2130	4.6
	UO_2	2878	10.96
	VO_2	1967	4.31
	V_2O_3	1970	4.87
	Y_2O_3	2410	5.01
	ZnO	1975	5.60
	ZrO_2	2700	5.89
Oxides (mixed)			
	$Al_6Si_2O_{13}$	1920	3.16
	$BaCO_3$	1740	4.43
	$BeAl_2O_4$	1870	3.76
	$CaCr_2O_4$	2090	4.8
	Ca_3SiO_5	1900	------
	$CaTiO_3$	1975	4.10
	$CaZrO_3$	2550	4.78
	$Li_2Al_2O_4$	1900	2.55
	$MgAl_2O_4$	2135	3.6
	Mg_2SiO_4	1910	3.21
	$ZrSiO_4$	2550	4.56

Candidate fiber materials, as described, must be nonreactive (stable) with the atmosphere and with the composite matrix, they should have a thermal expansion behavior compatible with the matrix in order to avoid thermal stresses which often result in gross mismatch of fiber and matrix at high temperature, they must have high melting points and low vapor pressures to prevent sublimation. Strife [1988] compared the vapor pressures of several high melting point oxides with those of selected carbides and nitrides using data obtained from Schick, 1960; Ackermann et al., 1961; Batha et al., 1973; Long et al., 1961; and Storms, 1967. Finally, a candidate material should also experience a limited number of phase transitions in the temperature range of interest. With these criteria in mind, the most promising materials concepts are based on the use of oxides for the continuous fiber reinforcement of metal-matrix composites.

A knowledge of the processes by which the fibers, hence the composite deform, are critical in order to define the high-temperature long-term mechanical behavior of these structural components. It is therefore necessary to review the high-temperature creep behavior of the candidate fiber materials which meet the criteria necessary for a viable composite reinforcement (i.e. high melting point, low density, low vapor pressure, high refractoriness, limited phase transitions, matched CTE and chemical compatibility with the matrix).

This paper presents a comprehensive review of the creep data for oxide ceramics in order to identify alternative materials as reinforcements for high-temperature composites. The data which exist are scattered throughout many publications and have previously not been compiled. Therefore, the emphasis of this review is to compile this information and provide an overview of the current understanding of the deformation of oxides at high-temperatures in order to suggest the best possible candidate oxides for fiber reinforcement of metal and ceramic matrix composites.

In presenting these data, it is important to note that for most mechanisms controlling the creep behavior of the material a secondary or steady-state creep rate, $\dot{\varepsilon}$, is predicted

over some period of time while the material is experiencing a constant load at temperature. It is this steady-state creep regime which usually dominates the creep behavior of the material and it is in this range that the material experiences significant operational life. The steady-state rate may be described by the following equation [Langdon, 1975]

$$\dot{\varepsilon} = ADG\ \vec{b}/kT\ \left[\vec{b}/d\right]^m\ [\sigma/G]^n \qquad (1.1)$$

where A is a dimensionless constant, D is a diffusion coefficient (= D_o exp (-Q/kT)), Q is the activation energy for creep, T is the absolute temperature, G is the shear modulus, $\vec{b}$ is the Burgers vector of the gliding dislocations, k is Boltzmann's constant, d is the grain size, σ is the applied stress, and m and n are the exponents for the inverse grain size and stress dependence, respectively. This equation is most often referred to as the Dorn equation and it is an empirical equation used as the basis for many of the proposed creep mechanisms, herein discussed. It can be seen from this equation that any mechanism describing the process of creep in a material at a constant stress, temperature, and grain-size can be specified by the values of three constants A, m, and n and the value of D. The value of D is a function of the diffusion path, either through the lattice (D_l), along the grain boundaries (D_{gb}), as pipe diffusion along the dislocation cores (D_p), or through a second phase at the grain boundary (D_{ph}).

Based upon the criteria for an ideal fiber candidate, several oxide materials have been singled out and are listed with relevant physical property information in Table 3. Discussion of the creep behavior of each class of oxide is given separately. The vast majority of existing creep data is on the behavior of alumina. For this reason, the creep of alumina will be discussed first and used as a reference for the creep behavior of alternative oxides at high temperature and constant loads. It will be shown in the course of this

Table 3. Physical Properties of Candidate Oxides

Material	Modulus GPa	Thermal Expansion ($x10^{-6}$, K^{-1})	T_M, °K	Density g/cc	Structure
BeO	295-380	9.1	2793-2823	3.0	Hexagonal
MgO	210-300	13.8	3073	3.6	Cubic
Al_2O_3	360-400	8.5	2288-2323	3.97	Hexagonal
ZrO_2 (fully stabilized with Yttria)	97-207	7.6	2950-2983	5.56-6.1	Cubic
ThO_2	145	9.5	3323-3573	9.8-10	Fluorite
Mullite $3Al_2O_3 \cdot 2SiO_2$	145	5.3	2083-2093	3.15-3.23	Orthorombic
$MgAl_2O_4$	240	9.8	2400	3.58	Complex Cubic
Garnet (YAG)		8.9	1957	6.46	Complex Cubic

discussion that the creep rates of single crystal oxides are significantly less than those of polycrystalline oxides and for this reason the discussion focuses primarily on single crystal materials. More often than not, no creep data exists for a specific class of single crystal oxides and it is, therefore. necessary to compare polycrystalline to single crystal behavior.

It is difficult to interpret creep data for single crystals in terms of the mechanisms developed for polycrystals because most single crystal deformation is the result of glide on primary or secondary slip systems. In order to compare data between single and polycrystalline systems it is more appropriate to discuss or reference single crystal creep data which is the result of slip on the most difficult slip system, typically the system having the highest Peierls barrier.

2.0 DEFORMATION BEHAVIOR OF SINGLE CRYSTAL ALUMINA

Sapphire (single crystal alumina) fibers for example, oriented such that the basal (0001) plane is perpendicular to the fiber axis is referred to as 0° or c-axis oriented. These fibers possess a high degree of creep resistance when oriented in this manner which is explained by the extreme anisotropy of the psuedo-hexagonal crystal structure of Al_2O_3. The reason for the creep resistance exhibited by c-axis sapphire is explained by the material's highly anisotropic crystal structure resulting in few slip systems available to activate. Alumina also has a 63% ionic bond character so that the existing bonds have a highly covalent contribution to their bond strength further increasing the Peierls force needed to initiate slip. This anisotropy of creep behavior can be clarified with a more complete description of the structure of single crystal alumina.

Sapphire (single-crystal alumina, α-Al_2O_3) is rhombohedral (pseudo-hexagonal) in structure with oxygen atoms forming an hcp lattice and aluminum ions filling 2/3 of the available octahedral sites [Kronberg, 1957]. Figure 1 is a schematic of the structure of sapphire indicating the relative positions of oxygen and aluminum ions. In this structure the vacant octahedral sites form the basis of the Al_2O_3 unit cell. The slip systems of this unit cell are given schematically in Figure 2. In the case of a single crystal filament the crystal orientation is defined with respect to the crystal c-axis and the axis of the filament. For instance, a 0° filament has the c-axis parallel to the filament axis and a 60° filament has the c-axis 60° off of the filament axis, etc. Three slip systems have been macroscopically identified in sapphire. They are basal (0001) $<11\bar{2}0>$, prismatic $\{11\bar{2}0\}$ $<01\bar{1}0>$, and pyramidal $\{10\bar{1}1\}$ $<01\bar{1}1>$ slip systems [Bretheau et al., 1979]. Basal and prismatic slip have been determined conclusively via TEM investigations and slip trace analyses. There is a question, however, as to whether the pyramidal dislocations $1/3<01\bar{1}1>$ are confined to simply one slip plane [Busovne, 1981].

Some discussion continues regarding the anisotropy of deformation when pyramidal planes operate as slip planes. Pyramidal slip can be initiated when a stress is

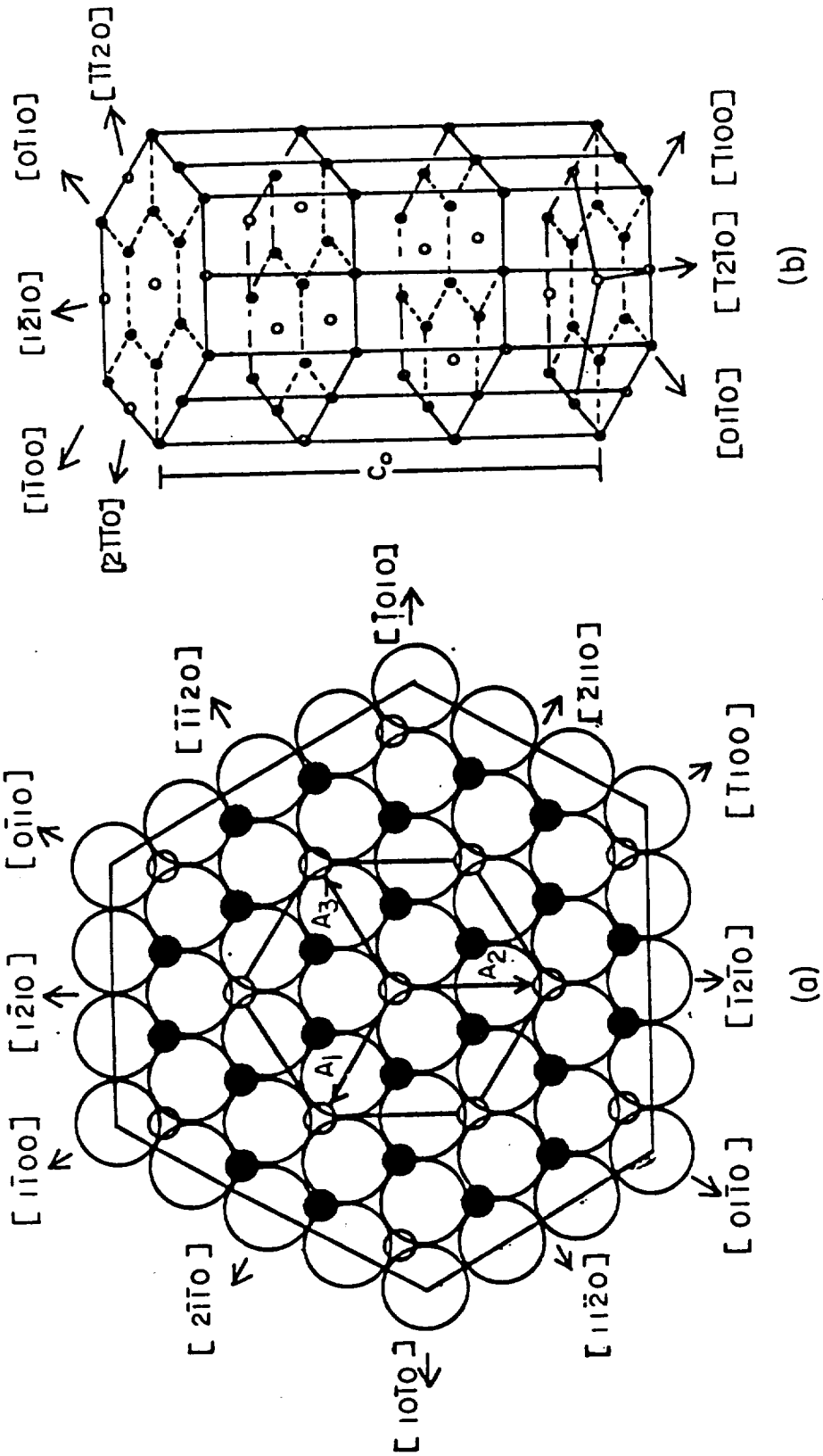

Figure 1. Structure of sapphire after Kronberg [1957]. (a) Arrangement of oxygen ions (large open circles), aluminum ions (solid circles), and holes (small open circles) on the basal plane. (b) Distribution of aluminum ions (solid) and holes (open) on the simple hexagonal lattice.

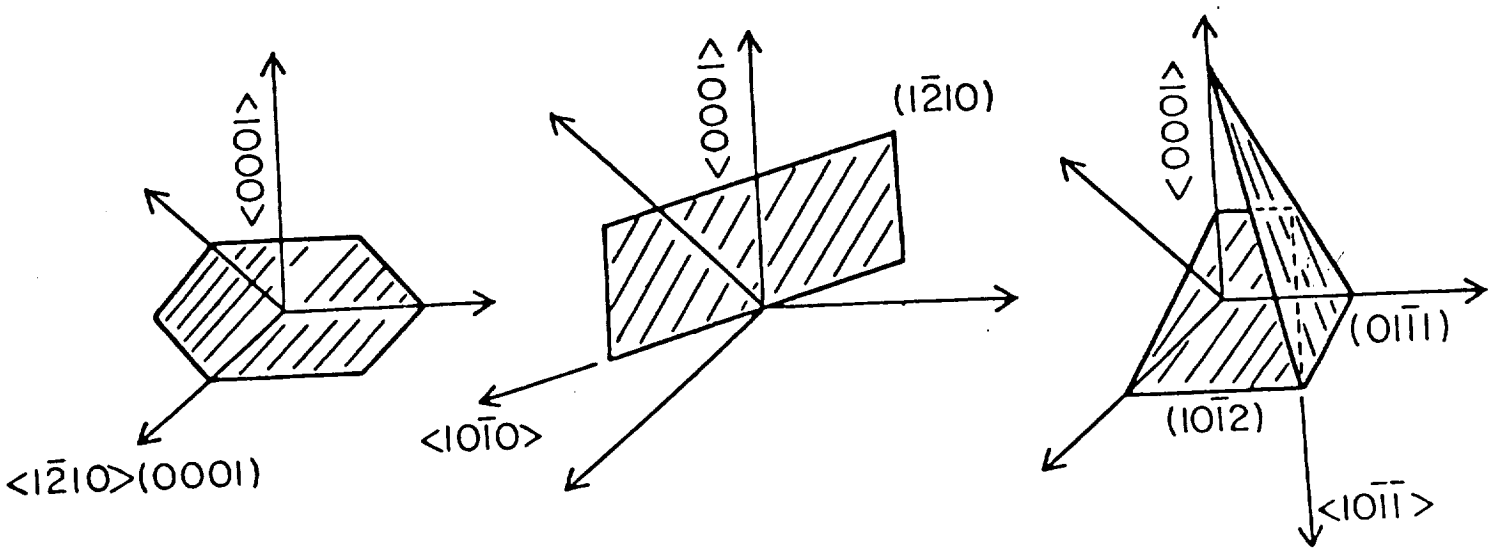

Basal
{0001} <11$\bar{2}$0>
$\vec{b}$ = 4.76 Å

Prismatic
{11$\bar{2}$0} <1$\bar{1}$00>
$\vec{b}$ = 8.24 Å

Pyramidal
{10$\bar{1}$1} <01$\bar{1}$1>
$\vec{b}$ = 5.12 Å

Figure 2. Schematic representation of basal, prismatic, and pyramidal slip systems in sapphire

applied parallel to the c-axis of sapphire and either the $\{01\bar{1}2\}$ or $\{10\bar{1}\,\bar{1}\}$ planes can act as glide planes. These planes refer to the morphological and structural faces of the rhombohedra and have Schmid factors of 0.45 and 0.25 respectively [Cadoz and Pellissier, 1976]. The structural unit cell is twice as high as the morphological cell. In referring to glide on the pyramidal system we will reference the structural hexagonal unit cell of sapphire as defined by Kronberg [1957] in which the c/a ration is 2.73. The marked anisotropy of the critical resolved shear stress (τ_{crss}) for the three slip systems shown in Figure 3 indicates that basal slip can occur in general orientations unless the stress is either parallel or perpendicular to the c-axis of the crystal. Basal slip has the lowest τ_{crss} in alumina. For sapphire crystals oriented so that the applied uniaxial stress is perpendicular (90° orientation) or parallel (0° orientation) to the c-axis, the basal slip system is not operative. In 90° orientation, the prismatic slip system $\{11\bar{2}0\}\ <01\bar{1}0>$ is operative at temperatures as low as 1150°C [Gooch and Groves, 1972]. In the 0° orientation, macroscopic flow (creep) occurs only at much higher temperatures ($\cong$ 1600°C) [Wachtman and Maxwell, 1957]. The temperature at which pyramidal slip occurs may actually be much lower, and with the advent of much more sensitive testing techniques pyramidal slip at 1600°C and lower requires further study.

The various slip systems have been studied via mechanical testing under tensile, compressive and bending modes. Inspection of the sample has been accomplished via etch pit techniques, slip trace analysis and/or much more conclusively by transmission electron microscopy.

The yielding behavior of sapphire has been attributed to a dislocation multiplication mechanism rather than to the unpinning of existing dislocations [Firestone and Heuer, 1976; Kotchick, 1978; Mitchell, 1979]. It has been suggested that the mechanism controlling yielding is temperature and strain-rate sensitive [Busovne, 1981], because the drop in the yield usually observed for basal, prismatic and pyramidal slip increases in magnitude as the temperature decreases or as the strain-rate increases. Pre-straining of the

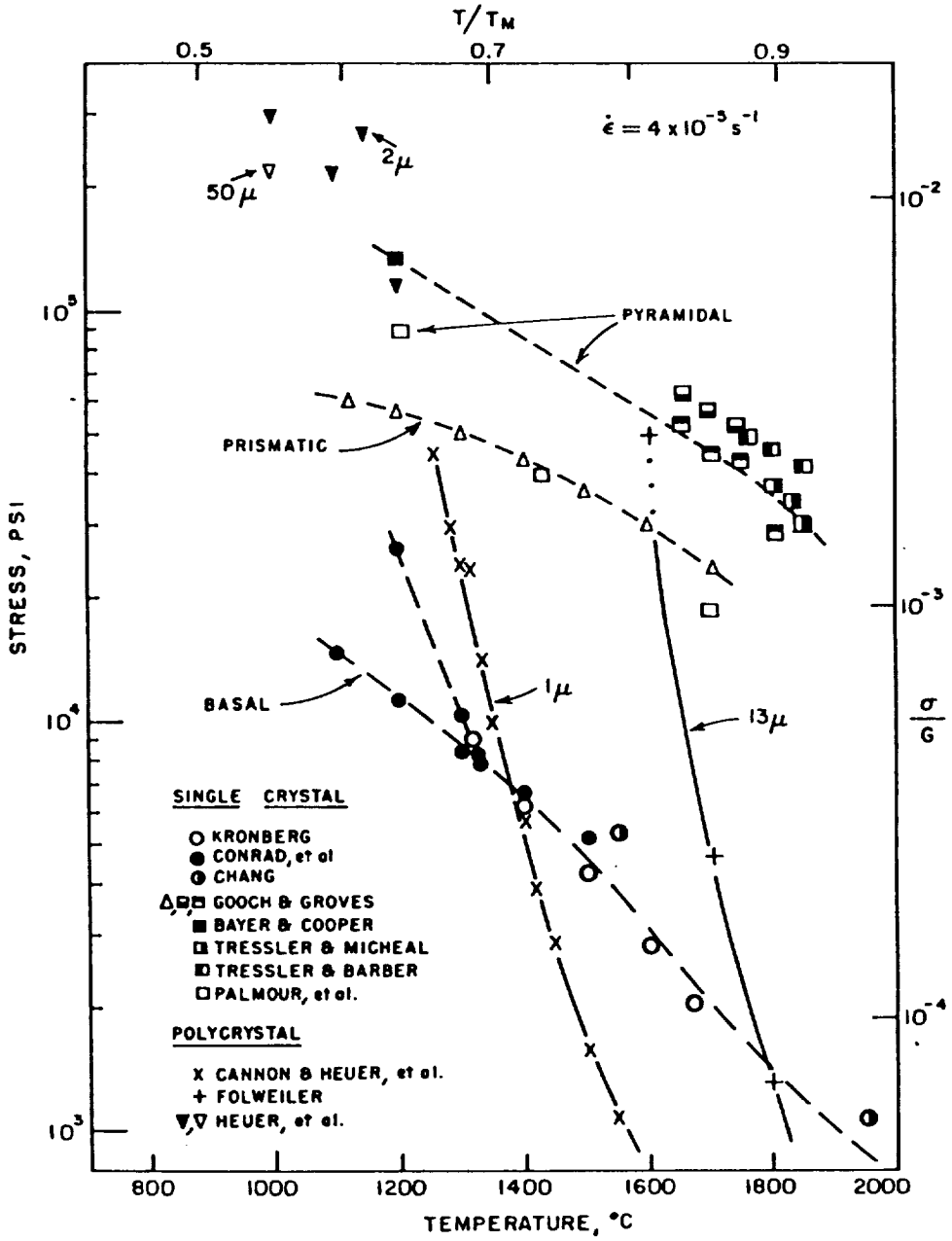

Figure 3. Tensile flow stress versus temperature for basal, prismatic, and pyramidal slip in sapphire [Cannon and Coble, 1975]

crystal is necessary in order to observe this yielding behavior which results from the accumulation of a sufficient number of dislocations [Tressler and Barber, 1974]. If these dislocations do not accumulate, fracture will occur before yielding. In the oxides, dislocation generation processes have, in general, been shown to control yielding behavior. For sapphire, in particular, the yield stress is sensitive to the thermal/stress history of the samples.

2.1 The Mechanism of Basal Deformation

Sapphire deforms plastically along the basal (0001) plane by slip in the $<11\bar{2}0>$ direction in both tension and compression in the temperature range of 900-2000°C. This deformation has been investigated thoroughly, and for complete reviews see Conrad [1965], Conrad et al. [1965], Bertolotti and Scott [1971], and Pletka et al. [1974]. A brief overview is given here to highlight these reviews. Kronberg [1962] first investigated the dynamical flow properties of sapphire via basal slip and found a sharp transition between brittle fracture and plastic flow as a function of both temperature and strain-rate. He concluded that rapid multiplication of dislocations caused the yield drop rather than the unpinning of existing dislocations. Kronberg [1957] previously had proposed that $1/3<11\bar{2}0>$ dislocation dissociation would be energetically favorable and slip would occur by the "synchro-shear" motion of four partial dislocations. This mechanism had not been verified since these partial dislocations have rarely been observed in TEM investigations and in terms of atomic structure the $1/3<11\bar{2}0>$ dissociation is not favored because the motion of this dislocation requires oxygen atoms of one plane to move directly over top of close packed oxygen in the adjacent plane, thereby, disrupting the close packed structure. The dislocation structure of sapphire deformed in compression by basal slip consists of long, straight dislocations in the basal plane with Burgers vector $1/3<11\bar{2}0>$ [Pletka, Heuer, and Mitchell, 1977]. Slip lines are straight and distinct, no evidence of cross-slip

has been observed since the other slip systems are not activated until much higher temperatures. With increased strain, loops, dipoles, and dislocation tangles become evident and evidence of dislocation climb has been observed at temperatures greater than 1200°C. The overcoming of the Peierls force appears to control basal flow at T< 1700°C while at higher temperatures dislocation climb is probably rate-limiting [Pletka, Heuer, and Mitchell, 1977]. Creep studies of Bertolotti and Scott [1971] and Chang [1960] have supported the Peierls force and dislocation climb as rate-controlling mechanisms in the basal creep of sapphire at high temperature.

Chang [1960] conducted creep tests in tension at temperatures of 1500-1900°C, $\dot{\varepsilon} = 3.6 \times 10^{-3}$ hr^{-1}) and resolved shear stresses of ≈10 MPa. Under these conditions he found that the creep of sapphire was controlled via a dislocation climb mechanism. Bertolotti and Scott [1971] argued on the basis of activation energies from compressive creep tests that the deformation of sapphire single crystals at temperatures between 1400 and 1700°C was controlled by overcoming the Peierls stress. Conrad et al. [1967] extended the temperature range over which the Peierls stress was rate limiting to 900-1700°C when resolved shear stresses were 10-60 MPa and strain rates were 10^{-3} to 10^{-1} hr^{-1}. Pletka, et al. [1977] tested 60° sapphire over the temperature range of 1200 to 1500°C, ($\dot{\varepsilon} = 9.45 \times 10^{-2}$ - 0.468 hr^{-1}) and stresses of 30-60 MPa in compression and developed a quantitative model for basal work-hardening by correlating stress-strain behavior with careful TEM observations of dislocation substructure. They observed that dipoles formed by the extension of dislocations on parallel basal planes and resulted in subsequent edge trapping, screw components annihilate by cross-slip and faulted dipoles, formed by climb dissociation, then form loops via self-climb. The transformation of narrow dipoles to loops was carried out by first forming the faulted dipoles through climb dissociation by the reaction $1/3[11\bar{2}0] \text{----> } 1/3[10\bar{1}0] + 1/3[01\bar{1}0]$, with one pair of partials annihilating to form the faulted dipole. The formation of faulted dipoles broken up into strings of loops by self-climb was rate limited by the diffusion of oxygen. These

interactions between gliding dislocations and loops caused the observed work-hardening. Zero work-hardening was observed after further straining and was attributed to the creation of new loops which were completely balanced by the annihilation of existing loops by diffusion. Therefore, the typical stress-strain curve for basal slip in sapphire at a constant strain rate shows a rapid decrease in stress (upper yield stress) with initial plastic strain. A lower yield stress was observed at small plastic strains where work hardening begins at a relatively high rate and gradually decreases until a zero work hardening region is reached at higher strains.

In the flow region, data for basal slip in sapphire have generally been fit to two equations. For dislocation barriers such as over coming the Peierls stress, creep data have been fitted to an equation in which the strain rate is an exponential function of the applied stress.

$$\dot{\varepsilon} = A \exp (-H_{(\sigma)}/ RT) \qquad (2.1.1)$$

where $\dot{\varepsilon}$ is strain rate, A is constant, $H_{(\sigma)}$ is the stress dependent activation enthalpy, R is the gas constant and T is the absolute temperature. This equation has been found to apply well with relatively low temperature (900 - 1700°C) creep behavior [Conrad, 1965; Bertolotti and Scott, 1971; and Pletka et al., 1974].

In instances where diffusion controlled climb dictates the creep rate (higher temperatures) the strain rate is dependent upon the stress to some power.

$$\dot{\varepsilon} = (A/T)\, \sigma^n \exp (-H_o/RT) \qquad (2.1.2)$$

where A and n are constants, and H_o is the activation enthalpy which is independent of stress [Chang, 1960].

Conrad's review [1965] in which data were taken from several sources having widely different strain-rates concluded that basal deformation of sapphire could take place

in the temperature range of 900 - 2000°C by either of the two thermally activated processes described by Equations 2.1.1 and 2.1.2.

2.2 Deformation by Prismatic Slip System

Prismatic $\{11\bar{2}0\}$ $<01\bar{1}0>$ slip was first observed by Klassen-Neklyudova, et al. [1970] on 90° oriented sapphire deformed above 1800°C. Scheuplein and Gibbs, [1960] and later Gooch and Groves, [1972] observed slip on the $\{11\bar{2}0\}$ $<01\bar{1}0>$ system determined from slip trace analysis and TEM for bend tests under conditions which were much less extreme than previously thought necessary to activate prismatic slip. Temperatures less than 1800°C and as low as 1150°C at a strain rate of 10^{-3} hr^{-1} and a stress of 350 MPa were found to activate prismatic slip in sapphire cut form a verneuil-grown boule and deformed in four point bending. Gooch and Groves [1973] observed that the stress-strain curve for prismatic deformation at 1150 to 1800°C for 10^{-3} - 10^{-2} hr^{-1} and 350 -120 MPa had three major characteristics: a sharp yield point, an appreciable work-hardening rate, and a saw-tooth character to the curve in the plastic region. They also noted a very low strain-rate sensitivity to deformation when prismatic slip was controlling.

Bilde-Sorenson, et al. [1976] unambiguously identified the $\{11\bar{2}0\}$ $<01\bar{1}0>$ slip system by deforming 90° Verneuil-grown sapphire in four-point bending and observing the dislocation structure via TEM. They carefully sectioned $\{11\bar{2}0\}$ foil planes from deformed samples and used TEM weak-beam and dark field techniques to analyze the dislocation structure. The majority of dislocations were of $<01\bar{1}0>$ type with a few $1/3<01\bar{1}0>$ partial dislocations observed. The $1/3<01\bar{1}0>$ dislocations were usually associated with faulted dipoles or faulted prismatic loops lying along the [0001] direction. Since the Burgers vector associated with prismatic slip is relatively long (8.24 Å), it does not appear to be energetically favorable over shorter possible Burgers vectors such as $1/3<11\bar{2}0>$.

However, the slip plane consisted of parallel rows of close packed oxygen atoms in the $<01\bar{1}0>$ direction with the appearance of interlocking grooves and ridges perpendicular to $<01\bar{1}0>$ in the slip plane. Gooch and Groves [1972] rationalized that such a long Burgers vector in a hard sphere model, where slip in the $<01\bar{1}0>$ requires surmounting a hill of 0.35 Å while slip in $1/3<11\bar{2}0>$ requires surmounting a hill of 0.79 Å. On the basis of the Burgers vector length alone, prismatic slip should be more difficult to activate than basal slip.

Kotchick and Tressler [1980], Cadoz [1978], and Castaing, et al. [1980], investigated work-hardening and deformation mechanisms in sapphire deformed by prismatic slip. Kotchick and Tressler [1980] deformed a-axis (90° orientation) sapphire filaments in tension ($\dot{\varepsilon} = 2.2 \times 10^{-1} - 4.2 \times 10^{-3}$ hr^{-1}) over the temperature range of 1550 to 1850°C in vacuum and observed $\{11\bar{2}0\}$ $<01\bar{1}0>$ slip from slip trace analysis. Typical stress-strain curves showed a yield drop, a small region of low work-hardening ($\theta \sim G/500 - G/5000$), and a region of constant flow stress. At 1850°C, work-hardening was not observed as the lower yield stress merged with the flow stress. Yielding was attributed to a dislocation multiplication process. Activation parameters [$V^* \sim (2 - 5)\,\vec{b}^3$, $\Delta H = 60 - 250$ kcals/mole (251 - 1046 kJ/mole)] and stress exponents ($n \sim 6$-14) strongly indicated that the rate-limiting barrier to flow was the chemical force derived from a supersaturation of vacancies caused by the motion of jogs on glide dislocations which formed by the intersection of glide dislocations with basal debris. The high density of basal debris was verified by TEM. The flow behavior did not confirm to simple diffusion or Peierls process models, but was rationalized on the basis of the creation of supersaturation of vacancies generated by the motion of jogs on gliding screw dislocations.

Cadoz [1978] deformed 90° sapphire in compression ($\dot{\varepsilon} = 4.8 \times 10^{-1} - 4.8 \times 10^{-2}$ hr^{-1}) at 1400-1800°C in air. Samples were oriented such that a $\{11\bar{2}0\}$ glide plane made an angle of 30°, 45°, or 60° to the compression axis. Slip trace analysis and TEM observations verified the $\{11\bar{2}0\}$ $<01\bar{1}0>$ slip system. Loop/glide interactions, cross-slip,

and evidence of climb were observed by TEM. Two work-hardening regions ($\theta_1 \sim G/80$, $\theta_2 \sim G/30$) and a constant flow region ($\theta_3 \sim 0$) were observed after yielding. Prismatic work-hardening is thought to be caused by the rapid build-up of a dislocation network structure caused by the decomposition of prismatic dislocations [Mitchell, 1979]. The activation volume [$V^* \sim (1\text{-}10)\vec{b}^3$] was nearly constant with temperature while the activation enthalpy [$\Delta H \sim$ 150 - 500 kcals/mole (627.6 - 2092 kJ/mole)] decreased with temperature. Cadoz [1978 and 1981] suggested that the overcoming of the Peierls stress is indicated to be controlling the rate of yielding (e.g. critical resolved shear stress) at low temperatures while at high temperatures oxygen diffusion could be controlling yielding.

Castaing, et al. [1980] extended the investigation of Cadoz [1979] at low temperatures (200° to 950°C) by deforming 90° sapphire in compression ($\dot{\varepsilon} = 7.2 \times 10^{-2}$ hr^{-1}) under hydrostatic pressure. Deformation under these conditions occurred by prismatic $\{11\bar{2}0\}\ \langle 01\bar{1}0\rangle$ slip rather than by twinning or cracking. Yield stresses were 4 - 60 times higher than those at high temperatures determined by Cadoz [1978]. Activation volumes [$V^* \sim (0.11\text{-}0.45)\vec{b}^3$] were smaller and stress exponents (n) ranged between 19.5 and 10.4. The critical resolved shear stress τ_{crss} between 200 and 1800°C fit an Arrhenius relation ($\ln \tau_{crss}$ vs. $1/T$), suggesting that one thermally activated mechanism controls the yielding behavior over the entire temperature range. The rate-controlling mechanism was suggested to be the overcoming of the Peierls barrier or barriers due to dislocation dissociation out of the glide plane. Further TEM studies are needed to improve the understanding of the creep rate-controlling mechanism of prismatic slip.

2.3 Deformation by Pyrimadal Slip Systems

Of the three macroscopically identified slip systems in Al_2O_3, pyramidal slip is of primary interest in this discussion because it is the most difficult slip system to activate. Most studies of the pyramidal system have been carried out on either the bulk sapphire

boules grown by the Verneuil or Czochrolaski techniques or on sapphire filaments grown by modified Czochrolaski methods [Pollock, 1972 and Haggerty, 1973]. Pyramidal slip has been activated by placing a tensile or compressive stress parallel to the c-axis of alumina at temperatures above 1600°C. Application of stress in this direction produces a zero critical resolved shear stress, τ_{crss} on the basal plane (perpendicular to the c-axis) and the prismatic planes (parallel to the c-axis). Sapphire oriented for application of stress along the c-axis is referred to as either 0° sapphire or c-axis sapphire.

Wachtman and Maxwell [1957] first observed deformation above 1600°C in 0° sapphire in four-point bend experiments but did not identify the slip system. Tensile tests confirmed that a temperature of 1600°C and stress of ~100 MPa were required to initiate creep by a mode of deformation other than shear on a (0001) plane in a $[11\bar{2}0]$ direction [Wachtman and Maxwell, 1957]. Bayer and Cooper [1967] tension tested a c-axis whisker and at 1200°C and concluded that a unique slip system, $\{10\bar{1}2\}\ <01\bar{1}1>$ was operative from slip trace analysis. This slip system was previously unobserved and is not considered representative of pyramidal slip. Shahinian [1971] reported that the strength of his 0° oriented sapphire filament specimens were controlled by a mechanism other than basal or prismatic slip; however, he did not persue this further. Hockey [1971], Tressler and Barber [1974], and Gooch and Groves [1973] performed deformation experiments on c-axis sapphire filaments and concluded $\{10\bar{1}1\}\ <01\bar{1}1>$ pyramidal slip was probable.

Tressler and Barber [1974] performed differential temperature and differential strain rate tests on c-axis Tyco* filaments (which contain microvoids of about one micron) and found a power law dependence, with n values increasing from 8.5 at 1775°C to 12.4 at 1875°C. They also found a zero stress activation enthalpy of approximately 80 kcals/mole.

Michael and Tressler [1974] deformed c-axis sapphire filaments grown by laser heating floating zone techniques (A. D. Little filaments)[Haggerty, 1973] in tension

* Currently Saphikon fiber

($\dot{\varepsilon} = 1.2 - 2 \times 10^{-1}$ hr^{-1}) at 1800 -1850°C and concluded from slip trace analysis that $\{10\bar{1}1\}$ $<01\bar{1}1>$ slip had occurred. Activation enthalpy [$\Delta H \sim 120 - 170$ kcals/mole (502-711 kJ/mole)] and activation volume [$V^* \sim (800\text{-}1200)\bar{b}^3$] suggested the overcoming of the Peierls barrier as the rate-limiting mechanism for the motion of a $1/3<10\bar{1}1>$ dislocation since the activation volume was too large for diffusion mechanisms, the stress exponents were too large for diffusion models previously reported by Conrad, 1965 and Conrad et al., 1965, and the activation enthalpies appeared to be a decreasing function of stress and an increasing function of temperature. They did not, however, rule out diffusion controlled processes since the apparent activation enthalpies included the 152 kcals/mole (636 kJ/mole) measured for O^{2-} in Al_2O_3. Finally, they noted the distinct difference between porous Tyco c-axis filaments and pore free c-axis crystals in flow stress and activation parameters in the temperature range studied, suggesting that they may show different rate-controlling deformation mechanisms.

Both Tressler and Barber [1974] and Michael and Tressler [1974] concluded that slip was taking place on $\{10\bar{1}1\}$ with a probable $1/3<10\bar{1}1>$ Burgers vector from direct SEM analysis of oriented macroscopic slip traces in deformed c-axis filaments. Gooch and Groves [1973a] had tested c-axis Tyco filaments in tension at 1600 - 1800°C at strain rates of 10^{-3} hr^{-1} and stresses of 180 - 65 MPa. They found a stress exponent (n) of about six and activation enthalpies with marked stress dependence, but did not speculate as to the rate controlling mechanism. They determined from etch pit studies, TEM analysis and macroscopic slip traces that the $\{10\bar{1}1\}$ $<01\bar{1}1>$ slip system was primarily responsible for deformation under these conditions. They proposed that the Peierls stress controlled the motion of a $1/3<10\bar{1}1>$ dislocation to 1800°C and observed that the $1/3<10\bar{1}1>$ dislocation was not restricted to one glide plane.

The rate controlling mechanism for plastic deformation via pyramidal slip has not been convincingly determined. Heuer et al. [1970] and Firestone and Heuer [1976] proposed pure Nabarro-climb deformation for 0° Czochrolski sapphire deformed from

1600 - 1800°C in tensile creep under low loads 70 - 114 MPa which resulted in low strain rates (10^{-5} - 10^{-3} hr^{-1}). In Firestone and Heuer's [1976] tensile creep study in which they tested 0° sapphire at 1600 -1800°C they generated dislocation structures which consisted of heterogeneous distributions of arrays containing long dislocations, loops, and nodes. They also found that the nonbasal $1/3<10\bar{1}1>$ dislocation did not lie in any particular glide plane although the $\{1\bar{1}02\}$, $\{1\bar{1}01\}$ and $\{2\bar{1}\bar{1}3\}$ planes were glide plane possibilities. Even though nonbasal dislocations were present, they concluded from the mechanical behavior that most of the deformation occurred via vacancy diffusion between a stable network of climbing dislocations (Nabarro climb). They based their conclusion on the stress exponent ($n = 3$) from a relationship of the form $\dot{\varepsilon} = \sigma^n$ and a fit of the apparent oxygen diffusion coefficient calculated assuming Nabarro climb.

Cadoz and Pellissier [1976] compression tested ($\dot{\varepsilon} = 1.8 \times 10^{-2}$ - 3.6×10^{-3} hr^{-1}) Verneuil-grown c-axis sapphire at 1700°C and observed an R1 $1/3 < 01\bar{1}\bar{1} > \{0112\}$ and an R2 $1/3 < 0\bar{1}1\bar{1} > \{01\bar{1}\bar{2}\}$ glide system operating. The R1 system had a higher flow stress due to much higher loop and debris densities. The R2 system had a lower flow stress and long, straight edge dislocations with $<01\bar{1}1>$ Burgers vectors associated with its activation.

Kotchick [1978] deformed c-axis sapphire at 1300 - 1850°C in tension ($\dot{\varepsilon} = 2.16 \times 10^{-1}$ - 4.2×10^{-3} hr^{-1}). The dislocation substructure consisted of long, straight parallel dislocations. By slip trace analysis, he concluded that $\{10\bar{1}1\}$ $<01\bar{1}1>$ glide was probable. Activation enthalpy [$\Delta H \sim 60$ - 120 kcal/mole (251 - 502 kJ/mole)] and activation volume [$V^* \sim (200 - 400)\ \vec{b}^3$] indicated that flow was controlled by the thermally activated overcoming of the Peierls barrier at T<1750°C. From 1750 to 1850°C the tensile flow data fit the Kuhlmann-Wilsdorf model which describes the temperature dependence of the Peierls stress when associated with the uncertainty of position of the dislocation core caused by thermal fluctuations.

2.4 The Influence of Doping on the Creep Resistance of Sapphire

Since sapphire does deform plastically, albeit relatively slowly; it would be desirable to extend its creep resistance by increasing the barriers to dislocation motion. There are three means by which this can be accomplished this and they are: (1) work hardening, (2) solution hardening, and (3) precipitation hardening. Work hardening is an intrinsic process caused by dislocation interactions which probably cannot be changed very much by dopants except as they affect the point defect equilibria and thus the recovery process. Solid solution hardening and precipitation hardening are extrinsic processes in which the additives interfere with dislocation motion. Precipitation hardening places finely dispersed precipitates throughout the structure to pin or interfere with dislocation motion. Solid solution hardening can impede dislocation motion by direct elastic interactions of solute atoms with dislocations. Solute atoms can also change the Peierls-Nabbarro barrier to dislocation motion or the defect equilibrium for diffusional rate controlling processes such as dislocation climb.

Chromium and titanium are known hardeners of sapphire at room temperature. Bradt [1967] showed that the microhardness of fine grained alumina increased continuously with the addition of up to 12.5 mole % chromia. Several investigators [Bratton, 1971; Busovne [1981], Kotchick [1978], Tressler et al. [1974], and Rasmussen et al., 1965; Hsu et al., 1967] have shown that the microhardness on the basal plane of single crystal sapphire is increased for additions of Ti^{3+} and Ti^{4+} solid solutions and for precipitated star sapphire. The precipitates in titanium doped sapphire nucleate and grow at about 1300 - 1450°C in air when the solid solubility limit is exceeded (~ 0.5 mole % TiO_2 at 1500°C) [Rozz and Coble, 1968; McKee et al., 1963; and Winkler et al. 1966]. The acicular precipitates which lie on the basal plane in the three $<10\bar{1}0>$ directions cause the asterism in star sapphire, are known to be faulted rutile from TEM lattice imaging experiments by Philips, et al. [1977]. Philips et al. [1977] also found that prismatic

dislocations are associated with the misfit of the precipitates along $<2\bar{1}\bar{1}0>$. Bratton [1971] aged 0.11 weight percent titanium doped Czochrolski sapphire in air at temperatures between 1100 and 1600°C and found that the precipitates are mainly localized at grown-in dislocations or subgrain boundaries. He also showed that the precipitates increased the Knoop hardness with increased aging time, observing an optimum hardening after aging at 1300°C for 13 days in air. Busovne and Tressler [1981] aged plastically deformed and undeformed Ti^{4+} doped (0.08 and 0.17 weight percent TiO_2) single crystal sapphire at 1300°C and found that dislocations acted as preferential nucleation sites for precipitation.

Wachtman and Maxwell [1957] tensile creep tested 90° sapphire rods (oriented for basal slip) containing 0.75 weight percent chromia at 1200 - 1300°C and found approximately a 50% increase in the creep stress. Chang and Groves [1965] measured an increase in resolved shear stress from 7 MPa for pure sapphire to 12 MPa for 0.50 weight percent Cr_2O_3 doped sapphire at a steady state creep rate of 10^{-3} hr^{-1} at 1500°C, 10^{-1} hr^{-1} in air and found that 4500 ppm Cr increased the critical resolved shear stress from 10 to 60 MPa and additions of 350 ppm Ti increased the critical resolved shear stress from 10 to 75 MPa. They also found evidence of slip on nonbasal systems which appeared to be more extensive in the impurity doped crystals.

Pletka, et al. [1975] deformed titanium and chromium-doped sapphire by basal slip and explained the relative hardening effect of these ions by the size difference and type of distortion they produce in the lattice. They also examined the effect of precipitation hardening on basal slip and observed that there was no significant difference from solid solution hardening with Ti^{4+} due to the fact that the precipitates lie in the glide plane and the dislocations can by-pass them by glide and climb with relative ease.

Busovne and Tressler [1981] investigated the effects of thermomechanical working (prismatic slip) of Ti^{4+}- doped sapphire. They found that the heat treatment of Ti^{4+} - doped sapphire in air at 1300°C resulted in the precipitation of rutile (TiO_2) needles oriented in the $<10\bar{1}0>$ direction. Precipitates were found to nucleate preferentially at

dislocations in samples deformed between 1600 and 1800°C ($\dot{\varepsilon}$ = 1.65 x 10^{-2} - 8.82 x 10^{-2} hr^{-1}) by the prismatic $\{11\bar{2}0\}<1\bar{1}00>$ slip system prior to aging in air. Dislocations had little or no effect on the particle growth process. The presence of TiO_2 precipitates in sapphire increased the room temperature microhardness in the $<11\bar{2}0>$ direction by 5-20% (~ 23 GPa) for Ti^{4+} doped and aged sapphire versus ~ 18 GPa for undoped sapphire.

The effect of TiO_2 precipitates on prismatic $\{11\bar{2}0\}<1\bar{1}00>$ slip behavior was investigated by deforming a-axis (90°) sapphire filaments in tension at 1450°C ($\dot{\varepsilon}$ = 3.7 x 10^{-2} hr^{-1}). It was found that specimens aged for 3 days fractured. These specimens were tested under conditions in which the applied stress was higher than the critical resolved shear stress for flow. This result indicates that barriers to slip (i.e. the TiO_2 precipitates) allow enough localized stresses to develop to propagate microflaws unstably instead of initiating deformation. The hardening of the prismatic slip system by rutile precipitates was attributed to image forces generated by elastic mismatch between rutile and sapphire.

Michael and Tressler [1974] deformed Ti^{4+} doped (0.024 to 0.077 weight percent Ti) c-axis sapphire over the range between 1800°C and 1850°C in air and found no significant difference in activation parameters and flow stresses concluding that the Ti^{4+} has no effect on c-axis sapphire and pyramidal slip. This study ruled out the possibility of a cation defect diffusion rate-controlling deformation mechanism. They concluded that the rate controlling mechanism appeared to be the thermally activated overcoming of the Peierls-Nabarro stress.

Kotchick [1978] investigated the effect of Ti^{4+} and Ti^{3+} additions to a-axis (90°) and c-axis (0°) sapphire filaments at 1550 and 1850°C ($\dot{\varepsilon}$ = 4.24 x 10^{-2} hr^{-1} and 0.18 x 10^{-3} hr^{-1}, respectively). It was found that a 30% reduction in flow stress anisotropy, due to softening of both the prismatic and pyramidal flow stresses, was achievable, compared to estimates for basal flow from Pletka [1975] in Ti^{4+} doped sapphire. An example of this behavior is given in Figure 4 in which the tensile flow stress versus temperature for doped

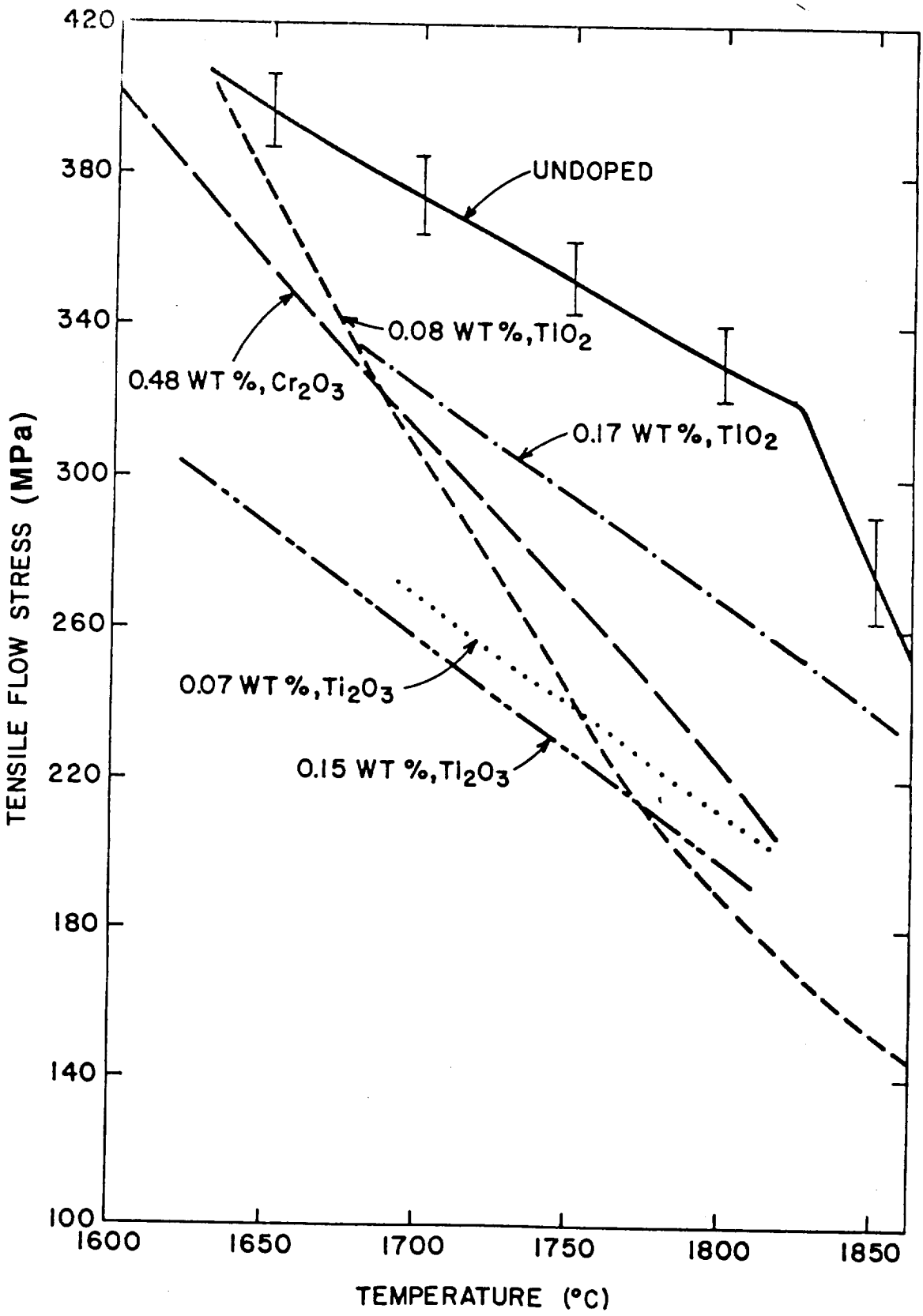

Figure 4. Influence of Ti^{4+}, Ti^{3+}, and Cr^{3+} additions on the tensile flow stress of a 0° Sapphire filament at a $\dot{\varepsilon} = 0.114\ hr^{-1}$.

and undoped 0° sapphire is given at a strain-rate of 0.114 hr^{-1}. The doped 0° sapphire filaments exhibited significant solid solution softening for all dopants. This was most pronounced for the more heavily doped Ti^{3+} samples which had an almost 40% drop in their flow stress at 1800°C. In the 0° sapphire, this softening behavior was attributed to a disruption of the dislocation core by the large ionic radius dopants (e.g. Ti^{3+} - 0.81Å) which are thought to cause a reduction of the Peierls barrier [Kotchick, 1978]. Figure 5 illustrates this anisotropy reduction for all three slip systems in sapphire.

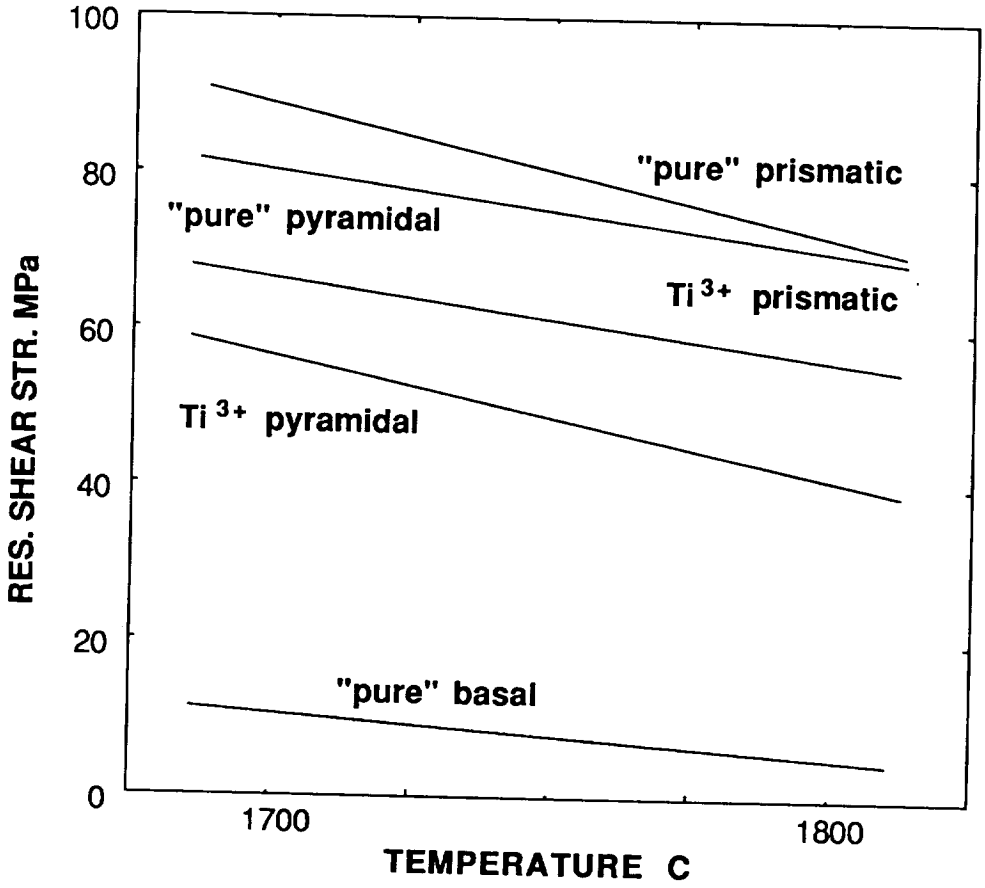

Figure 5. Flow stress anisotropy reduction in sapphire via Ti^{3+} Doping, from Kotchick [1980].

3.0 DEFORMATION BEHAVIOR OF POLYCRYSTALLINE ALUMINA

The high-temperature creep data and flow behavior of polycrystalline Al_2O_3 are difficult to interpret for a number of reasons which include variability in test parameters, purity of the aluminas, fabrication techniques, grain sizes, and microstructures. Also, a great deal of the creep testing of polycrystalline Al_2O_3 has been performed in flexure. The stress in a bend or flexure test is redistributed as the material creeps and, thus, the maximum tensile stress is not known accurately as a function of creep strain. Also, since there is a stress gradient, multiple mechanisms may influence the creep behavior.

For the purposes of this overview, the deformation of fine-grained (1 to 15 μm) alumina is of interest since it is the fine-grained materials which are useful as strong filaments at room temperature. Plastic deformation of fine-grained polycrystalline alumina may exhibit three distinct deformation mechanisms; (1) diffusional creep; (2) basal slip and; (3) unaccommodated grain boundary sliding.

With regard to diffusional creep, both lattice and grain-boundary diffusion are important since the creep rate is generally believed to be controlled by the slowest species along the fastest path. The diffusion of the aluminum ion, therefore, is believed to be rate controlling because the diffusion of oxygen is very slow through the lattice, yet rapid down the grain boundary. For very fine grains sizes, diffusional creep can become interface controlled resulting in non-Newtonian creep behavior of fine-grained materials [Cannon et al., 1980].

Another important behavior of polycrystalline ceramics is that under certain conditions the creep of polycrystalline ceramics can be greater than a single crystal in the most favorable orientation (such as basal slip in sapphire) [Gilman, 1966]. This interest in deformation and the role of diffusion on deformation behavior has lead to the extensive study of the creep of polycrystalline alumina

Stress-directed vacancy (or interstitial) diffusion between climbing dislocations [Nabarro, 1967 and Weertman, 1968] or grain boundaries [Nabarro, 1948; Herring, 1950

and Coble, 1963] gives rise to macroscopic deformation. Diffusional creep usually refers to migration of these vacancies between grain boundaries, and this behavior appears to dominate the low stress deformation of many ceramic polycrystals. In the constitutive relationship previously given to describe creep (Eq. 1.1) it is assumed that grain boundaries act as perfect sources and sinks for vacancies and that they easily slide. In cases where this is not true, diffusional deformation is believed to be interface reaction controlled [Ashby, 1969; Greenwood, 1970; Burton, 1972 and Ashby and Verrall, 1973].

Diffusional creep with grain boundaries as defect sources has been analyzed extensively as compared to other creep theories. Folweiler was the first to study the deformation of fully dense polycrystalline Al_2O_3 as a function of temperature, grain size and strain rate. Folweiler [1961] tested fine- to medium-grained MgO-doped, sintered Al_2O_3 in air under three point bend. His data satisfied the relationship $\dot{\varepsilon} \propto \sigma$ over a wide temperature range of 1400 - 1800°C for specimens with grain sizes of ≈6 - 34 μm. A grain size dependence of the rate of $1/d^2$ was found. Folweiler concluded that Nabarro-Herring creep was operative; however, one must keep in mind that this conclusion was based on flexure data in which more than one stress state is necessarily operative.

Warshaw and Norton [1962] tested commercial Al_2O_3 having grain sizes ranging between 10 and 100 μm under four point bend at low stresses (up to ~ 10 MPa) in the temperature range of 1600 - 1800°C. Warshaw and Norton apparently confirmed the validity of a diffusional deformation model for polycrystalline alumina. However, diffusion coefficients calculated were an order of magnitude lower than those of Folweiler [1961]. Fine grained (3 - 13 μm) alumina exhibited viscous (n = 1) behavior with an activation enthalpy of 130 kcal/mole (543.9 kJ/mole). Grain size dependence for the fine-grained materials $\left(\dot{\varepsilon} \propto 1/d^2\right)$ also supported a Nabarro-Herring diffusion controlled creep mechanism. Warshaw and Norton [1962] also noted that dislocation mechanisms

contributed to the creep process of the Al_2O_3 and grain boundary sliding was noted in this material on surfaces under compression.

Passmore and Vasilos [1966] crept tested undoped, hot-pressed alumina under constant load in four point bending over the temperature range of 1400 to 1500°C. The purpose for their work was to establish whether cation diffusion was controlling the creep rate of very small (≈2μm) grain size material. At low stresses, Nabarro-Herring diffusional creep was proposed as the controlling mechanism and a diffusion coefficient of 8×10^{-13} m^2/sec was calculated over the temperature range of 1400 to 1500°C from the creep data for the rate controlling species (believed to be Al^{3+}). The belief that cation diffusion was controlling the creep of these fine-grained aluminas was based on the work of Paladino and Kingery [1963] and their observations of cation diffusion independent of the grain size in alumina. Results of Oishi and Kingery [1960] showed that this was not true of the anion - the oxygen diffusivity increased with decreasing grain size. Therefore, Passmore and Vasilos proposed that creep in polycrystalline alumina was controlled by stress-directed cation (Al^{3+}) diffusion (e.g. for grain sizes < 20μm).

Others who have studied the flexural creep of polycrystalline alumina and support the belief that Nabarro-Herring diffusion is the major contribution to creep include Hewson and Kingery, 1967; Hollenberg and Gordon, 1973; and Lessing and Gordon, 1975 and 1977. Much of this work focused on the influence of various aliovalent dopants on the diffusivity of the Al^{3+} cation [Ikuma and Gordon, 1983 and Burton, 1973] and the nature of the solid solution and precipitation structure resulting from doping [McKee et al., 1963; Roy and Coble, 1968; Winkler et al., 1966; Pletka et al., 1972; Burton, 1973; and Mohapatra et al. 1977]. Of these studies, it was found that MgO concentrations doped into sintered alumina did exhibit a retarding effect on the diffusivity of Al^{3+} in the temperature range of 1550 to 1860°C [Hewson and Kingery, 1967].

Doping of polycrystalline alumina with aliovalent impurities also appeared to influence the creep-rate dependence on the partial pressure of oxygen above the sample

[Hollenberg and Gordon, 1973]. High p_{O_2} enhanced creep in Ti doped Al_2O_3 and depressed the creep rate in Fe doped Al_2O_3. There was no influence of p_{O_2} on Cr doped alumina. Hollenberg and Gordon [1973] also found that the precipitation of TiO_2 increased the activation energy for the rate controlling diffusion mechanism which was believed to be Al lattice diffusion via a vacancy or an interstitial mechanism.

Hollenberg and Gordon [1973] reported studies involving four point loading of pure and transition element doped polycrystalline alumina in a range of oxygen partial pressures. The aliovalent dopants caused a marked p_{O_2} dependence of the steady state creep rates. High p_{O_2} enhanced creep in Ti doped Al_2O_3, depressed the creep rate in Fe doped Al_2O_3, and had no effect on isovalent Cr-doped alumina. In general, slightly non-viscous ($n = 1$ to 1.35) behavior was recorded for a p_{O_2} range of 0.86 to 10^{-10} in the temperature range of 1375 to 1525°C and under stresses of 0.2 to 11 MPa. Grain sizes ranged from 3 to 6 μm in Cr doped, 10 to 28 μm in Fe doped and 28 to 42 μm in Ti doped aluminas. These data suggest that the Nabarro-Herring lattice diffusion mechanism was indeed the dominant mechanism. Precipitation of a second phase TiO_2 was responsible for the increased activation energy of the basic diffusion mechanism. The rate controlling mechanism throughout was thought to be Al lattice diffusion via a vacancy or an interstitial mechanism.

Lessing and Gordon [1975] extended this study by working with hot pressed pure, Cr, and Fe doped aluminas having a range of grain sizes from 6 to 1200 μm. Testing was accomplished under four point dead load at 1350 to 1550°C, stress levels of 4 to 50 MPa and p_{O_2}'s ranging from 0.86 to 10^{-9}. Stress exponents of 1.03 to 1.43 were found for grain sizes between 9 and 110 μm and these data agreed well with the Nabarro-Herring creep equation. Slightly non-viscous behavior ($n = 1.4$ to 1.8) was exhibited by the 70 to 306 μm pure and Cr-doped aluminas at 1450°C. Stress exponents up to ≈1.7 were characteristic of creep deformation in bending and compression of Al_2O_3, pure and doped, over a wide range of experimental conditions. Grain size and p_{O_2} effects, activation

energies and calculated diffusion coefficients indicated that the Nabarro-Herring mechanism was a major contributor to creep deformation.

In large grained specimens (> 100 μm) and in higher stress regimes non-viscous creep dominated the strain-rate behavior, with stress exponents higher than two exhibiting (in general) a grain size independence. In this regime, chromium was an effective hardener, significantly depressing the steady-state creep rate compared to undoped, large grained alumina. It was also concluded from this study that the steady-state creep of pure and doped, polycrystalline Al_2O_3 is controlled primarily by lattice diffusion of aluminum ions either by a vacancy or an interstitial mechanism. Lessing and Gordon [1977] established that the steady-state creep of polycrystalline pure (undoped) Al_2O_3 and Al_2O_3 doped with chromium, at low stresses was rate limited primarily by the lattice diffusion of aluminum ions and independent of chromium concentration. Doping alumina with Fe^{2+} in solid solution enhanced the lattice diffusion of Al^{3+} ions. The steady state creep of iron-doped alumina; however, was found to be mixed in character in that both aluminum lattice and oxygen grain-boundary diffusion are comparable in magnitude. At high concentrations of the divalent iron (i.e. high iron dopant levels and low oxygen partial pressures) aluminum lattice diffusion was too rapid to be rate limiting. Under these conditions, Coble creep which was rate-limited by oxygen grain-boundary diffusion was dominant.

Cannon, Rhodes and Heuer [1980] studied the behavior of hot pressed pure and MgO doped sintered aluminas under four point loading. Fine grain sizes (1 to 15 μm) exhibited diffusion controlled behavior over the temperature range of 1200 to 1850°C and at stress levels between 3 and 310 MPa. Newtonian-viscous deformation was not always observed because of either interface control reaction of the diffusion process or the occurrence of basal slip and nonaccommodated grain boundary sliding. Coble type creep was suggested at lower stress levels, while lattice diffusional creep seemed operative at higher stress levels. The interface-controlled diffusional deformation (n = 2) became important only if the grain boundaries did not serve as perfect sources and sinks for

vacancies, and if sliding was inhibited which is often the case for very small grain-sized material. Implicit in interface reaction controlled diffusional creep was a threshold stress, σ_o, below which no permanent deformation occurs. These researchers had found that as a result of creep testing in flexure, several deformation mechanisms occurred simultaneously and the controlling creep mechanism was difficult to define.

Cannon et al. [1980] concluded from their work that the control of the deformation is by an additive contribution of boundary and lattice diffusion of Al with rapid (but not rate controlling) oxygen boundary diffusion. A transition from Newtonian behavior at high stresses, to interface control is cited as the cause of the previously reported non-integral values of the stress dependence in creep studies of fine-grained aluminas.

Heuer et al. [1980] reported on the phenomena of basal slip and grain boundary sliding (GBS) which occur simultaneously in the fine-grained alumina. The deformation textures developed in the same materials and over the same range of stress and temperatures as given previously by Cannon et al. [1980] were described. Emphasized in their discussion where the controlling dislocation mechanisms, GBS, cavitation, and cavitation development during deformation. Grain boundary sliding resulted in triple point offsets that were observed in TEM studies, though their occurrence was not abundant. Voids due to cavitation, perhaps a consequence of the inability of diffusional processes to accommodate slip band/grain boundary interactions in favorably oriented grains were, noted. Grain boundaries were concluded to be the primary source for the basal dislocations observed in TEM studies. The low dislocation densities found seemed to indicate that grain boundaries were able to annihilate active dislocations. In all cases the low frequency of evidence of slip and grain boundary sliding suggests that neither mechanism is comparable in magnitude to diffusional deformation processes, as expected for the fine (1 to 5 microns) grain sizes investigated.

Slip was previously noted as a significant deformation process in polycrystalline Al_2O_3, as the grain size was increased. Rhodes et al. [1965 and 1966] investigated the

compressive creep behavior of both pure and doped alumina and hot pressed and forged from powders. Evidence for deformation by slip mechanisms was seen at temperatures between 1500 and 1700°C. Electron microscopy revealed that basal slip was the primary slip mechanism.

Several researchers have comprehensively examined the creep deformation of alumina under compressive loads (Sugita and Pask, 1970; Bacher, 1971, Mocellin and Kingery, 1971; and Hou et al., 1979] and their results are also interpreted in terms of diffusional controlled creep. The trends in these creep data which are evident are few, but important. Analysis of the creep rate of Al_2O_3 indicates that at low stresses creep is dominated by diffusional creep. At intermediate stresses which are above the basal yield yet below that of slip on a secondary slip system, slip will occur on favorably oriented basal slip systems with accommodation of the grain slope change by sliding.

For intermediate and fine-grained materials, much of the strain observed is the result of diffusion controlled creep; however, a contribution to the creep rate may result from basal slip which yields stress exponents slightly greater than one. Large-grained materials most often exhibit non-viscous behavior independent of grain size, while Newtonian ($\dot{\varepsilon} \propto \sigma$) behavior is always approximated by the fine-grained materials of various purity levels which appears to be controlled by the diffusion of the cation either through the lattice or along the grain boundaries.

3.1 Deformation of Single Crystal and Polycrystalline Al_2O_3

Single crystal alumina (sapphire) is extremely anisotropic in its deformation behavior, and it has been clearly illustrated that the basal slip system is the primary system and that prismatic or pyramidal slip systems are secondary. Therefore, the most creep resistant orientation of a fiber tested in uniaxial tension is the basal plane perpendicular to

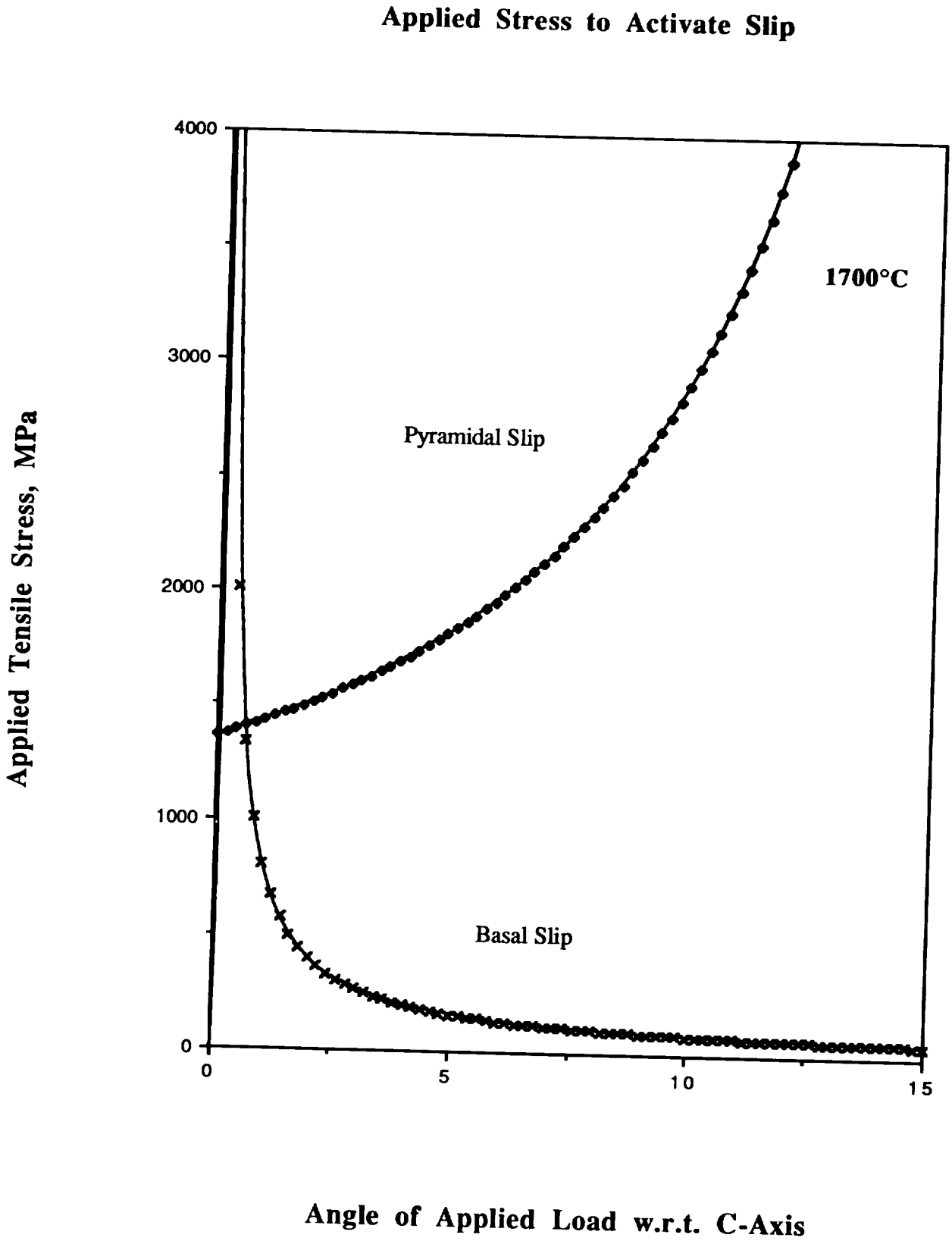

Figure 6. Applied stress necessary to activate slip in Sapphire as a function of the angle between the applied stress and the c-axis

the fiber axis (0° Sapphire). Figure 6 is a plot of the applied tensile stress necessary to activate a given slip system in a 0° Sapphire filament as a function of the angle between the applied tensile stress and the c-axis. The values for τ_{crss} for basal and pyramidal slip at 1670°C were taken from Kronberg [1962] and Tressler and Barber [1974], respectively. The critically resolved shear stresses were taken from tensile flow stresses extrapolated to zero elongation at 1670°C. A value of 14 MPa was used for basal slip, whereas a value of 392 MPa was used for pyramidal. Figure 6 clearly shows that basal slip in the 0° Sapphire fiber can occur in every orientation unless the stress is applied parallel (or perpendicular) to the c-axis of the crystal. Based upon Schmid's Law at an orientation of 0° to the fiber axis, activation of the pyramidal slip system, requires an applied tensile stress of 1374 MPa in a perfect crystal at 1650°C.

Slip on the basal system is much easier than on the prismatic or pyramidal systems as shown in Figure 3. Figure 3 presents the flow stresses versus temperature for the various slip systems from tests on single crystals of alumina. The stresses plotted are tensile yield stresses for 60° crystals for basal slip $1/3 < 11\bar{2}0 > (0001)$, for 90° crystals for prismatic slip, $1/3 < 1\bar{1}00 > \{11\bar{2}0\}$ and for 0° crystals for pyramidal slip, $1/3 < 0\bar{1}11 >$ on one or both of $\{10\bar{1}2\}$ or $\{10\bar{1}1\}$, respectively.

All of the data plotted in Figure 3 are for pure undoped samples taken for a strain rate of 0.144 hr^{-1} (4.0×10^{-5} sec^{-1}). The single crystal basal and pyramidal flow stresses have strain rate sensitivities in the range of n = 4 - 7.

Activation analyses of the single crystal yield behavior have not conclusively identified the barriers which control slip on any slip system. However, it has been inferred that the lower yield stresses (which are plotted in Figure 3) are representative of the Peierl-stress for the non-basal systems [Tressler and Michael, 1974 and Govorkov et al., 1972], and for basal slip at low temperatures [Conrad, 1965]. For temperatures >1600°C, climb around obstacles may limit slip in basal and nonbasal systems [Conrad, 1965].

Steady-state flow stresses for 1 and 13 μm polycrystalline material of the same strain rate are also plotted in Figure 3. Folweiler [1961] demonstrated that the kinetics indicated diffusional creep for the entire range of stress investigated. The stress exponents were typically n = 1 to 1.2 which is consistent with an increasing contribution of basal slip at higher stresses. This diffusionally controlled behavior was confirmed by others [W. R. Cannon, 1971; Heuer et al., 1969; and R. M. Cannon, 1975]. Similar plots can be contributed from Schmid's law for near a-axis orientation. The end result is that single crystal orientations very close to 0° orientation or c-axis are the most creep resistant.

Kotchick's [1978] creep results are evidence of the influence of pyramidal slip on controlling the creep rate of 0° sapphire in tension. Kotchick's data for 0° sapphire fibers are plotted in Figure 7 along with several other sets of data which bracket the creep rates of 0° sapphire and polycrystalline alumina over the temperature range of interest. All the data in Figure 7 and in the later figures which similarly plot strain-rates against the reciprocal of the temperature are extrapolated to a stress level of 100 MPa using the constitutive relationships as defined by each study. Kotchick's [1978] research was directed at defining the deformation dynamics in uniaxial tension of doped (Cr^{3+}, Ti^{3+}, and Ti^{4+}) and undoped c-axis single crystal sapphire at temperatures between 1600 and 1800°C via the pyramidal $\{10\bar{1}1\}$ $<10\bar{1}1>$ slip system. Plotted in Figure 7 are data for the undoped c-axis sapphire crept at a stress level of 180 MPa and extrapolated to 100 MPa. Doping (as previously described) served to facilitate slip on the pyramidal slip system. The rate controlling process for flow of these doped and undoped sapphire filaments in Kotchick's [1978] study was again believed to be limited by the thermally activated overcoming of the Peierls barrier. This mechanism was supported over the temperature range of 1600 to 1800°C by results which included observed dislocation substructures in the deformed samples which contained long straight dislocations perpendicular to the glide direction, calculated stress exponents were large and activation volumes were indicative of a Peierls

Creep of Single and Polycrystalline Al2O3

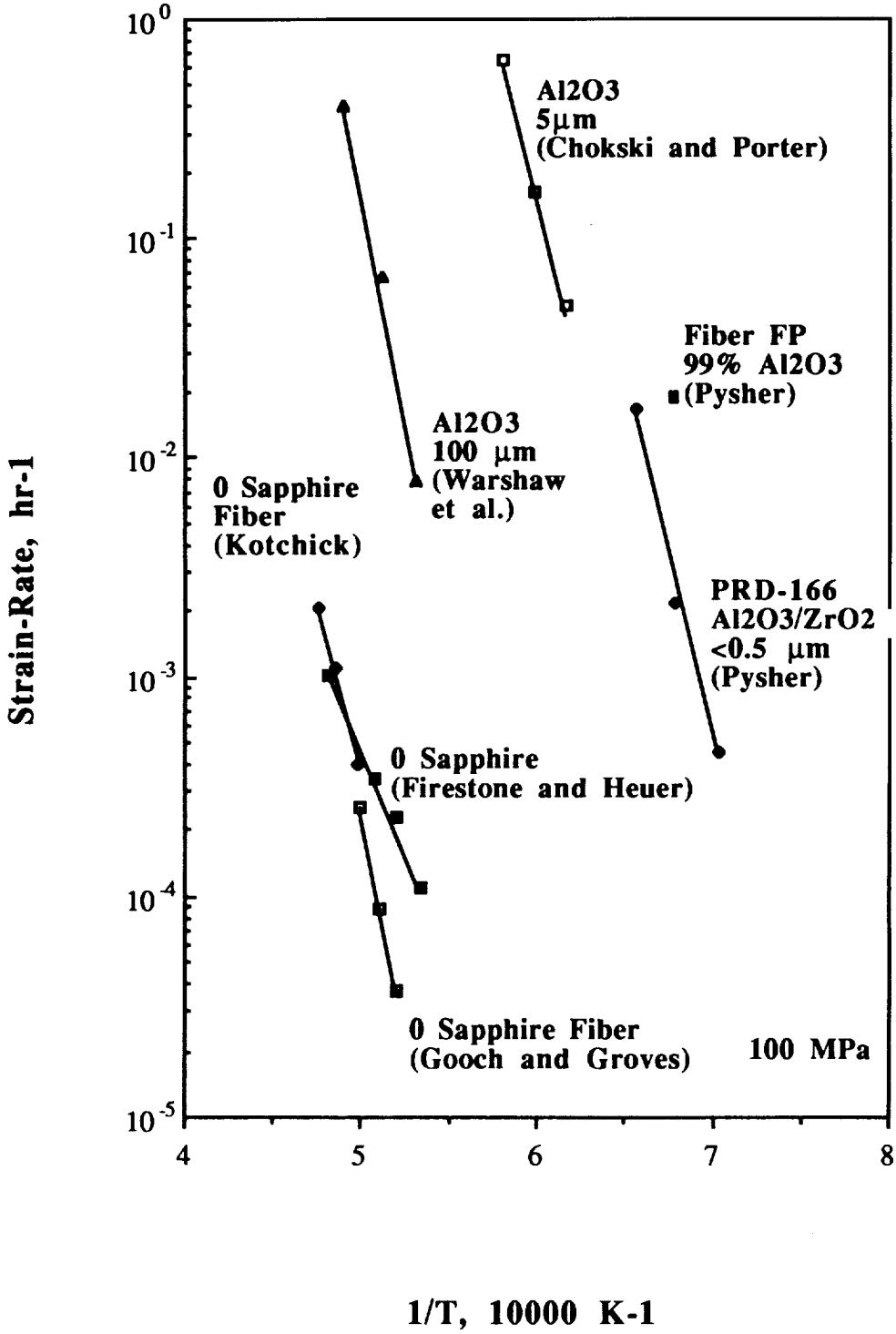

Figure 7. Steady-state strain-rates of single and polycrystalline alumina extrapolated to 100 MPa applied load

process ($\geq 10\ \vec{b}^3$). The apparent activation enthalpies also did not change when the crystals were doped with Ti^{4+}.

Creep deformation data for Firestone and Heuer's [1976] study of 0° oriented sapphire is also plotted in Figure 7. The deformation of this sapphire was studied between 1600 and 1800°C at stresses of up to 114 MPa. It should be noted that most deformation studies on single crystal alumina used extremely high stress (on the order of 200 MPa) to study the deformation behavior. This study by Firestone and Heuer [1976] is the one study which examined the behavior at much lower stresses, between 75 and 114 MPa. Pure Nabarro climb was suggested as the controlling deformation mechanism under these conditions. The high creep resistance of 0° sapphire, again, was attributed to the difficulty of activating pyramidal slip.

From the work on 0° sapphire (bulk and filaments) [Wachtman and Maxwell 1954 and 1957, Gooch and Grooves, 1973; Tressler and Barber, 1974; and Michael and Tressler, 1974] it is clear that there is little measurable deformation at temperatures below 1600°C and that the total strain before fracture is <10%. Disagreement remains as to whether the deformation process above 1600°C is controlled by a Peierls-Nabarro stress or by a diffusion mechanism such as cooperative climb at low stresses and Peierls controlled creep at high stresses. Also unknown is the influence of the specific creep mechanism on creep damage and, ultimately, creep rupture of sapphire.

The role of creep damage on rupture was briefly addressed in the Firestone and Heuer [1976] paper. Fracture surfaces of the 0° sapphire specimens exhibited mirror and hackle regions characteristic of brittle fracture. This was true even of the deformation specimen which was crept at 1800°C. The fracture planes were well defined. Evidence of ductile fracture was not present. Firestone and Heuer [1976] attributed this rupture behavior to slow crack growth which resulted in catastrophic fracture when the flaw had grown to such a size that the Griffith criteria was satisfied. This mirror radius was used to calculate the fracture surface energy. A value of 37.9 J/m^2 was obtained for a filament

under a stress condition of 114 MPa having a mirror radius of 0.42 mm. No mechanism was proposed for controlling the rupture behavior of 0° oriented sapphire.

For comparison, the creep rates observed for single crystal Al_2O_3 (0° oriented), fine-grained polycrystalline aluminas are also plotted in Figure 7. Chokski and Porter [1986] examined the flexural creep behavior of a polycrystalline Al_2O_3 having a grain size of $\leq 5\mu m$. The mechanism controlling the creep behavior at temperatures between 1600 and 1800°C was typical of fine-grained materials. Creep was controlled by Nabarro-Herring diffusion which is consistent with cation diffusion controlled creep. However, the creep rate decreased with time as a function of grain growth at high temperatures.

Also given in Figure 7 are the creep rates for two polycrystalline oxide filaments; the PRD-166 which is a commercial Al_2O_3 - ZrO_2 filament produced by DuPont having a grain size of $< 0.5\ \mu m$, and Fiber-FP which is a 99% polycrystalline Al_2O_3 fiber also having a grain size of $\approx 0.5\mu m$ [Pysher, 1989]. The rate controlling mechanism for the creep of these filaments is currently under investigation; however, based upon the evidence presented for the bulk polycrystalline Al_2O_3, the mechanism would appear to be an interface reaction controlled diffusional process.

Diffusive creep appears to be the controlling elongation process in fine-grained alumina over a wide range of temperatures and stresses, yet we do not know the rate limiting diffusion path and the influence of impurities on the diffusion process. Diffusion coefficients for ionic diffusion in single crystal and polycrystalline Al_2O_3 are highlighted in Figure 8 [Paladino and Kingery, 1962; Oishi and Kingery, 1959; Reddy and Cooper, 1982, and Reed and Wuensch, 1980]. Additional studies on the diffusion of O^{2-} in α - Al_2O_3 at temperatures above 1600°C include Oishi, et al. [1980], Oishi et al. [1983], and Cawley [1584].

The Paladino et al. [1962] study is the sole study to date of the cation mobility. Paladino et al. examined the diffusion of an ^{26}Al tracer ion through a polycrystalline Al_2O_3

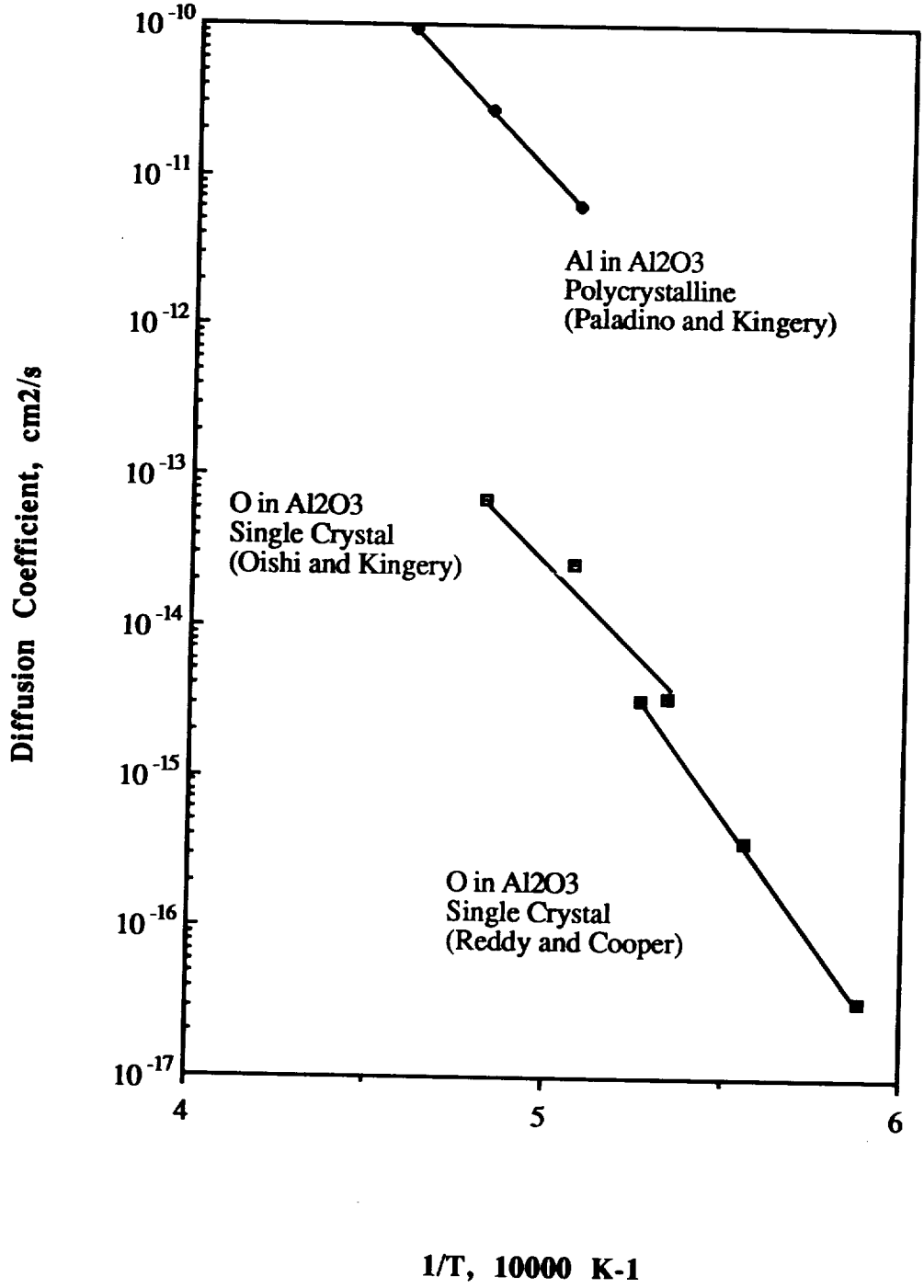

Figure 8. Diffusion coefficients for Al and O ions in alumina

over the temperature range of 1600 to 1905°C. An activation energy of 114 kcals/mole (477 kJ/mole) and frequency factor (D_o) of 28 cm^2/s were reported.

Oishi and Kingery [1960] evaluated the self-diffusion coefficient of oxygen as a function of temperature in both single crystal and polycrystalline Al_2O_3 over the temperature range of 1360 to 1780°C, utilizing the ^{18}O isotope. The single crystal diffusion data is reported in Figure 8 to bracket the lower end of the oxygen diffusion rates. Experiments indicated intrinsic diffusion with a frequency factor of 1.9×10^{-3} cm^2/s and an activation energy of 152 kcals/mole (636 kJ/mole). However, there did appear to be an intrinsic diffusion transition temperature at 1650°C [Oishi et al. 1977 and 1980] which implies some structure sensitivity. The oxygen diffusion coefficient in polycrystalline aluminum oxide was ≈ 2 orders of magnitude larger than that observed for single crystals. Diffusion results which are discussed in the later sections of this text will be referenced to the Paladino et al. [1962] and Oishi et al. [1959] results given here.

Reddy and Cooper [1982] studied oxygen self-diffusion in single crystal alumina using an ^{18}O tracer over the temperature range between 1480 and 1680°C. The diffusion direction in each of the undoped crystals was along $\{10\bar{1}2\}$ and this changed to the {0001} direction when the crystal was doped with either Ti or Mg. There was a strong influence of preannealing in air on the diffusion of oxygen through these crystals. Samples which were not preannealed showed a much greater penetration of ^{18}O and a large scatter in these data. Data from this study was in fair agreement with the high-temperature data of Oishi and Kingery [1959], but an order of magnitude lower than their low-temperature results. This was attributed to the fact that Oishi and Kingery did not preanneal their samples. Reed and Wuensch [1980] studied the diffusion of oxygen through preannealed sapphire and reported rates which were an order of magnitude lower. These results could not be explained.

Reddy and Cooper reported a pre-exponential term of 2.7×10^{-2} m^2/s and an activation energy of 147.5 kcals/mole (617 kJ/mole kcals) for preannealed samples. These

data supported the transport of oxygen via a vacancy migration mechanism. Doping sapphire with titania was also found to decrease oxygen diffusion as a result of lowering the oxygen vacancy concentration via the Schottky equilibria. Doping with Mg was believed to lower the oxygen vacancy concentration; however, the diffusion rate was not lowered, and, probably because spinel precipitates formed during crystal growth.

These studies suggest that oxygen rather than aluminum self-diffusion should be rate controlling in sapphire since O^{2-} diffuses ≈ 1000x slower than Al^{3+} in the temperature range between 1400 and 2000°C. This belief is supported by the work of Lagerlof et al. [1989] in which loop annealing data support oxygen self-diffusion as the rate controlling mechanism at high temperatures. Diffusion controlled by the mobility of O^{2-} is also consistent with relatively fast cation impurity diffusion kinetics observed in doped sapphires [Lesage, 1983].

4.0 CREEP BEHAVIOR OF OTHER CANDIDATE OXIDES FOR FIBER

The objective of this review is to identify oxide materials which may possess high-temperature properties necessary for their application as continuous fiber reinforcements for metal and ceramic matrix composites. Of the ceramic fibers which currently exist, none are expected to survive repeated use in ultra-high temperature turbine applications because of their property degradation with time and temperature.

The ultimate high-strength creep-resistant fiber material for composite reinforcement is a continuous single crystal fiber which has a high melting point, high stiffness, very slow mass transport rates at temperature, and oxidation resistance. As described, the oxides appear to be the most likely class of materials to meet these requirements. Several oxides could be singled out based on melting point alone. Thoria, for instance, has a melting temperature of 3220°C and could be considered one of these "candidate" oxides; however, melting points alone are clearly not sufficient. At high-temperatures mechanical properties coupled with stability limit the application of these oxides as fibers. Very little information on the properties of ceramic fibers exist at elevated temperatures. This information is even further limited in terms of assessing oxide fibers and their time-dependent strain and creep rupture behavior.

Presented here is a review of the available information on the creep behavior of several candidate oxides as alternatives to alumina. In discussing these oxides, a direct comparison of creep rates (extrapolated to a stress level of 100 MPa) based upon known constituitive relationships as a function of temperature is made for both the polycrystalline and single crystal oxides of each class. As a reference, these rate data are plotted against the data for polycrystalline alumina and sapphire. Information on the slip system is given when applicable for single crystal materials and diffusion coefficients are cited in order to completely reference the operative creep process for each class of oxide.

4.1 Creep of Thoria

Thorium dioxide crystallizes with the fluorite (CaF_2) structure which is unique among the oxide structures in that the metal ion is larger than the oxygen ion and, partly for this reason, diffuses more slowly. Thoria's structure can be thought of as an fcc stacking of metal ions, with oxygen ions contained in the tetrahedral holes. It is a structure which exists over a wide range of compositions, usually hyperstoichiometric, with the composition ThO_{2+x}.

At low temperatures fluorite-structured oxides exhibit a substantial lattice resistance to dislocation motion as a result of the size differences of the ions. This lattice resistance dominates the mechanical strength up to about 0.4 T_M. Above 0.4 T_M, oxides with the fluorite structure creep. Seltzer et al., [1971] has reviewed the creep data for oxides with the fluorite structure and reported a strong dependence of the creep rate on the partial-pressure of oxygen in the test environment. It is believed that excess oxygen (x) stabilizes vacancies on the cation sublattice, enhancing cation diffusion. This behavior is different from the "typical" cation diffusion controlled creep behavior of most oxides.

Under lower stress conditions, oxides with the fluorite structure show a well-defined regime of diffusional flow, sometimes with a threshold stress. The creep is almost linear-viscous ($n \approx 1$), and strongly dependent on grain size. Under high stress conditions and larger grain sizes, ThO_2 exhibits power law creep ($n > 1$) with an exponent of ≈ 4.0.

Thoria is of interest because of its extremely high melting point. Melting point depends on stoichiometry and the melting point of ThO_2 is 3220°C. For this reason alone, ThO_2 has been the subject of several creep investigations. Crystals with the fluorite structure slip on systems of the type {100} <110>, as opposed to {110} $<1\bar{1}0>$ which is the primary slip system of crystal with the rocksalt structure. ThO_2 slips with a slip vector of a <110> on {001}, {011} and {111} planes [Edington and Klein, 1966: Gilbert, 1965]. However, slip on the {111} and {011} planes primarily occur at higher temperatures. The metal is the slower-diffusing ion, and therefore the one likely to control

creep and diffusional flow. The activation energy for lattice diffusion of the thorium ion in ThO_2, is 149 kcal/mole (623.4 kJ/mole) [Frost and Asby, 1982].

The compressive creep of polycrystalline ThO_2 has been studied by Morgan and Hall [1966] and Poteat and Yust [1966 and 1968]. Morgan and Hall [1966] studied 97% theoretically dense ThO_2 with 10 μm grain size in air at 55 MPa and 1465°C in compression.

Poteat and Yust [1966 and 1968] examined the compressive creep of ThO_2, with a grain size of 10 μm; they observed an activation energy of 112.3 kcals/mole (470 kJ/mole) over the temperature range of 1400 to 1800°C. This activation energy was about three-quarters of that for lattice self-diffusion of Th ions. The absolute magnitude of the creep rate is faster, by a factor of 10^4, than that predicted by the Nabarro-Herring equation, but is consistent with the Coble equation. They reported creep rates for polycrystalline ThO_2 which are given in Figure 9 as a function of temperature. The microstructure of the deformed specimens contained intergranular voids which formed from the apparent growth and coalescence of pores along the grain boundaries. It was proposed that the mechanism for creep was one involving the diffusional transport of materials accounting for the intergranular voids. Grain boundary sliding was also observed during creep of this oxide. This mechanism can be described as one of viscous flow of the grain boundaries which resulted from short range diffusion of ions along the boundary. The creep rate was dependent on the stress raised to a temperature dependent power which varied from 1.04 to 1.59. Diffusion and creep in thoria depends on stoichiometry and on purity, and because of this, a low activation energy for creep, like that observed by Poteat and Yust [1966], may imply that diffusion is extrinsic.

Corman [1989a] has studied the creep behavior behavior of single crystal ThO_2 in which the crystal was subjected to a compressive stress in a [100] alignment. A strain rate of 0.144 hr^{-1} (4×10^{-5} s^{-1}) was reported at 1750°C under a constant applied load of 100

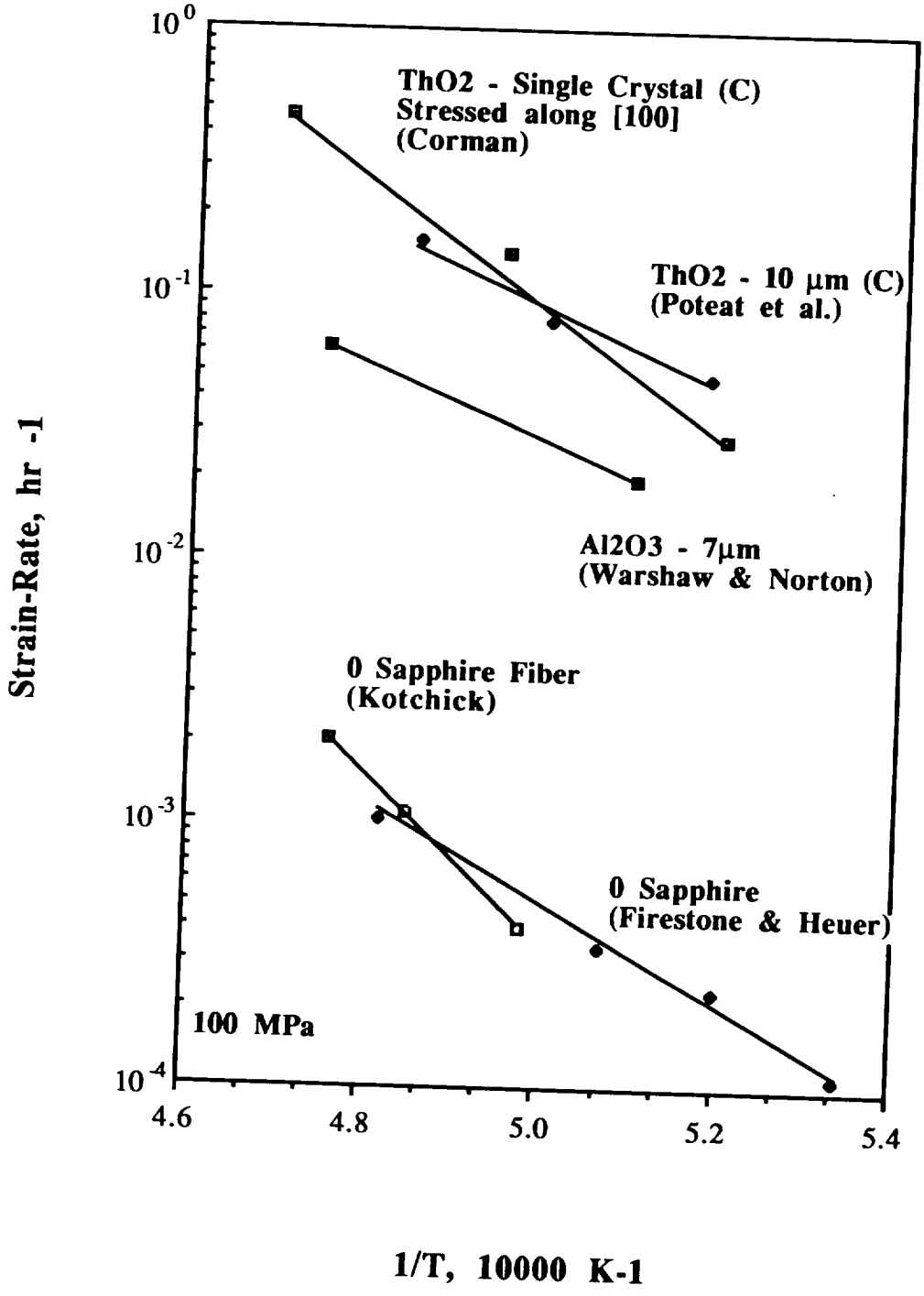

Figure 9. Influence of temperature on the creep rate of polycrystalline ThO_2 extrapolated to an applied load of 100 MPa

MPa. Corman has also reported that the stress limit for 1%/1000 hour creep rate at 1650°C was 45MPa. These data have been included in Figure 9.

Gilbert [1965] examined thin platelets of polycrystalline thoria and showed that cleavage (fracture) occurred primarily on {111} planes. Slip occurs on both {111} and {110} planes at high temperature. Campbell et al. [1959] reported that the fracture plane in polycrystalline ThO_2 was {100}. Edington and Klein [1966] examined slip and fracture in single crystal ThO_2 via etch pit and TEM techniques. The cleavage plane was indeed found to be the {111} in agreement with Gilbert [1965]. Slip was found to occur on the {110} planes.

The volume diffusion of Th in polycrystalline ThO_2 was studied by Hawkins and Alcock [1968] and was found to be independent of the oxygen pressure in the temperature range of 1600 to 2100°C. The diffusion coefficient can be described by the following equation:

$$D_{Th} = 1.25 \times 10^{-7} \exp \frac{\left(\frac{-58.8 \text{ kcals}}{\text{mole}}\right)}{RT} \text{ cm}^2/\text{sec}$$

Hawkins and Alcock's data [1968] for the diffusivities of Th in ThO_2 were approximately two orders of magnitude greater than the diffusivities determined by King [1971]. King assessed Th ion diffusion in single crystal ThO_2 in the temperature range of 1850 to 2050°C. The apparent volume diffusion coefficient as cited by King was:

$$D_{Th} = 0.35 \exp \frac{\left(\frac{-149.5 \text{ kcals}}{\text{mole}}\right)}{RT} \text{ cm}^2/\text{sec}$$

King felt that the diffusion coefficients of Th in the oxide was much lower than those previously reported, and that the diffusion coefficients reported were influenced strongly by the dislocation substructure allowing for short circuit diffusion to occur. These

data are plotted in Figure 10 and compared to the diffusion data for alumina. Thorium ion diffusion is quite slow as compared to that of Al in Al_2O_3 and appears to lower creep rates of polycrystalline ThO_2 which was not expected for a material having a fluorite crystal structure.

4.2 Creep of Zirconia

At ambient temperatures the crystal structure of zirconia is monoclinic; however, this structure transforms rapidly to tetragonal between 1000 and 1100°C. Accompanying this transformation is a large volume change which is detrimental to the materials structural application during thermal cycling; however, the ZrO_2 structure can be stabilized in the cubic, fluorite form upon the addition of several mole % of MgO, CaO, and Y_2O_3, among others. Toughness in these stabilized systems is related to the amount of tetragonal phase which acts to impede the movement of cracks through the materials by reverting back to the monoclinic phase in the vicinity of the crack.

Mecartney, Donlon and Heuer [1980] examined the deformation behavior of a single crystal of calcia-stabilized zirconia (CaSZ). The crystal studied contained 12 mol% CaO. Deformation was carried out at temperatures of 1350 to 1450°C at higher temperatures exhibit considerable ductility. Considerable climb occurred in addition to glide during deformation and as a result of the recovery little work hardening of this material was observed. The primary slip system $\{001\} < \bar{1}10 >$ was activated during the deformation of CSZ which is in agreement with slip in thoria (fluorite structure).

Previously, Ingel et al.[1982] noted that the strengths of two-phase partially stabilized zirconia single crystals (containing significant amounts of tetragonal phase, < 20 wt % Y_2O_3) considerably exceeded those for fully-stabilized cubic zirconia crystals. It was

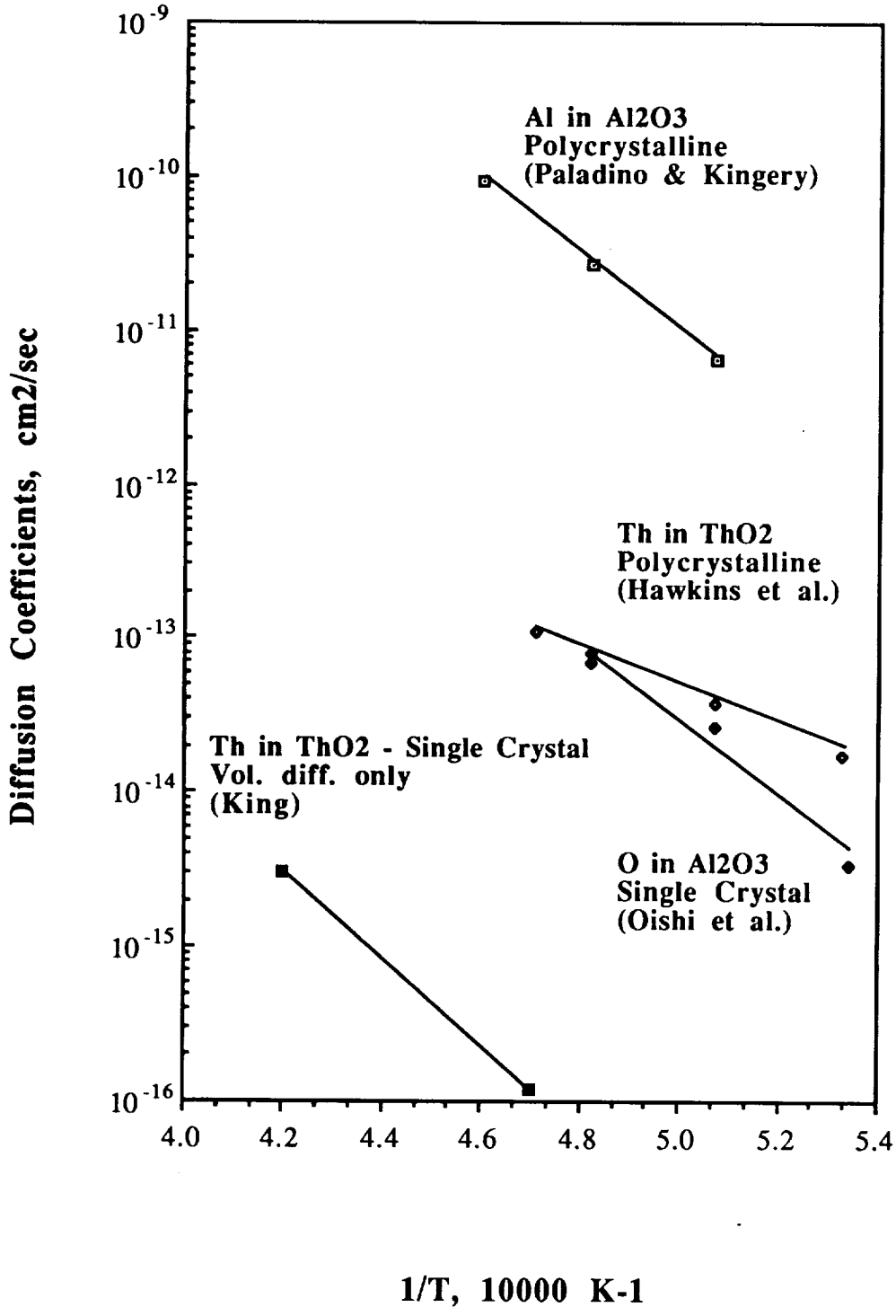

Figure 10. Influence of temperature on ionic diffusion in thoria

also noted that bend specimens of partially-stabilized (6 wt % yttria) exhibited very little plasticity at temperatures of 1500°C.

Deformation and failure mechanisms were studied for both fully and partially yttria-stabilized single crystal zirconia by Lankford [1986]. These materials lack grain boundaries and grain-boundary phases which tend to promote intergranular failure at elevated temperatures. The two compositions were 20 wt% Y_2O_3-ZrO_2 and 5 wt% Y_2O_3-ZrO_2. The former was fully stabilized and, therefore, had a cubic microstructure while the latter had a "tweed" microstructure composed of $\approx$ 50 vol% tetragonal precipitates within a cubic matrix. Specimens were tested in compression at temperatures between 23 and 1150°C. Both types of crystals exhibited plastic flow with rapid decreases in strength as the temperature was increased. No tetragonal to monoclinic transformations occurred during the deformation of the partially stabilized single crystal. The plastic deformation observed was attributed to dislocation activity alone. Plastic flow in the partially stabilized zirconia was found to be planar occurring on the {100} slip system; whereas, slip in the cubic stabilized zirconia was wavy and occurred on the {111} and secondary systems.

Deformation of single crystal cubic zirconia was also examined by Dominguez-Rodriguez, Lagerlof and Heuer [1986]. The orientation chosen for analysis favored {001} <110> slip. It was found that in addition to this slip system, slip on {111} <110> could also be activated. Activation energies were strongly influenced by the Y_2O_3 concentration. For instance, the activation energy for deformation of a crystal containing 9.4 mol % Y_2O_3 was 154.5 kcals/mole (646.4 kJ/mole). This activation energy increased to 191.4 and 225.8 kcals/mole (800.8 - 944.7 kJ/mole) upon the addition of 12 and 18 mol % Y_2O_3, respectively. The {001} <110> slip system was previously found to be the easy slip system in a single crystal CaSZ [Mecartney, Donlon, Heuer, 1980]. The experiments were performed at 1400°C at a strain rate of 4.7×10^{-2} hr^{-1} (1.31×10^{-5} s^{-1}).

Carter et al. [1988] proposed that creep in single crystal cubic zirconia probably occurs primarily as a result of the redistribution or motion of dislocations to lower energy

configurations, rather than further dislocation generation. From this they argued that it would be more difficult to generate dislocations in cubic YSZ than in cubic CaSZ, but that subsequent dislocation motion is easier in cubic YSZ than in cubic CaSZ.

Corman [1989b] examined the deformation behavior of 9.5 mol % yttria-partially stabilized single crystal zirconia (YSZ) for the temperature and stress ranges of 1650 to 1850° C and 12.5 to 100 MPa. Crystals were stressed along the [111] or [110] slip direction. He found that both of these alignments of the compressive load activated the primary slip system {100} <011>. The stress exponent for this deformation was found to be ≈4 and the activation energy was 104.2 kcal/mole (436 kJ/mole). This activation energy can again be compared to the lattice diffusion of cations (e.g. Zr in calcia-stabilized zirconia = ≈92 kcals/mole or Ca in CSZ = 100 kcals/mole [418.4 kJ/mole]). These results suggested a glide controlled by climb process where limited cation diffusion controlled the climb process. A similar yttria stabilized zirconia crystal was loaded along the [100] direction [Corman, 1989b] and in this case, the primary slip system was not activated. Creep occurred via slip on a secondary system, which may be either {110} $<\bar{1}10>$ or {111} $<\bar{1}10>$. The creep rate controlled by slip on this secondary slip was significantly lower than the strain-rate reported by MeCartney et al. [1980] for a fully stabilized single crystal zirconia having a fluorite structure.

Several researchers have performed studies of the creep behavior of polycrystalline zirconia. For instance, Straviolakis and Norton [1950] examined the torsional creep characteristics of calcia-stabilized zirconia under a load of 25 MPa and obtained a creep rate of 21 x 10^{-5} rad/in-hr. at 1300°C. St. Jacques and Angers [1972 and 1973] studied the compressive creep behavior of an 18 mole % CaO stabilized ZrO_2 in the temperature range between 1200 and 1400°C at stresses of 3.5 to 27.5 MPa. The zirconia studied was polycrystalline having grain diameters between 7 and 29 μm. A linear relationship was obtained between the creep rate and stress level applied. This behavior normally suggests diffusionally controlled creep [Nabarro, 1943; Herring, 1950; Coble, 1963; Grifkins,

1968; Ashby et al., 1970]; however, at higher stresses (~27.5 MPa) the creep rates are somewhat greater than those expected from the extrapolation of the rates obtained at lower stresses. This result was interpreted as resulting from a non-Newtonian creep at the higher stresses and has been shown by Heuer et al. [1970] to be common in instances where grain boundary sliding is the rate controlling mechanism. The activation energy for the creep of a CaO partially stabilized zirconia (Ca-PSZ) was 94 kcals/mole (393.3 kJ/mole), normalized for the grain size dependence [St. Jacques et al., 1972]. Examination of the crept Ca-PSZ specimen revealed voids along the grain boundaries. This behavior was also found to be true for polycrystalline ThO_2 (~10μm) [Poteat and Yust], polycrystalline Al_2O_3 (≤ 40μm) [Folweiler, 1961] and yttria- and scandia-stabilized zirconia [Evans, 1970]. The activation energy for the creep of CaPSZ in the St. Jacques et al. study was near that for the self diffusion of Ca (100.2 kcals/mole [419.2 kJ/mole]) and Zr (92.5 kcals/mole [387.0 kJ/mole]) in ZrO_2 stabilized with 16 mole % CaO; however, it was not clear whether volume or grain boundary diffusion controlled the creep of Ca by grain boundary sliding. The strain-rates for both fully- and partially-stabilized zirconia are given in Figure 11 as function of temperature. Ionic diffusion coefficients are given in Figure 12 and are compared to those for Al_2O_3.

Evans [1970] studied yttria- and scandia-partially stabilized zirconia in compression over the temperature range of 1163 to 1535°C and stress range of 4.1 to 7.1 MPa. The activation energies associated with creep for scandia-, yttria and heat-treated scandia-stabilized zirconia were 89, 86 and 74 kcals/mole (372.4 - 309.6 kJ/mole), respectively. The creep rates were found to be inversely proportional to the square of the grain sizes. Scandia-stabilized zirconia had a stress exponent of 1.5 while the yttria-stabilized zirconia had two regimes with n=1 and 6. The two regimes observed for the stress dependence in the yttria-doped zirconia were interpreted as cation diffusion control of the creep when n=1 with the coalescences of voids and propagation of cracks when n=6. In this treatment it was argued that n = 1.5 represents a transition region.

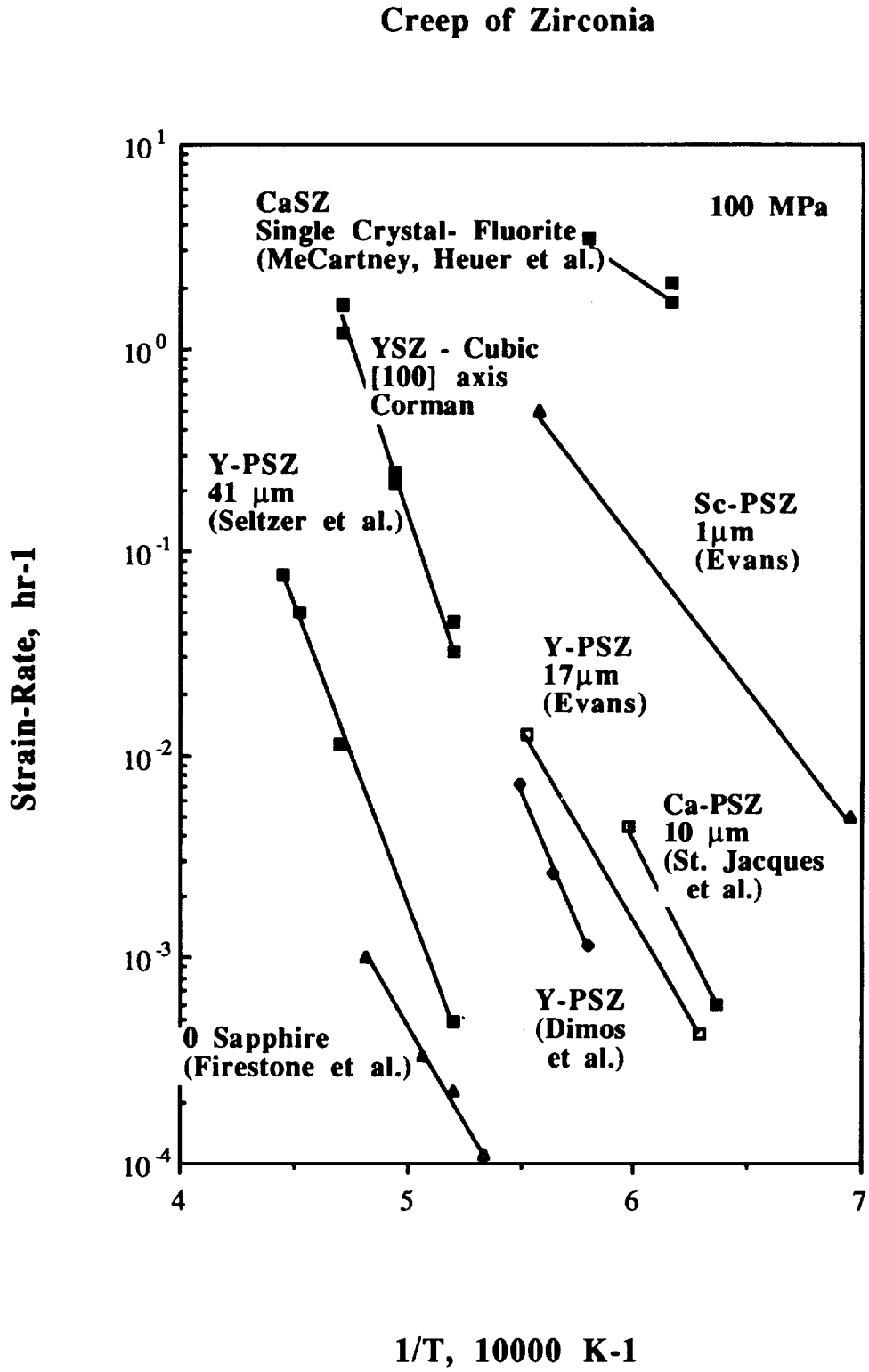

Figure 11. Influence of temperature on the creep rates of fully stabilized and partially stabilized zirconia

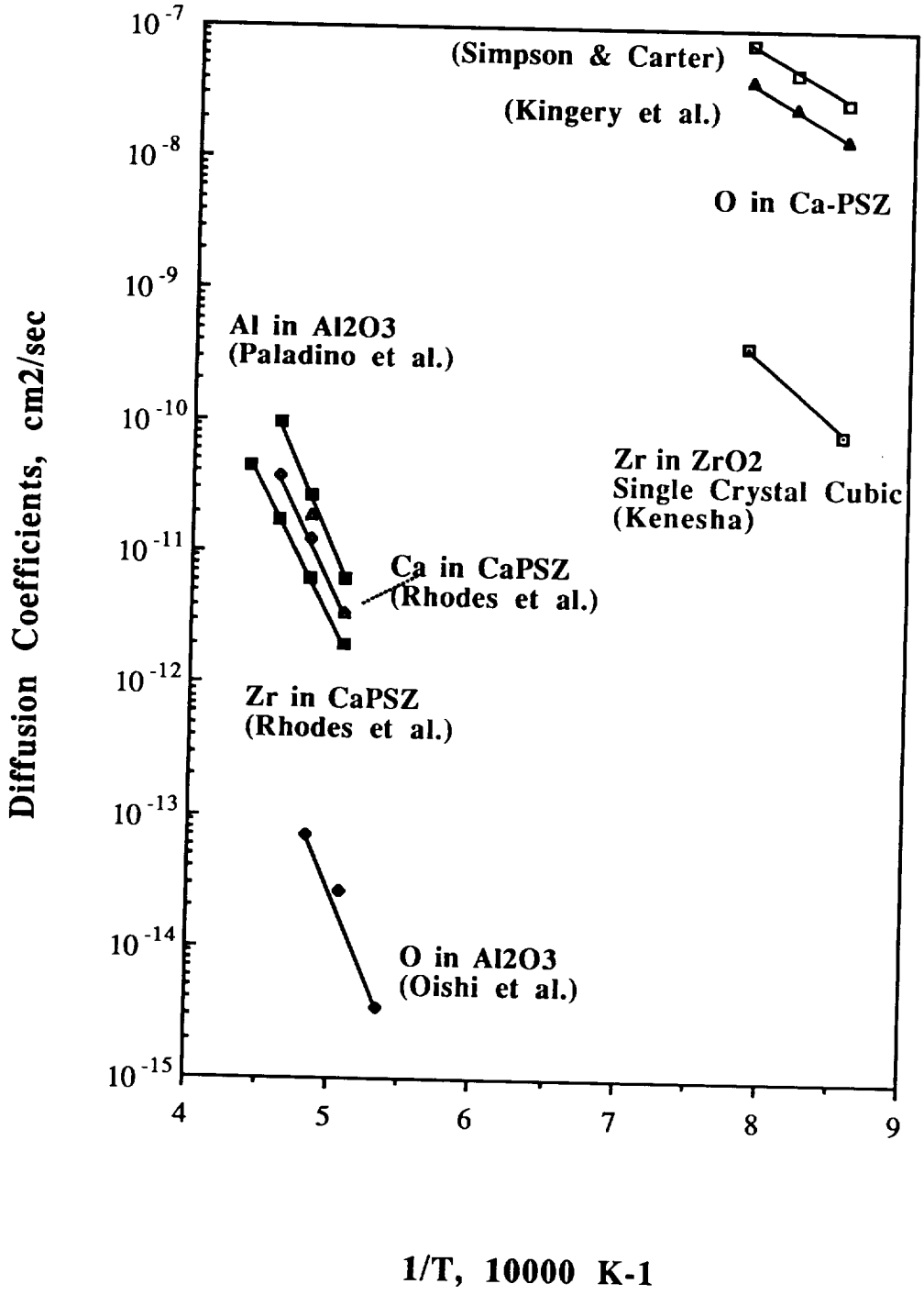

Figure 12. Influence of temperature on cation and anion diffusion in zirconia

Seltzer and Talty [1975] examined the high-temperature (up to 2000°C) compressive creep of Y_2O_3-stabilized ZrO_2 (Y-PSZ). Here again, a stress exponent of 1.5 was found for fine-grained samples (15-20μm) tested over a temperature and stress range of 1400 to 1535°C and 5.6 to 53 MPa. The reported activation energy was 127 kcals/mole (531.4 kJ/mole). No significant differences were found in the creep behavior for the high density Y-PSZ samples having different impurity contents and pore sizes. The lack of influence of the impurities on creep suggested that the atomic point defects which control the diffusion limited processes dictating high-temperature creep were not affected by aliovalent impurities.

From the Seltzer and Talty study, the activation energy for the creep of Y-PSZ was ≈128 kcals/mole (535.5 kJ/mole). Self-diffusion has not been studied in Y-PSZ; however, Rhodes and Carter [1966] measured cationic self-diffusion in calcia-stabilized zirconia from 1700 to 2150°C and found the lattice self-diffusion coefficients to be:

$$D_{Ca} = 0.444 \exp \frac{\left(\frac{\text{-100.2 kcals}}{\text{mole}}\right)}{RT}, \text{cm}^2/\text{sec}$$

$$D_{Zr} = 0.0.35 \exp \frac{\left(\frac{\text{-92.5 kcal}}{\text{mole}}\right)}{RT}, \text{cm}^2/\text{sec}$$

These diffusion coefficients for zirconia are plotted in Figure 14 over the temperature range of interest. Rhodes and Carter found that the Zr diffusivities were independent of CaO concentration for Zr stabilized with 12 and 16 mole % CaO. Simpson and Carter [1966] measured the diffusion of oxygen in calcia-stabilized zirconia between 800 and 1097°C and reported the diffusion coefficient to be:

$$D_o = 0.018 \exp \frac{\left(\frac{\text{-31.2 kcals}}{\text{mole}}\right)}{RT}, \text{cm}^2/\text{sec}$$

The measured oxygen diffusion coefficients were the same for both single and polycrystalline samples and these data agreed with those values calculated from electrical conductivity with an oxygen transport number of unity.

The data of Kingery et al. [1959] regarding oxygen ion mobility in cubic calcia-stabilized zirconia was corrected by Simpson and Carter [1966] and the diffusion coefficient was expressed as:

$$D_o = 6.9 \times 10^{-3} \exp \frac{\left(\frac{-30.4 \text{ kcals}}{\text{mole}}\right)}{RT}, \text{ cm}^2/\text{sec}$$

These diffusion results show the cation diffusion to be 10^6 slower than oxygen diffusion and support the argument that creep is controlled by cation diffusion. Kenesha [1971] reported an activation energy of 189.7 kcals/mole (793.7 kJ/mole) and a frequency factor of 2.34×10^{-2} cm^2/sec for a fully stabilized cubic ZrO_2. These data are also given in Figure 12.

Dimos and Kohlstedt [1987] also found that the steady-state creep rate in fine-grained yttria-stabilized (25 mole %) zirconia was roughly proportional to the applied stress and strongly dependent on the grain size. Again, this indicated a deformation process controlled by a diffusional creep mechanism. The stress exponent (n) was 1.2 and the activation energy for creep was ≈131.5 kcals/mole (550.2 kJ/mole). Both suggest cation lattice diffusion as the rate controlling process. This result is further supported by a grain size exponent m = 2.2 which indicates creep occurs primarily via a Nabarro-Herring mechanism. Cation diffusion through the lattice was reported to be:

$$D_L = 3.0 \times 10^{+3} \exp \frac{\left(\frac{-134.8 \text{ kcals}}{\text{mole}}\right)}{RT}, \text{ cm}^2/\text{sec}$$

This value agrees closely with that reported by Rhodes and Carter [1966].

4.3 Creep of Spinels

Spinels form a large class of oxides with the general formula AB_2O_4. They crystallize in a cubic structure which can be thought of as a combination of the rock-salt and the zinc blende structures. The unit cell of $MgAl_2O_4$ was first determined by Bragg [1915] and Nishikawa [1915], and consists of 32 oxygen ions in a slightly disturbed f.c.c. array with 8 magnesium (A) ions in tetrahedral sites and 16 aluminum (B) ions in octahedral sites. The oxygen ions are close packed in fcc stacking, with the cations contained in the octahedral and tetrahedral intercises. In normal spinels, the A^{2+} ions are contained in the tetrahedral holes, and the B^{3+} ions are in octahedral holes. Among the normal aluminate spinels are $MgAl_2O_4$, and those obtained on replacing Mg by Fe, Co, Ni, Mn or Zn. Certain ferrites, too have the normal spinel structure, among them are Zn Fe_2O_4 and $CdFe_2O_4$. The inverse spinel structure is adopted by many other ferrites, notably $MgFe_2O_4$ and those obtained on replacing Mg by Ti, Fe or Ni. Spinels are often used as refractories and their high-strength and transparency makes them attractive for windows which must resist heat, impact or abrasion. Stoichiometric $MgAl_2O_4$ has a melting point of 2135°C and exists over a wide range of composition at elevated temperatures. When Al_2O_3-rich spinel is slowly cooled under equilibrium conditions the excess Al_2O_3 is precipitated. It is possible to retain the Al_2O_3 in supersaturated solid solution by quenching, and is common in Verneuil-grown crystals.

The mechanical behavior of this class of oxide closely resembles that of α-alumina. Their structures are closely related, they show high lattice resistance and retain their strength to high homologous temperatures (0.5 T_M and above). Diffusion rates in these materials vary somewhat with temperature but are also comparable to alumina.

Magnesium aluminate spinel, $MgAl_2O_4$, is cubic with a lattice parameter of 8.08 Å. The easiest slip system has a Burger's vector of a/2 <110> which is dissociated into a/4

<110> partials. The slip plane in crystals of the spinel type is the {111} plane which is analogous to the basal plane of corundum, the nearly close packed oxygen plane.

Hornstra [1960] first attempted to define the deformation of spinel from a theoretical standpoint. He predicted that dislocation glide would occur parallel to the close-packed {111} oxygen anion planes and along the close-packed <110> directions.

The creep of stoichiometric $MgAl_2O_4$ was investigated by Palmour [1966] in 4 point bend over a temperature range between 1450 and 1700°C. The stress exponent varied from less than 2 to ≈5 with an average value of ≈2.7. From these data an activation energy of 214 kcals/mole (895.4 kJ/mole) was calculated and a mechanism of dislocation climb was proposed as the rate-controlling mechanism.

Hornstra's earlier predictions were confirmed by the work of Newey and Radford [1968] in which they deformed single crystal Verneuil grown spinels of compositions 1:1 and 1:3 ($MgAl_2O_3$) in compression. Slip on the {110} <110> system was also observed, and in fact it was the primary slip system in the 1:2 composition. The controlling slip processes were again suggested to be dislocation climb which operated over the temperature range between 1350 and 1800°C.

Another single crystal composition was examined by Donkhan et al. [1973], a 1:1.8 ($MgAl_2O_3$). These researchers found that deformation of the single crystal was indeed controlled by dislocation climb and this occurred on the {110} <110> slip system. The stress dependence was found to be ≈3.9 and activation energy was 122 kcals/mole (510.4 kJ/mole). Hwang, Heuer, and Mitchell [1975] studied the creep behavior of single crystal Czochralski grown $MgAl_2O_4$ at stresses of ≈200 MPa ($\dot{\varepsilon} = 0.504\ hr^{-1}$ [$1.4 \times 10^{-4}\ s^{-1}$]) at 1810°C. Slip occurred on the {111} <110> system in this stoichiometric spinel. In nonstoichiometric spinel the preferred plane changes to {110}.

The study of the plasticity of alumina spinel solid solutions has allowed researchers to investigate "metallic" slip {111} <110> versus "ionic" slip {110} <110> in crystals since both have been produced in this oxide as a function of the stoichiometry or molar

ratio of MgO to Al_2O_3. Mitchell et al. [1976] probed the transition from {111} to {110} slip in spinel single crystals when the MgO:Al_2O_3 ratio was decreased. These workers proposed that the octahedral cation vacancies present in nonstoichiometric spinel diffuse to dislocations during deformation and favor {110} slip. The data of Newey and Radford [1968] and Mitchell et al. [1976] showed that {111} slip was characteristic for stoichiometric compositions. The high strength of the stoichiometric crystals was attributed to a large Peierls force on {111} planes, and it was assumed that a still larger force was required to slip the {110} planes. The transition to {110} slip as the stoichiometric composition changes from 1:1 to 1:2 could be attributed to a steeper lowering of the Peierls barrier on the {110} planes than on {111} planes, owing to the diffusion of the excess cation vacancies.

The yield stress was found to be high in spinel and comparable to that for sapphire oriented to suppress both basal and prismatic slip. For instance, at 1790°C the yield stress was 215 MPa [Mitchell et al., 1976]. Initial work-hardening rates are high ($\approx\mu/70$) except at the highest deformation temperatures (1895°C). Work softening sets in at the higher strains which may be due to recovery by climb. The work hardening rate in spinel is several times larger than that for sapphire deformed by basal slip. The reason for this is that the work hardening mechanism in sapphire is the interaction of dislocations on parallel slip planes to form dipoles, which is a less effective hardening process than the interaction with dislocations on intersecting secondary planes (as is the case with spinel).

Highly non-stoichiometric (1:3) crystals deformed plastically at temperatures 300°C below that for the stoichiometric crystals. A yield stress was detected at 0.73 T_M in the 1:1 composition and at 0.64 T_M in the 1:3 composition, where T_M is the particular solidus temperature [Newey and Radford, 1968]. Easier deformation of these crystals was attributed to the defect structure. Figure 13 presents the creep rates for several stoichiometric or nearly-stoichiometric spinels plotted along with polycrystalline and single crystal Al_2O_3 (all data were extrapolated to a 100 MPa stress level).

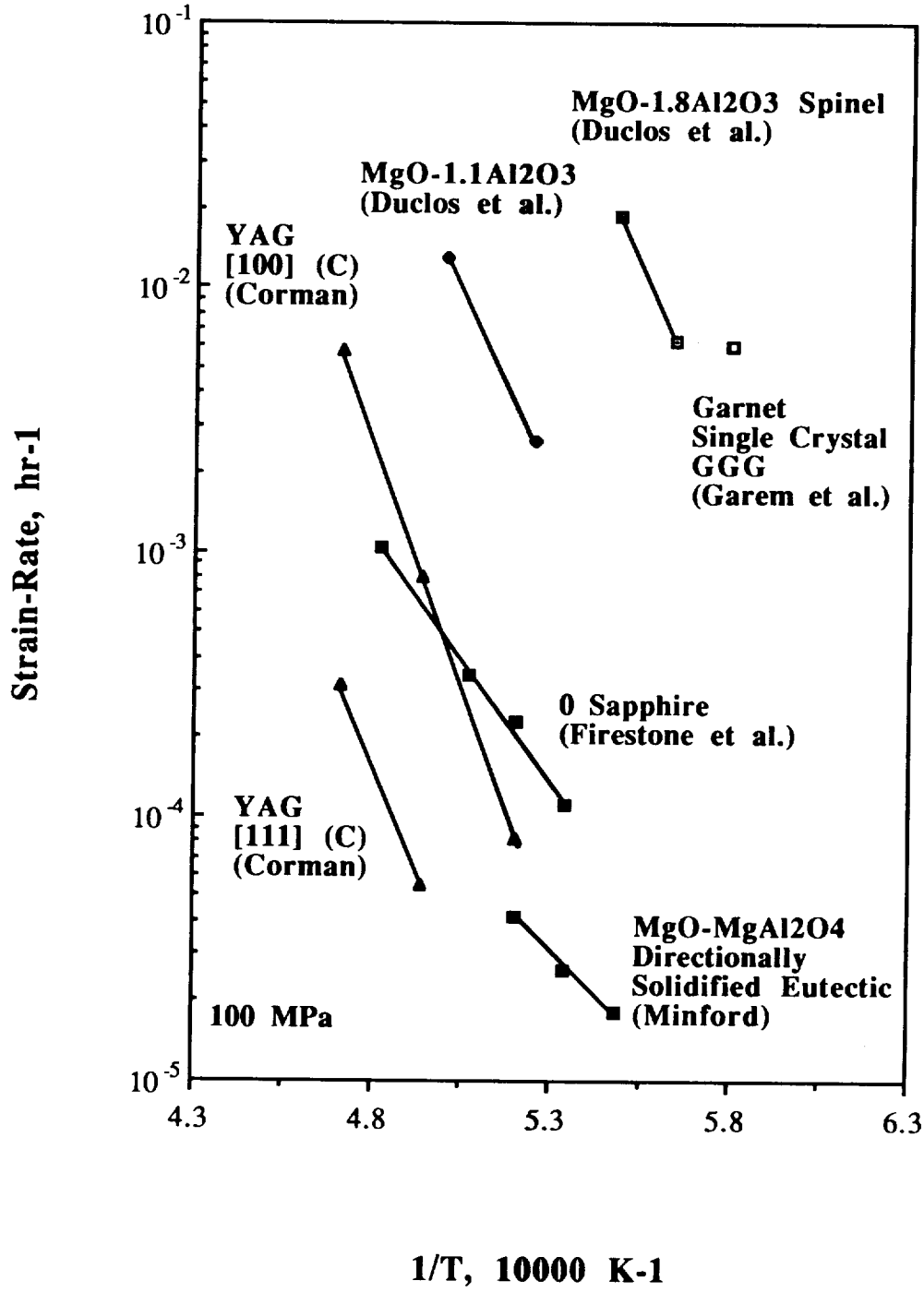

Figure 13. Influence of temperature on the steady-state creep rates of spinel and garnet

The creep behavior of a nearly stoichiometric spinel 1:1.1 ($MgO \cdot nAl_2O_3$) was investigated by Duclos et al. [1978] in compression along a [001] axis at temperatures of 0.77 to 0.83 T_M and loads between 88 and 120 MPa. Their results indicated that {100} <110> slip system was activated at a very early creep stage. No evidence of {111} slip planes were observed; however, for the case of uniaxial stress along the of [110] direction, {111} slip was observed. It was suggested that deformation continued under these experimental conditions after slip was inhibited (sessile splitting of dislocations) by pure climb strain alone. The mechanism of climb-creep accounts for the experimental observed creep rates and for the dependence on stoichiometry (which was shown to influence the pre-exponential term).

Duclos et al. [1978] argued against considering the {111} <110> slip as the easiest slip system for stoichiometric spinel as it had previously been cited in the literature [Radford and Newey, 1968] [Mitchell, Hwang, and Heuer, 1976]. Duclos et al. [1978] showed that {110} slip is favored for Schmid factors of 0.5 and 0.41, respectively (ratio of 1.22). These values support a slightly higher lattice resistance on the {111} plane.

Duclos [1981] deformed <111> axial aligned with the compression direction spinel specimens of the composition 1:1.8 at a constant strain rate over the temperature range of 1420 to 1630°C. Deformation of these specimens was found to be controlled by dislocation climb rather than the expected glide. The stress exponent was found to be 3.7 ± 0.1 and activation energy of 133.8 kcals/mole (559.8 kJ/mole). No work hardening was observed beyond yielding for this compression axis. The same composition stressed along the <100> or <110> compression orientations showed considerable work hardening. Slip traces were observed for specimens of the <100> and <110> orientations, but not however for the <111> orientation. These results also suggested dislocation climb. A steady-state creep rate was calculated based upon the Nabarro-Weertman model [1955] for pure climb controlled by oxygen diffusion, and it agreed well with the experimentally determined creep rates. Deformation of <111> samples proceeded as edge dislocations (the least mobile

dislocation) were produced and the strain rate resulting from their climb became high enough to accommodate the imposed strain rate; this caused the stress to drop making further glide more difficult. Duclos's results suggested that, when dislocation glide was hindered, non-stoichiometric spinel could exhibit a mechanical behavior as hard as stoichiometric, and that the higher plasticity observed for the non-stoichiometric composition results from factors favoring a higher glide mobility.

Directionally solidified eutectic melts were investigated by Minford [1977] for creep behavior. One of the key cubic compositions in this study were a MgO - $MgAl_2O_4$ system in which all the planes and directions of this eutectic phase was parallel and the [111] direction was parallel to the solidification direction. The creep behavior of this directionally solidified eutectic with colony and grain structures was examined in 4 point bend and the data is given in Figure 14 (extrapolated to 100 MPa). The extremely low creep rates observed for this system were attributed by the author to the crystallographic orientation of the eutectic phases. Dislocations were thus impeded by the existing fibrous phases preventing any extensive plastic deformation of this "in-situ" developed composite. The deformation process of the directionally solidified MgO - $MgAl_2O_4$ eutectic with colony structure had a stress exponent of approximately one and an activation energy of 27 ± 5 kcals/mole (113 kJ/mole) over a temperature range of 1550 to 1650°C and 69 to 124 MPa. Minford also found that the creep resistance of the grain structure was greater than that of the colony structure. The overall creep behavior of this eutectic was believed to be controlled by a void nucleation and growth mechanism. The creep rates, however, for this specimen are suspect because the stress distributions in the bend specimens are complex and were not well defined in these experiments.

Oxygen is the slowest diffusing species in single crystal spinel [Ando and Oishi, 1974; Reddy and Cooper, 1981]. The self-diffusion coefficient of the oxygen ion was smaller by several orders of magnitude than that of the magnesium ion over the temperature

range form 1432 - 1739°C. The self-diffusion coefficients over the temperature range studied in stoichiometric $MgAl_2O_4$ can be described by:

$$D_o = 8.9 \times 10^{-1} \exp\left(\frac{-105 \text{ kcals/mole}}{RT}\right) \text{cm}^2/\text{sec}$$

Excess alumina added to the spinel does not affect the self diffusion of the oxygen ion and , hence, the concentration of defects associated with the oxygen ion. As previously described, the oxygen ions in $MgAl_2O_4$ are close-packed. This structure is similar to MgO and α-Al_2O_3, in which oxygen ions are in a nearly close-packed state and cations are in octahedral sites. Because of this [Ando and Oishi, 1974] anticipated a similarity in the diffusion behavior of the oxygen ions in these three crystals. It was found that activation energy for O diffusion in $MgAl_2O_4$ (105 kcals/mole [439.3 kJ/mole]) was twice that of extrinsic diffusion in α-Al_2O_3 and MgO and nearly that of intrinsic diffusion in Al_2O_3 (152 kcals/mole [636 kJ/mole]) [Oishi and Kingery, 1960]. It was also found that the activation energies for sintering $MgAl_2O_4$ are close to that for the self-diffusion of the O ion [Bratton, 1969]. The work of Ando and Oishi [1974] confirms that the sintering of $MgAl_2O_4$ is by a volume diffusion mechanism, and that the rate controlling species is oxygen which has the smallest self-diffusion coefficient. The data for ion diffusion in spinel is given in Figure 14.

Oxygen is the biggest ion in this structure; however, evidence exists which suggests that the diffusion of the cation can limit the creep rate as it does in Al_2O_3 and this implies that similar complications are experienced by spinel.

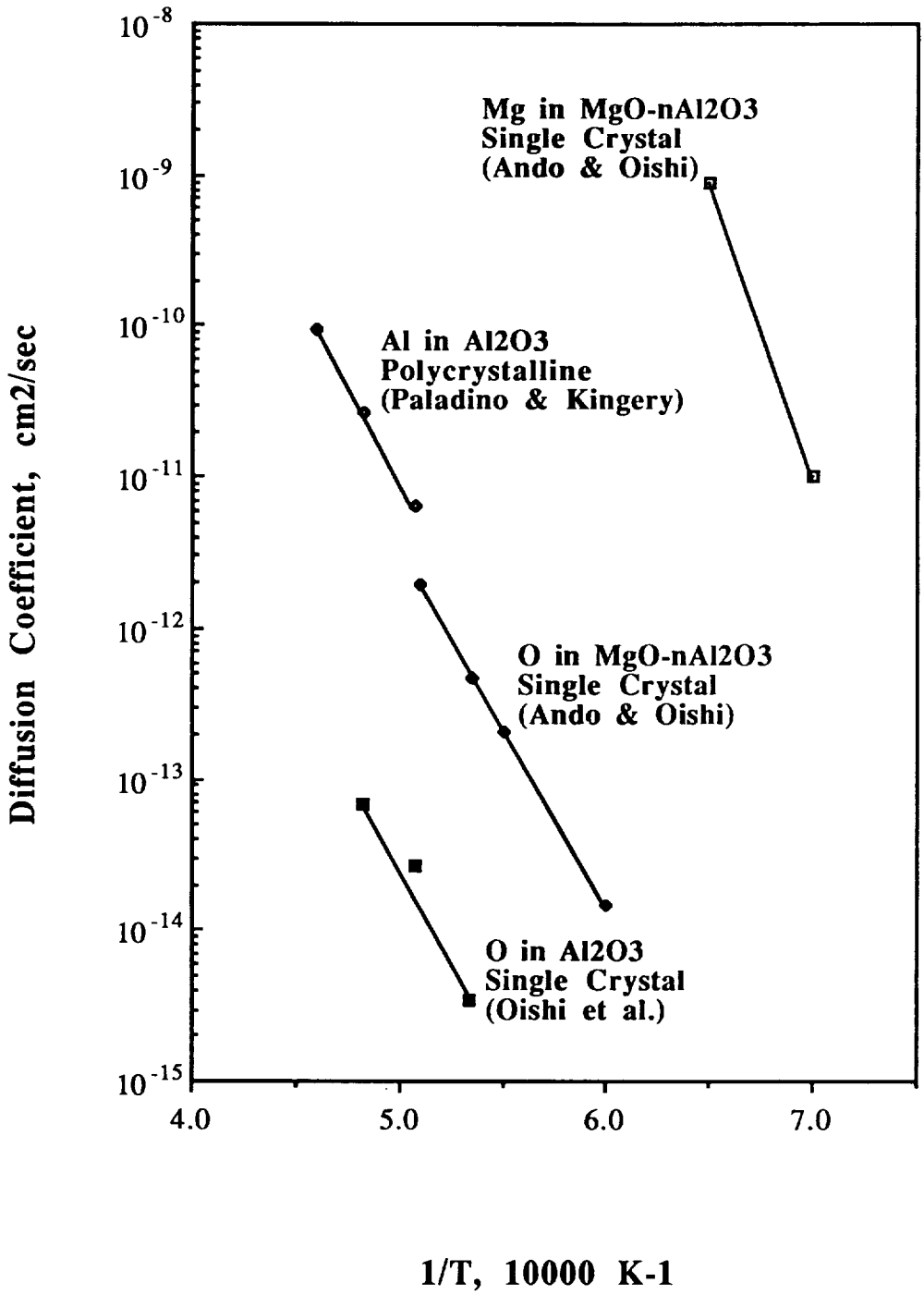

Figure 14. Influence of temperature on cation and anion diffusion in single crystal spinel

4.4 Creep of Garnets

The garnet structure is a body-centered, complex cubic structure in which the largest cations occupy dodecahedral interstices in the oxygen sublattice and other cations are in tetrahedral and octahedral positions. In this complex cubic structure there is no close packed plane in the oxygen sublattice. The garnet structure is expected to exhibit good mechanical properties since the dislocations have to overcome high lattice friction stresses [Garem et al., 1982].

Garnet oxides are known to have very good mechanical properties at high temperatures. This is the case for synthetic garnets such as $Y_3Fe_5O_{12}$ (YIG), $Gd_3Ga_5O_{12}$ (GGG) and $Y_3Al_5O_{12}$ (YAG) as well as natural garnets. Some work has been conducted on the plastic properties of these materials because of the use of these materials in the electronic industry in applications where they are used as bubble memory devices (GGG) or as insulators (YIG). Rabier and Garem [1984] investigated the plastic deformation of single crystal GGG in compression between 1300 and 1500°C (0.79 - 0.92 T_M). To induce deformation high stresses were used (≈200MPa) and low strain-rates resulted ($\dot{\varepsilon}$ = 3.3×10^{-6} s^{-1} at 1450°C). They observed a glide anisotropy. The orientation of the compression axis was <100> or <110> and the activated glide planes were {110} or {112}, respectively. The primary slip system is unknown; however, this slip behavior is analogous to that of bcc metals which is attributed to the sessile glide dissociation of a/4<111> screw dislocation. In the garnet structure it is believed that a high-temperature substructure is built in at low strains and is composed of segmented glide loops and climb loops.

Garem, Rabier, and Veyssiere [1982] investigated the slip systems in gadolinuim gallium garnet single crystals in compression in air at 1400°C and 1550°C. Slip was activated on the {110}, {112}, and {123} planes as a function of the compression

orientation. The single crystals had extremely low dislocation densities ($1cm^{-2}$) and a melting temperature of 1720°C.

It was found that in order to induce deformation, high stresses were required even at temperatures close to the melting point of GGG (0.92 T_M). This high resistance to deformation is a general trend for crystals with the garnet structure. TEM observations of crept samples support a mechanism of creep controlled by high lattice friction stresses which oppose the movement and multiplication of dislocations. The strain-rate of Garem et al. [1982] for GGG is plotted with the spinel data for reference in Figure 13.

Very recent work of Corman [1990] indicates that garnet structures may indeed be promising fiber candidates because they possess a high resistance to creep . This resistance is attributed to the complex garnet structure with accompanying large lattice parameters which limits dislocation motion. The lowest creep rate was found for crystals in which the applied stress was aligned in the [111] direction and the highest for the [100] alignment [Corman, 1990]. The steady-state creep rate of the [111] aligned garnet is given in Figure 14. The stress exponent for garnet stressed in the [111] direction was 5.68. It was not clear whether this alignment resulted in the activation of a secondary slip system. The role of diffusion in the deformation of garnet was also unresolved since the activation energy was 169 kcals/mole (710 kJ/mole) which is more than twice that for the diffusion of O in YAG which is 71 - 77.7 kcals/mole (297-325 kJ/mole) [Haneda et al., 1984]. There are no reported values for cation diffusion in the garnet structure. The creep mechanism and active slip systems for YAG are still uncertain. The creep mechanism and active slip systems for YAG are still uncertain.

4.5 Creep of Beryllium Oxide

Beryllium oxide (BeO) is the only oxide of beryllium and shows no detectable variation from stoichiometric composition. It possesses high chemical stability and has been studied for electrical insulating and thermal conducting applications. BeO also possesses excellent properties as a moderator for thermal nuclear reactors since Be and O nuclei have low scattering cross section for thermal neutrons.

BeO possesses two polymorphs, a low temperature form (α-BeO) which is stable to 2100°C and a high-temperature form (β-BeO) above 2100°C. The α-BeO has a hexagonal (wurtzite) structure formed by the interpenetration of hexagonal close-packed lattices of oxygen and beryllium. This displacement of the lattices relative to one another is not symmetrical, giving a structure which is electrostatically polar in the c-axis direction (Figure 15). One basal plane $(000\bar{1})$ is terminated by oxygen atoms (a negative surface) while the other (0001) is terminated by beryllium atoms (a positive surface). The β-BeO has a tetrahedral coordination (zinc blende structure) and is based on the cubic close packing of the anions. In the transformation of α-β, the α-BeO c-axis increases by 6.8% and the a-axis dimension decreases by 0.8% [Smith, 1964].

Austerman [1964] initiated a study to fabricate and investigate the properties of α-BeO single crystals. In this study he used a molten oxide (Li_2MoO_4-MoO_3) as a solvent flux with a steady-state thermal gradient method to form the crystal. This process reportedly can be tailored to control the growth rates and crystal purity. The lattice constants for the crystals grown by Austerman were found to be:

$$a_o = 2.69783 \pm 0.00015\text{Å}$$

$$c_o = 4.3777 \pm 0.0005\text{Å}$$

$$c/a = 1.6227 \pm 0.0002\text{Å}$$

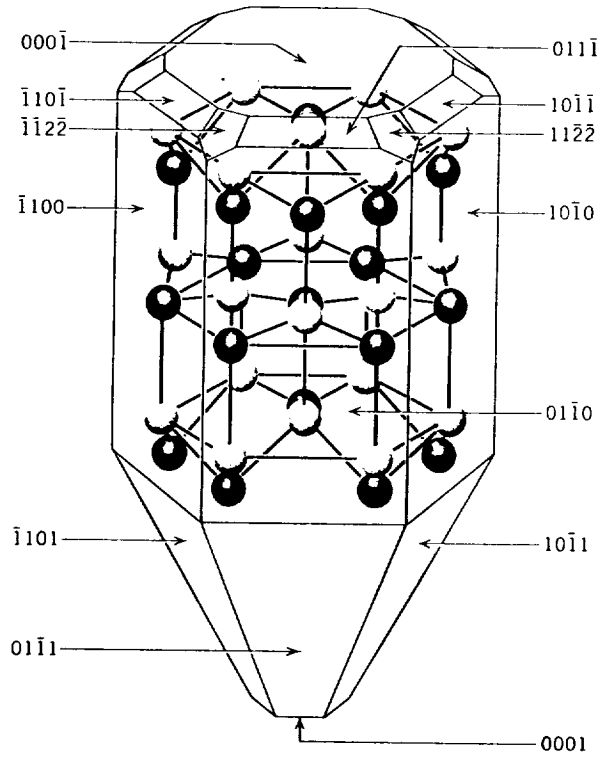

Figure 15. Polar lattice structure of beryllium oxide [Rothman, 1965]

when examined via CuK_α radiation = 1.5405Å. These values agree with the lattice values of Bellamy, Baker, and Livey [1962] for pure polycrystalline BeO. From this study it is clear that under controlled growth conditions (below the congruent melting point), single crystals of BeO can be made; however, no effort was undertaken to examine the mechanical behavior of single crystal BeO. Studies directed toward examining the creep behavior of BeO have all been conducted on polycrystalline materials.

Chang [1959] examined the high temperature tensile creep and anelastic behavior of polycrystalline BeO and Al_2O_3 having grain sizes of 25-30 μm. Chang reported activation energies for steady-state creep as 200 kcals/mole (836.8 kJ/mole) for Al_2O_3 and 120 kcals/mole (502.1 kJ/mole) for BeO [1959 and 1963]. These values reported for the activation energy associated with grain boundary relaxation and steady state creep were approximately equal to those for self-diffusion of the cation. In other words, the activation energy for self-diffusion in BeO was 115 kcal/mole (481.2 kJ/mole) [Chang, 1959] and in Al_2O_3, 180 kcals/mole (753.1 kJ/mole) based on the sintering data of Coble [1958]. Chang correlated the steady state creep rates for BeO with those calculated according to the Nabarro-Herring model for vacancy controlled diffusional creep. Using the self-diffusion data for Be, he proposed that this mechanism is the rate controlling mechanism for creep in polycrystalline BeO in the temperature range studied (1400 - 1745°C).

Austerman [1964b] using radioactive Be^7 and nonradioactive O^{18} isotopes studied self-diffusion in polycrystalline BeO. His data indicated that cation diffusion through the lattice via vacancies occurred without significant grain boundary diffusion. Results from these experiments also indicated that there was little or no anisotropy of cation diffusion in single crystals. Oxygen, on the other hand, diffuses in polycrystalline BeO, primarily through grain boundaries.

From the strain rate measurements of Vandervoort and Barmore [1963] the diffusion coefficient was computed, and the data for creep were comparable to the diffusion coefficient for Be through BeO. The activation energies for creep in both compressive and

tensile experiments, and for self-diffusion below ≈1700°C all lie in the range of 90-120 kcal/mole (376 - 502 kJ/mole). However, at temperatures in excess of 1700°C the activation energies drop off to a range of 30-70 kcals/mole (125.5 - 292.9 kJ/mole).

Figure 16 gives the experimental values for the creep of BeO. These creep data are plotted along with those values calculated from a vacancy-diffusion mechanism of the Nabarro - Herring type. The model which was used accounted for conditions under which the grain-boundaries were completely relaxed. Herring has previously shown that under these circumstances, the steady-state tensile creep rate is related to the tensile stress, σ as follows [Herring, 1950].

$$\dot{\varepsilon} = \left(\frac{10}{3}\right)\left(\frac{4\pi}{3V}\right)^{\frac{2}{3}} \frac{ND\,\Omega\sigma}{RT} \qquad (4.5.1)$$

$$D = D_o \exp\left(\frac{-Q}{RT}\right)$$

where V is the mean volume of a grain, Ω is the volume of a vacancy which is assumed to be equal to the volume of a BeO "molecule", σ is the applied tensile stress, R is the gas constant, T is the absolute temperature, D_0 the diffusivity constant for self-diffusion, and Q the activation energy for self-diffusion.

As previously described, Vandervoort and Barmore [1963] investigated the compressive creep of behavior polycrystalline BeO (grain sizes between 7.5 and 10μ) in the temperature range of 1370 to 1540°C. An activation energy of 96 kcal/mole (401.6 kJ/mole) was reported for the steady state creep. These results are consistent with the diffusional data of Austerman [1964b] and the Nabarro-Herring creep mechanism. The reported creep rates varied linearly with the applied stress which supported the proposed stress-directed diffusion of vacancies and a stress dependence of 1. A comparison of cation and anion diffusion data is made for both BeO and Al_2O_3 in Figure 17.

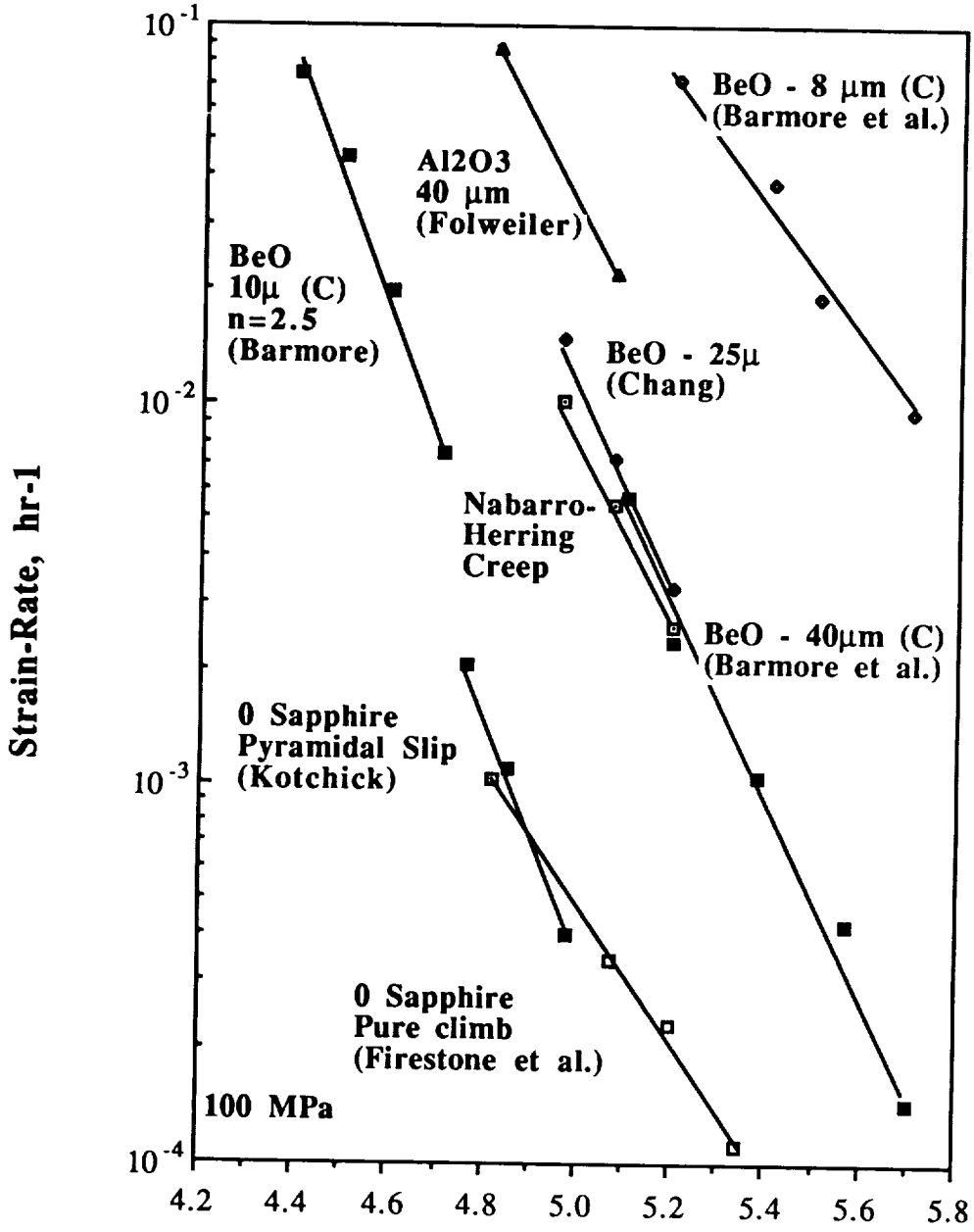

Figure 16. Influence of temperature on the creep rate of beryllium oxide

The compressive creep data of Vandervoort and Barmore [1963] were compared to the self diffusion data of Austerman [1964b] and Austerman and Chang [1964] using a

The compressive creep data of Vandervoort and Barmore [1963] were compared to the self diffusion data of Austerman [1964b] and Austerman and Chang [1964] using a relationship which accounted for relaxed grain boundaries during uniaxial compressive creep:

$$D = \left(\frac{3}{40}\right) \frac{\dot{\varepsilon}\, kTd^2}{\Omega\sigma} \qquad (4.5.2)$$

where k is Boltzmans constant and d is the mean grain diameter. These diffusion data agree well with the results of Austerman. Compressive creep data were converted to diffusive coefficients by this equation and compared to Austerman's work on Be diffusion in BeO

$$D = 1.37 \exp\left(\frac{-91.9 \text{ kcals/mole}}{RT}\right).$$

Barmore and Vandervoort [1965] examined plastic deformation of BeO under four point bending stresses (7 - 31 MPa) at temperatures between (1400 and 1700°C). They found an activation energy for creep of ≈99 kcals/mole (414 kJ/mole), a linear relationship between the applied stress and the creep rate, and an inverse square of the grain diameter dependence of the creep rate, consistent with a Nabarro-Herring type mechanism. Using equation 4.5.1 the diffusion coefficient can be calculated from the creep data for the oxide and compared to the mobility of the cation or anion. It has been proposed that oxygen migrates via grain boundaries at a rate faster than the cation through the volume in these oxides. Barmore and Vandervoort also found creep behavior to be the same in tension as it was in compression. These values are plotted in Figure 16 for comparison.

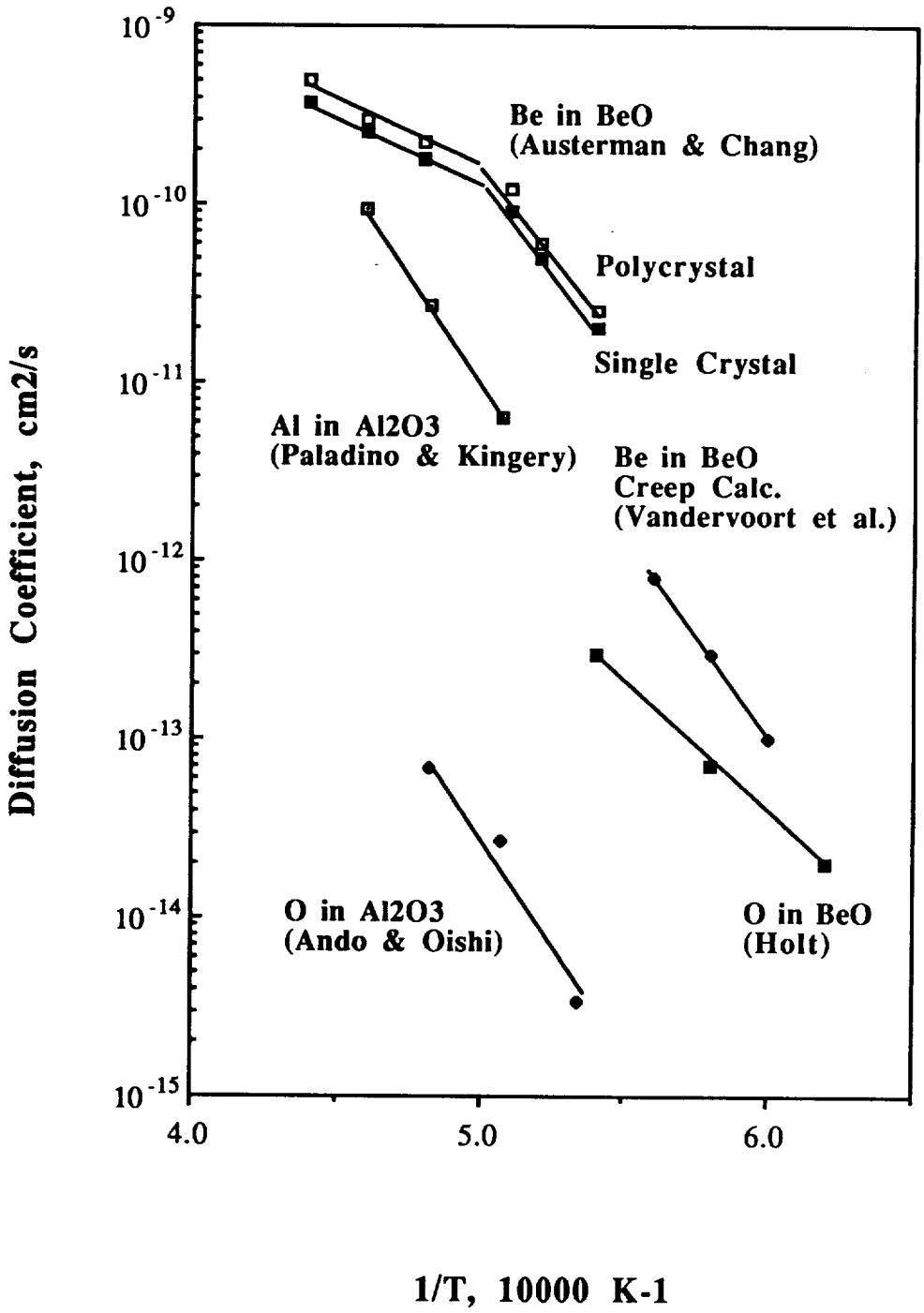

Figure 17. Influence of temperature on cation and anion diffusion in beryllium oxide

A study of the compressive creep behavior of polycrystalline BeO (grain size ≈ 63μm) in the temperature range of 1850 to 2050°C was undertaken by Barmore and Vandervoort [1967] in which they found a stress dependence of 2.5 and activation energy of 145 kcals/mole (607 kJ/mole). Tests were conducted at stresses of 10 to 42 MPa over the temperature range of 1850 to 2050°C. These rates were dictated by a dislocation mechanism yet unidentified. Note that in the the high-temperature study of BeO deformation the upper temperature was limited by the rapid (α-β) phase transformation at T > 2050°C. Previous studies of the creep behavior of BeO examined the deformation processes at temperatures much less than 1750°C [Bentle et al., 1965; Barmore et al., 1965; Vandervoort et al., 1963; Fryxell et al., 1964; Chang, 1959; Walker et al., 1971; and Cline et al., 1967]. It was found that from 1300 to 1700°C, the creep rate is linearly dependent on the applied stress and proportional to the inverse square of the grain diameter. The viscous deformation behavior in this temperature range for BeO was attributed to a Nabarro-Herring mechanism of stress-directed diffusion of vacancies. Behavior of this type has also been found for small grain size polycrystalline Al_2O_3 and MgO.

Mechanisms which describe the creep-rate dependence on stress where n is greater than 1 are controlled by dislocation motion and can be listed as follows:

1. Motion of jogged screw dislocations (when dislocation density is a function of the applied stress) [Dorn and Mote, 1963]
2. Peierls process (overcoming lattice resistance) [Weertman, 1957]
3. Dislocation climb [Weertman, 1955]

On the basis of the stress exponent, the most likely dislocation controlling process was that of overcoming Peierls forces or viscous glide mechanisms.

The underlying cation diffusional process in the high temperature region was reported to be not that of stress induced vacancy diffusion, but rather a process of volume diffusion of the anion. This was supported by the increase in the activation energy from ≈

100 kcals/mole (418 kJ/mole) to 145 kcals/mole (607 kJ/mole) at the higher temperatures. Beryllium diffusion occurs via a vacancy migration process and the authors believed it was likely that oxygen diffusion occurred in a similar manner because of its large ionic size. The diffusion coefficient for the beryllium ion varies with the level of impurities [Austerman, 1964b] and the activation energy for this process was ≈ 60 kcals/mole (251 kJ/mole) [DeBruin et al., 1964]. The activation energy for grain boundary diffusion of Be should be much less. Because of the relative high activation energy for creep in these experiments, it was proposed that the volume diffusion of the anion controlled the deformation rate in the high temperature region and that the value of 145 kcals/mole (607 kJ/mole) is the activation energy for volume diffusion of the anion in BeO. Values which can be found in the literature for the activation energy of oxygen diffusion in BeO are 43 and 68 kcals/mole (179.9 - 284.5 kJ/mole) [Austerman, 1964b and Holt, 1964]. These reported values are low in comparison to those for oxygen diffusion in Al_2O_3 which is 152 kcals/mole (636 kJ/mole) [Oishi et al., 1960].

The creep mechanism changed from that of Nabarro-Herring at lower temperatures (1300 - 1700°C) to one involving dislocation motion at high temperature; however, the specific dislocation mechanism was not determined. Since Al_2O_3 and BeO both have hexagonal close packed oxygen sublattices with nearly the same packing density, and with Al in octahedral interstices (Al_2O_3) and Be in tetrahedral interstices [Cotton and Wilkinson, 1980] the diffusion of the cations becomes significant in predicting ultimate creep behavior (at least at temperatures below 1700°C). In comparing the diffusion coefficients in these two structures, it's been found that both the cation [Paladino et al., 1962] and anion [Oishi et al., 1960] diffusion coefficients are an order of magnitude lower in Al_2O_3 than in BeO; however, the activation energies are higher. From this it can be argued that ionic mobility is greater, at any given temperature, for the structure having the higher melting temperature (BeO, ≈ 2500°C and Al_2O_3, 2010°C).

$$D_{Al} = 28\ cm^2/s \exp\left(\frac{-114\ kcal/mole}{R\ (1973\ K)}\right) = 6.5 \times 10^{-12}\ cm^2/s$$

$$D_{Be} = 1.35\ cm^2/s \exp\left(\frac{-92\ kcals/mole}{R\ (1973\ K)}\right) = 8.6 \times 10^{-11}\ cm^2/s$$

DeBruin et al. [1964] reported values for self-diffusion in polycrystalline cold-pressed and sintered BeO which were considerably different and this was attributed to differences in fabrication of the oxide, densities and purity. The activation energy for the self-diffusion of Be in BeO was found to be 62.5 kcals/mole (261.5 kJ/mole) with a frequency factor of 2.5×10^{-3} cm^2/s. This is significantly different than Austermans values of ≈111 kcals/mole (464.4 kJ/mole) below 1725°C and 36 kcals/mole (150.6 kJ/mole) above this temperature. DeBruin also cited a diffusion controlled mechanism based on the movement of the cation via the interstacies of the wurtzite structure to a vacancy. It was also predicted from this diffusion model that for single crystal of BeO the activation energy for diffusion will be the same in the a and c crystallographic direction as was noted by Austerman [1964b].

There is only one work on the creep behavior of single crystal c-axis oriented BeO [Corman, 1990]. The extreme anisotropy of this crystal was found to result in significant creep at temperatures as low as 650°C when tested slightly off axis. Slip apparently occurred on the primary (basal) slip system.

Single crystal c-axis BeO appears to be a good alternative oxide to single crystal Al_2O_3 in terms of its creep resistance; however, the issue of single crystal BeO fabricability must be addressed further since fabricating single crystal BeO from the melt is a challenge. The melting temperature is considerably higher (T_M = 2520°C) than the α-β phase transition. Beryllium oxide single crystals have been observed to degrade (cracking and crumbling) when heated above 2100°C as a result of a very rapid change in the crystal structure when the material is transformed from the α-BeO to the β-BeO phase.

Microcrystals of BeO have been grown by oxidizing beryllium, decomposing beryllium hydroxide vapor, and by hydrologizing gaseous beryllium fluoride at temperatures [Hutchinson et al., 1949].

Growth by the oxidation of the Be metal powder (99.9+ % Be) was accomplished using a Be boat to contain the powder in an alumina tube furnace with flowing H_2 atoms at 1525°C for 16 hours. One of the products of the alumina - H_2 reaction is steam. The reaction with the liquid Be metal is as follows:

$$Be_{(l)} + H_2O_{(g)} \leftrightarrow BeO_{(s)} + H_{2\,(g)}$$

$$\Delta F^\circ = -165 \text{ kcals/mole}$$

Beryllium may also react with the volatile aluminum oxide species, $Al_2O_{(g)}$ as follows: $Al_2O_{(g)} = 1/2\ BeO + Al_{(l)}$. The observed average growth rate for a microcrystal was 0.1μm/sec and occurred within the interior of the Be boat [Hutchinson et al., 1949].

These favorable reactions indicate that there are possibilities for the growth of BeO whiskers via the hydrolysis reaction or through decomposing beryllium hydroxide vapor:

$$BeO_{(s)} + H_2O_{(g)} \leftrightarrow Be(OH)_{2\,(g)} \qquad \Delta F^\circ = +30 \text{ kcals/mole}$$

Volitilization is due to the presence of water vapor in contact with beryllium oxide. A reaction with water results in the formation of a volatile compound which condenses at lower temperatures with decomposition to beryllium oxide. The formation of the volatile oxide occurs at temperatures of 1250°C or greater [Hutchinson et al., 1949]. This phenomenon is one which poses a problem for utilization in wet environments.

Experiments by Newkirk and Smith [1964] used a dense polycrystalline BeO cylinder (99.9% BeO) and placed this within the hot zone (1525°C) of an alumina tube

furnace. BeO substrates were placed downstream from the nutrient in a lower temperature zone (1400°C). The BeO nutrient and substrates were heated in a flowing, water-saturated He atm for 24 hours.

Whiskers were made having [001], $[0\bar{1}1]$, and [100] crystallographic orientations of the growth axis. The [001] or c-axis whiskers were common regardless of the growth conditions [Newkirk and Smith, 1964]. This c-axis oriented BeO whisker would be the most favorable orientation in terms of resistance to creep. The second principal growth direction was found to be $[0\bar{1}1]$. Rarely was the [100] growth direction found. Significantly, the c-axis direction was found to be the principal growth direction at temperatures greater than 1200°C. It is also clear from the data that the mechanisms for the whisker growth are complicated by the presence of impurities which were also volatile and deposited along with the BeO.

The growth of BeO macrocrystals was described by Austerman [1964]. He used a molten flux of lithium molybdate - molybdenum trioxide (Li_2MoO_4 - MoO_3). A thermal gradient technique was used in which the top of the furnace was heated slowly and a gradient exists form top to bottom. The continuous source of BeO solute was a large block of dense polycrystalline BeO at the upper surface of the flux contained within a crucible. The BeO source is suspended by a Pt wire a the top of the flux which itself supports a thermal gradient. The cooled zone is at the base of the flux and in this zone a super saturation of the BeO in the flux exists. The degree of super saturation depends upon the difference in temperature (ΔT) between the source block and the floor. Actual ΔT values were only $\approx$ 30°C for the processing techniques reported by Austerman [1964]. At the highest temperatures of the crucible floor for any given flux concentration, crystals nucleated and on any BeO that might have been present in the floor. As the temperature has lowered crystals began to grow on nucleating sites within the flux. The best crystal growths were found under conditions where nucleation occurred on seeds.

The growth of BeO macrocrystals was also described by Newkirk and Smith [1965]. The growth of high quality polyhedral and dendritic crystals approaching 1 cm on edge was described, and growth was discussed in terms of three possible mechanisms: (1) crystallization from molten salt solvents, (2) hydrothermal synthesis and vapor-phase decomposition/deposition reactions. A wide variety of BeO crystal habits were achieved as a function of the molar concentration of the specific flux and temperature of growth. Needles of BeO having a [0001] orientation were grown at 1200°C with increasing additions of MoO_3 (6 moles) to Li_2MoO_4 flux [Newkirk and Smith, 1965]. The mechanisms of growth are thought to be associated with [001] screw dislocation network along the central core of the crystal.

It is feasible that a single crystal filament may be grown from a polycrystalline feedstock via a laser floating zone technique if plastic relaxation is fast enough to accommodate the volume change which occurs during the α-β BeO phase transition. This possibility needs to be explored further.

4.6 Creep of Aluminosilicates - Mullite

A classical study of the equilibrium relationships of mixtures of pure $Al_2O_3 \cdot SiO_2$ and at high temperatures was conducted by Bowen and Grey [1924]. The principal compound was found to be $3Al_2O_3 \cdot 2SiO_2$. Since this time, considerable research has been directed at the synthesis of polycrystalline stoichiometric $3Al_2O_3 \cdot 2SiO_2$ (mullite). The incongruent melting point of mullite is ≈1825°C.

A major problem in the synthesis of stoichiometric mullite is that, regardless of the starting $Al_2O_3 \cdot SiO_2$ ratio (in the range of 3:2 or 2:1), sintering in the absence of a liquid phase produces a 3:2 mullite with an equiaxed grain morphology, [Davis and Pask, 1971]. Rapid cooling from a liquid phase produces a 2:1 composition of an acicular-type habit [Davis and Pask, 1971]. In both cases, there is always an excess of SiO_2 or Al_2O_3 in the product. Mazdiyasni and Brown [1972] prepared stoichiometric mullite by vacuum hot-pressing high-purity, submicron mixed oxide powders which were prepared by the hydrolytic decomposition of mixed metal alkoxides. This process formed, initially, amorphous needlelike particulates which transformed to highly crystalline structures at 1200°C.

Creep measurements on specimens such as these have been reported by Lessing, Gordon and Mazdiyasni in 1975 and Plenty and Hasselman in 1972. Lessing et al. [1975] tested the acicular, interlocking needle materials (grain size ≈ 5 μm) between 1400 and 1500°C in 4-point bend under stresses ranging between 9.8 to 49 MPa. An activation energy of 165 kcals/mole (690 kJ/mole) was reported along with a stress exponent of ≈ 1.0. They found this mullite to be significantly more creep resistant than polycrystalline Al_2O_3 from 1350°C

to near the melting point of mullite, and related creep to a diffusionally controlled process. Dokko, Pask and Mazdiyasni [1977] examined the compressive strength and creep behavior at temperatures between 1400 and 1500°C of polycrystalline mullite as prepared

by Mazdiyasni et al. [1972] and a single crystal mullite boule of composition $2Al_2O_3 \cdot SiO_2$ growth by the Czochralski technique by Austerman.

The creep resistance of the Mazdiyasni mullites as measured by Dokko et al. [1977] is similar to the data taken by Lessing et al. [1975] which was taken in 4-point bending. Both data sets exhibit a linear stress dependence (n = 1.0) with an activation energy for creep of 170 kcals/mole (711.3 kJ/mole).

The activation energy agrees well with the activation energy for lattice diffusion of 168 kcals/mole (703 kJ/mole) [Askay, 1973]. There was also a grain size dependence of 2, which together with the stress exponent and activation energy suggest a Nabarro-Herring controlled creep mechanism for mullite.

The mullite single crystal subjected to a stress of 480 MPa at 1400°C for 200 hours had no detectable plastic strain. Specimens with slip orientations as much as 6° off of the c-axis also exhibited no plastic strain under a stress of 620 MPa. These results indicate that dislocations are not mobile under these testing conditions.

Plenty and Hasselman [1972] obtained data for creep from fine-grained mullite under 4-point bending. They obtained a value of 167 kcals/mole (699 kJ/mole) for the activation energy and stress exponents ranging from 1.1 to 1.4. This activation energy for creep of mullite is in good agreement with Hulse and Pask [1966], Ghate [1972] and Kreglo and Smothers [1967]. The minimum temperature at which this mullite exhibited observable rates of creep is on the same order as polycrystalline alumina [Folweiler, 1961] and well above magnesia [Heuer, Cannon and Tighe, 1970]. For instance, a polycrystalline alumina of a 1.2 μm grain size had an observed steady-state creep rate of 0.36 hr^{-1} (1 x 10^{-4} s^{-1}) at 56 MPa at 1415°C the mullite studied by Plenty et al. [1972] exhibited a creep rate of 1.2 x 10^{-2} hr^{-1} (3.3 x 10^{-6} s^{-1}) at 1430°C and 56 MPa. The difference in the stress exponents between data taken in bending [Penty et al., 1972] and data taken in compression [Dokko et al., 1977] indicate the difficulties in interpreting flexural creep data.

The creep rates for the mullite specimens studied by Plenty and Hasselman [1972] were faster than that predicted by the grain-size dependence alone as compared with specimens fabricated by the Mazdiyasni technique which had an elongated grain structure, whereas the Penty et al. [1972] specimens do not. Evidence does suggest that columnar (elongated) grain structure increases creep resistance [Wilcox and Clauer, 1972] through a mechanism of inhibiting diffusionally controlled creep [Green, 1970]. Figure 18 gives the steady-state creep rates for stoichiometric polycrystalline and a single crystal mullite stressed at 686 MPa.

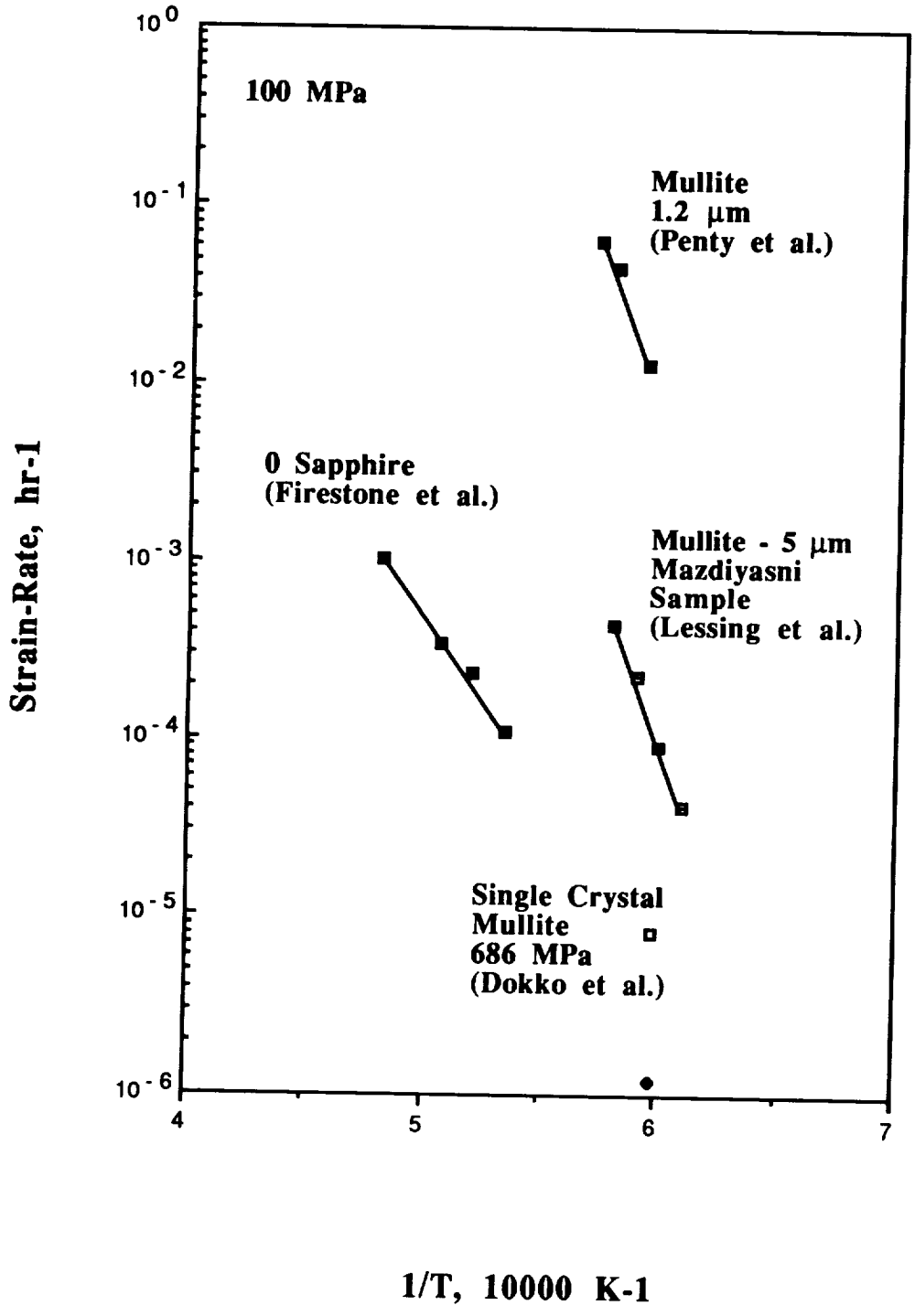

Figure 18. Influence of temperature on the steady-state creep rate of single and polycrystalline mullite

4.7 Creep of Oxides With the Rock-Salt Structure

A number of simple oxides crystallize with the rock-salt structure including MgO, CaO, MnO, NiO, SrO and BaO among others. Some, such as MgO, are stable as the stoichiometric oxide; whereas, others exist as the hyperstoichiometric oxide such as $Co_{1-x}O$ which is oxygen-rich because of the presence of Co^{3+} ions. Oxygen is the larger of the two ions in these structures. They are packed in a fcc array, with the metal ions occupying the octahedral interstices. The bonding in rock-salt structured oxides is largely ionic. The easiest slip system is on $\{110\}\ \langle 1\bar{1}0\rangle$ at low temperatures [Parker, 1961]. This provides two independent slip systems. At high temperatures polycrystal plasticity is made possible by slip on $\{100\}\ \langle 0\bar{1}1\rangle$ where five independent slip systems are possible. Slip on the harder $\langle 1\bar{1}0\rangle\ \{100\}$ system is observed in single crystals loaded along a $\langle 111\rangle$ axis, and in polycrystals at high temperatures, and it is presumed to occur in tests on polycrystals at low temperatures [Hulse and Pask, 1960; Hulse et al., 1963; Day and Stokes, 1966]. Slip due to compression in the $\langle 110\rangle$ direction is more difficult than in the $\langle 110\rangle$ or $\langle 100\rangle$ directions for MgO single crystals (at 1300°C) [Copley et al., 1966].

Oxides with the rock-salt structures are not considered good candidates for reinforcement materials. For instance, the steady-state creep data at 1500°C for a pure polycrystalline (218μm) MgO specimen is approximately one hr^{-1} when extrapolated to 100 MPa [Lessing and Gordon, 1974]. These values for creep rates are exceedingly high when compared to those of aluminas with comparable grain sizes ($\approx 10^{-3}$ - 10^{-4}, hr^{-1}) at similar stress levels. For these reasons oxides having the rock salt structure are not considered viable candidate oxides for fiber structures.

4.8 Creep of Silicon Carbide

In discussing candidate materials for application as fiber reinforcements, silicon carbide must be considered. Although not an oxide, SiC is extremely refractory and possesses excellent creep resistance. Silicon carbide is compiled of a single basic structural unit composed of a plane of tetrahedra, either SiC_4 or CSi_4 which are stacked sequentially in parallel or non-parallel arrays. The manner in which the structural unit is ordered determines the specific polytype of silicon carbide. There are approximately 170 different polytypes of silicon carbide with the most common being the 6H and the 3C stacking sequences representing the hexagonal and the cubic structures, respectively. These two silicon carbide structures are more commonly known as alpha and beta silicon carbide. Both structural forms are covalent solids which deform by dislocation motion only at temperatures high enough to overcome the Peierls barrier [Adewoga, 1981].

The primary slip system in hexagonal silicon carbide crystals is the (0001) $< 11\bar{2}0 >$ at temperatures below 2000°C [Stokes, 1966]. This system yields two independent slip systems. Others have reported slip systems which include the $\{4\bar{4}01\}$ and the $\{1\,\bar{1}01\}$ planes in the $< 11\bar{2}0 >$ direction [Amelinck et al., 1960; Farnsworth and Coble, 1966]; however, these systems are only activated at stress of 275 MPa or greater and temperatures in excess of 2000°C. Appreciable deformation of α-SiC single crystals has been reported in the temperature range between 2000 to 2100°C [Frantsevich et al. 1971]. Deformation was attributed to slip along the (0001) plane in the $< 11\bar{2}0 >$ direction.

Numerous studies have been undertaken to clarify the deformation behavior of polycrystalline SiC. The most creep resistant SiC is the α-SiC (6H) polytype. The hexagonal crystal structure of α-SiC results in deformation behavior which is extremely anisotropic. One of the first studies involving the creep deformation of alpha silicon carbide was conducted by Farnsworth and Coble [1966] at temperatures between 900 and 2200°C and constant strain-rates between 2.7×10^{-3} hr^{-1} (7.5×10^{-7} s^{-1}) and 6.0×10^{-4}

hr^{-1} (1.7×10^{-7} s^{-1}). Flow stress resulting for these test conditions ranged form 34.5 to 206.7 MPa. A viscous deformation behavior was found to dictate the creep behavior in this range.

Lane, Carter, and Davis [1988] examined the creep rates of sintered α-SiC under compressive stresses between 138 and 414 MPa and temperatures between 1400 and 1800°C. The stress exponent increased form 1.44 to 1.71 with temperature. There was a sharp change in the slope of the creep rate as a function of temperature at 1650°C. Below 1650°C the activation energy was 81-104.3 kcals/mole (339 -436.4 kJ/mole) and above 1650°C it was 192-218 kcals/mole (803 - 912 kJ/mole). The controlling creep mechanism at low temperatures was believed to be grain boundary sliding accommodated by grain boundary diffusion; whereas, at high temperature the controlling mechanism was grain boundary sliding accommodated by lattice diffusion.

More recently, Carter and Davis [1984] studied the creep of a CVD SiC under constant load (110 to 220 MPa) over the temperature range between 1575 and 1750°C. Stress exponents between 2.3 and 3.7 were reported along with an activation energy of 41.8 kcals/mole (174.9 kJ/mole). The controlling cree creep mechanism was shown to be highly temperature dependent. Dislocation glide was the reported creep controlling mechanism with the rate controlled by the Peierls stresses at temperatures less than 1600°C. At temperatures greater than 1600°C, the creep mechanism became dislocation glide controlled by climb. The creep of CVD SiC was strongly anisotropic. No deformation was observed for the planes oriented perpendicular to the applied stress at temperatures to 1650°C and stresses to 220 MPa.

Corman [1990] examined the steady-state creep behavior of a single crystal of (6H) SiC in the temperature range between 1600 and 1800°C. As anticipated the creep behavior was highly anisotropic with the most resistant orientation being the c-axis perpendicular to the compression axis. A stress exponent of 3.32 was reported and an activation energy of 67 kcals/mole (280.3 kJ/mole). The activation energy is lower than that for the diffusion of

C (171 kcals/mole [715 kJ/mole]) or Si (167 kcals/mole [699 kJ/mole]) in α-SiC [Hong and Davis, 1988 and Hong et al., 1981]. The creep resistance of the single crystal data is poor in comparison to the creep resistance of polycrystalline α-SiC [Carter et al., 1984 and Lane et al., 1988].

These data are compared to data on the creep of single crystal (c-axis oriented) alumina in Figure 19.

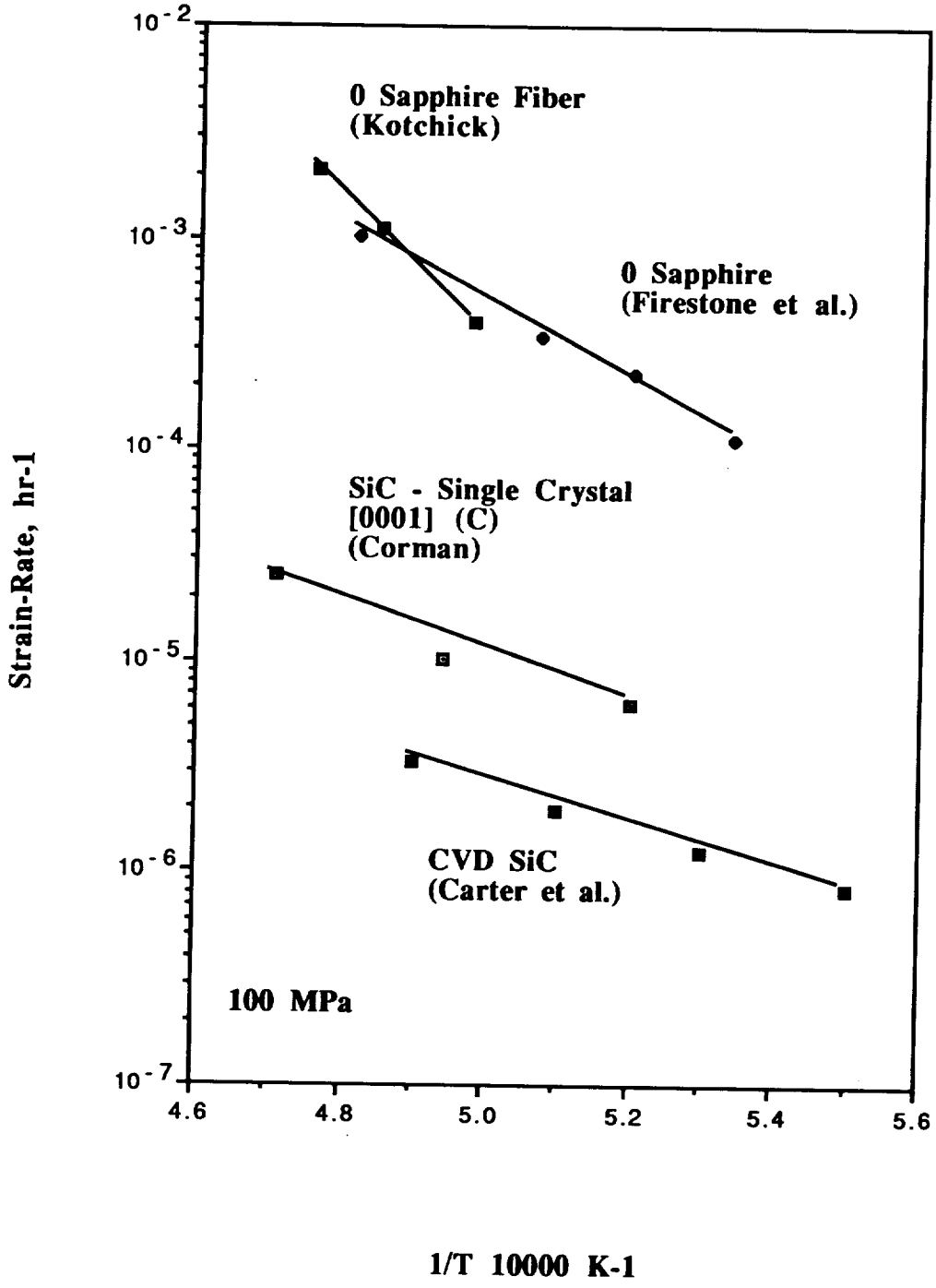

Figure 19. Influence of temperature on the steady-state creep rates of silicon carbide

5.0 SUMMARY

The emphasis of this review was to compile existing data on the creep behavior of oxide fibers and oxides which may be candidates for fabrication into fibers. The creep behavior of several classes of high melting point (≈2000°C) oxide ceramics has been presented in order to clarify which oxides could best serve as creep-resistant continuous fiber reinforcements for ceramic, intermetallic or metal matrix composites.

From this review several general trends in creep behavior emerge. In general, the deformation of polycrystalline oxide is controlled by diffusion of the slowest species along the fastest path, either through the lattice, along grain boundaries, or through a second phase located at the grain boundaries. Many subtleties affect the details. For example, the diffusional creep of fine grain aluminas appears to be controlled by the interface reactions to create or sink vacancies, a process which leads to non-Newtonian behavior. Dislocations can play a more or less important role depending on the specific oxide. For example, polycrystalline oxides with the rock salt structure have five independent slip systems and, thus, can deform or creep entirely by dislocation glide or glide controlled by climb processes.

Deformation of single crystals, on the other hand, is typically controlled by dislocation glide on the most favorable slip system (e.g. lowest critically resolved shear stress system depending on the crystal orientation and stress direction). Anisotropic crystals, which can be aligned so that primary slip is totally suppressed so that they deform via secondary slip during creep, are preferred over crystals with many independent slip systems as is the case of the rock salt structure. Sapphire, when oriented with the basal plane perpendicular to the fiber axis (c-axis orientation), is extremely creep resistant. The creep rate for 0° oriented sapphire is on the order of $10^{-8}/s^{-1}$ at 1600°C with a stress of 100 MPa since the secondary or pyramidal slip system $(01\bar{1}1)$ $\{10\bar{1}1\}$ is preferentially activated and the primary, basal, slip system is completely suppressed. The specific experimental data for single crystal and polycrystalline oxides are given in Figures 20 and 21. Under

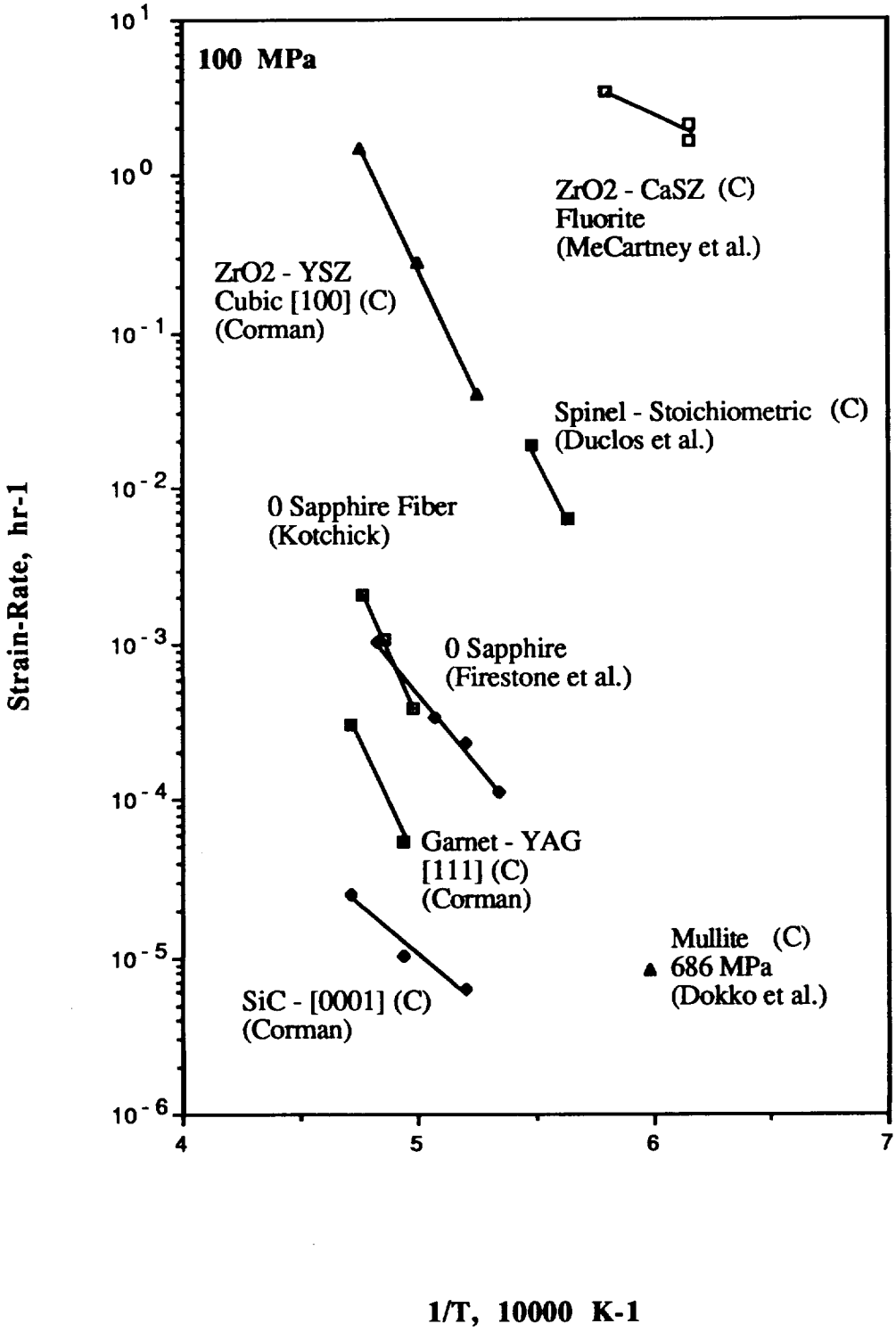

Figure 20. Influence of temperature on the steady-state creeprates of single crystal oxides.

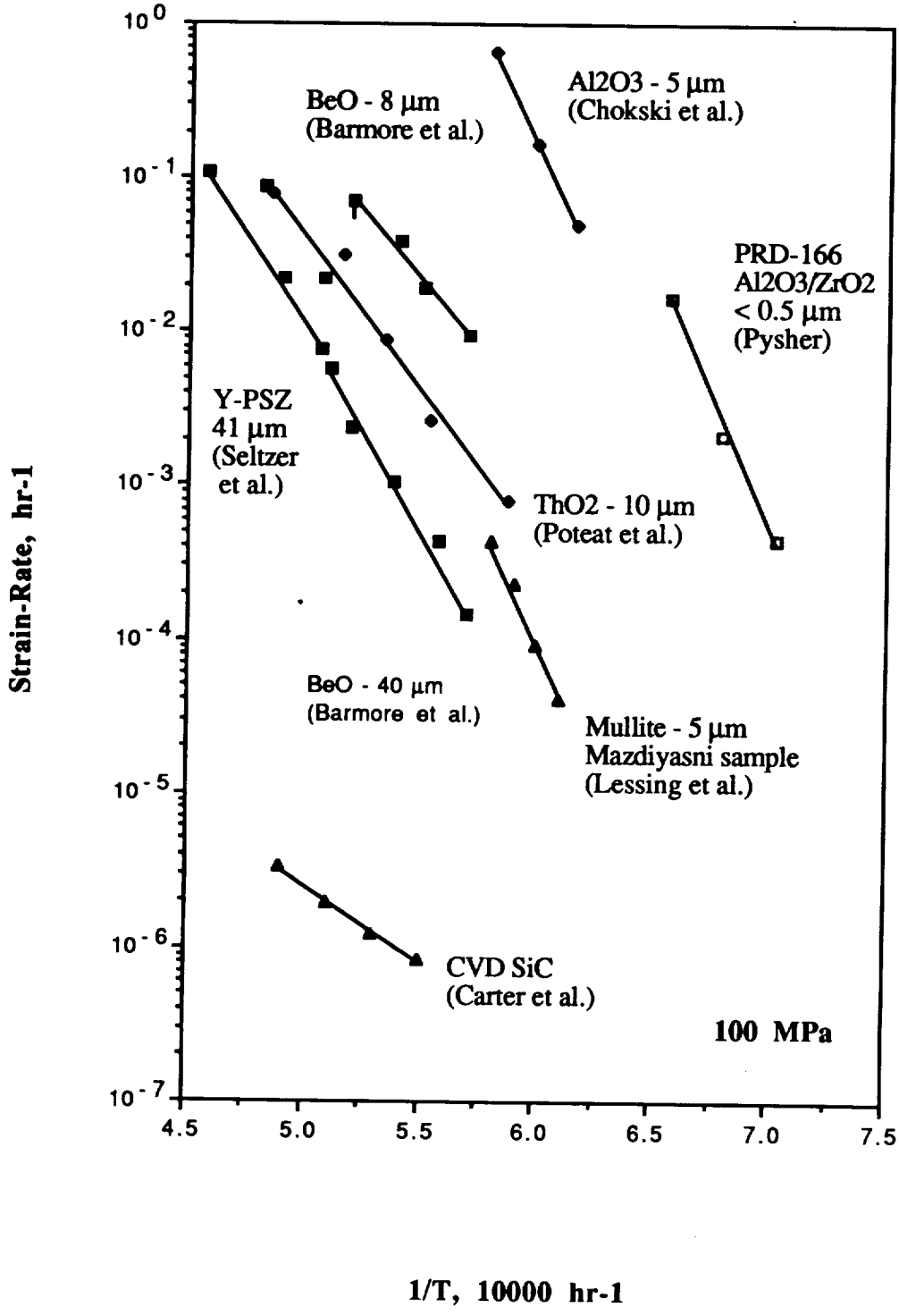

Figure 21. Influence of temperature on the steady-state creep rates of polycrystalline oxides.

low stresses at high temperature pure Nabarro climb (cooperative climb of edge dislocations) has been suggested as the process of creep of 0° sapphire at stresses below those necessary to activate pyramidal slip (≈120 MPa at 1100°C) [Firestone and Heuer, 1976]. Diffusion, therefore, can be an important process in the mechanisms for creep in both polycrystalline and single crystal oxides.

Vacancy diffusion in sapphire may also result in cavity nucleation and growth or in diffusion induced crack growth. Either of these rupture processes can lead to delayed failure of the fiber while in use. The identification and quantification of these processes is an important area for research.

Because of the importance of diffusion controlled creep and rupture processes in both polycrystals and single crystals, diffusion coefficients are key parameters in the prediction of creep and rupture. Diffusion coefficients for the oxides of interest are given in Figure 22. From the diffusion coefficients the relatively low creep rate of polycrystalline ThO_2 which has a fluorite crystal structure can be explained by the slow diffusivity of the Th^{4+} ion as compared to the Al^{3+} in Al_2O_3 and Be^{2+} in BeO. Diffusion of the ions along larger paths in materials with elongated grain structures is effective in increasing the creep resistance as in spinel and mullite [Minford, 1977 and Lessing et al, 1975]. Therefore, tailoring the microstructure of currently available polycrystalline oxide fibers by increasing the aspect ratio of the grains along the fiber axis is expected to decrease the creep-rate.

In terms of other fruitful areas for research this review has pointed out that c-axis oriented sapphire possesses an extremely high resistance to deformation; however, little is known about the creep of 0^o sapphire under low stresses (<100 MPa) and temperatures (< 1650 C) and the mechanisms controlling rupture under these conditions. C-axis oriented beryllia has been suggested as a candidate material based on the creep resistance of polycrystalline BeO. However, beryllia in poses problems in the fabrication of single crystal fibers and moisture sensitivity. From the work of Corman [1990] yttrium aluminum garnet (YAG) with its complex crystal structure and high Peierl's resistance

Oxide Diffusion

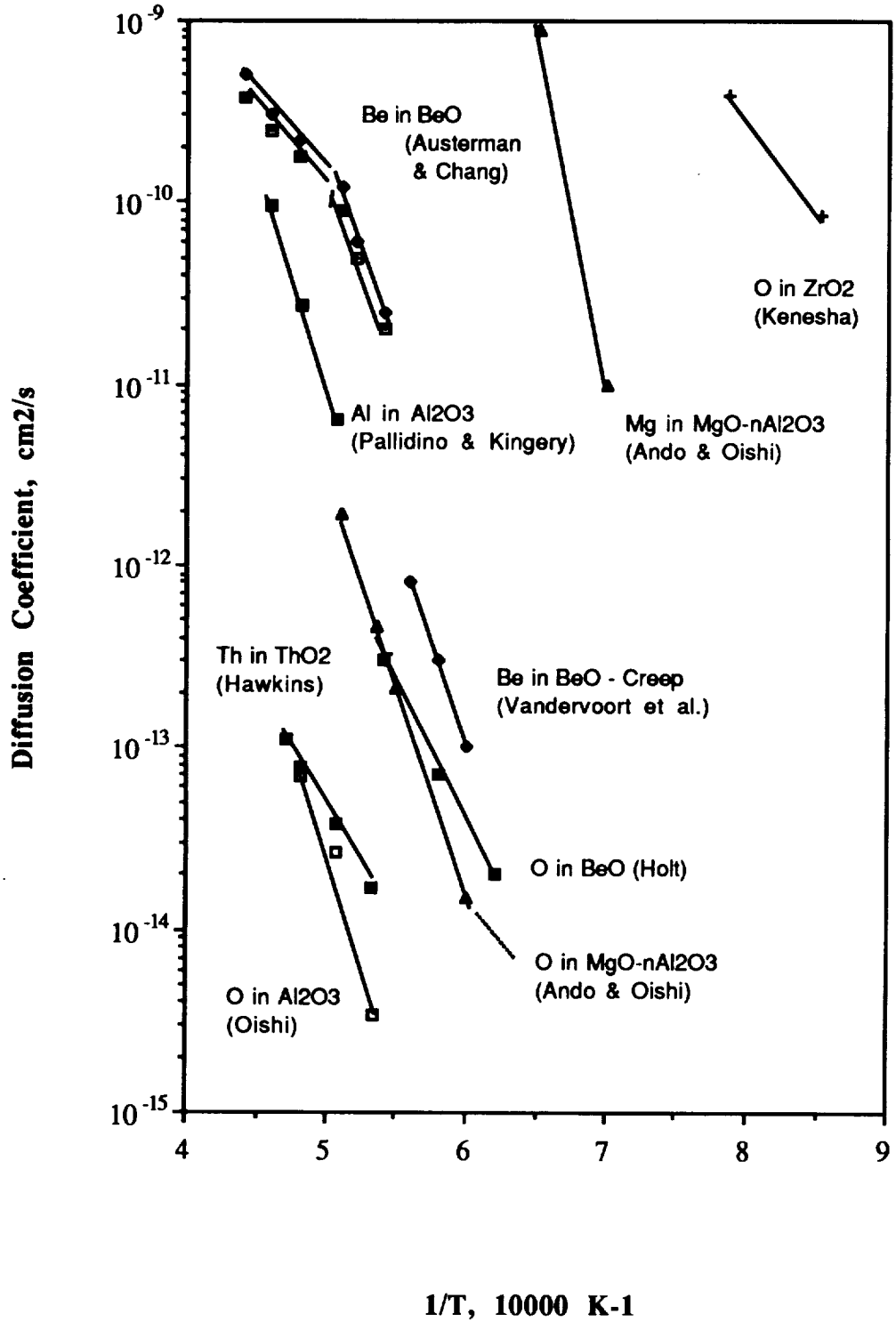

Figure 22. Diffusion coefficients in single and polycrystalline oxides.

appears to be a good candidate material for an oxide fiber. The high creep resistance of garnet suggests that there may be other complex ternary oxides such a single crystal mullite which may be viable candidates for fiber . Finally, CVD and single crystal SiC although not oxides do possess high resistance to creep in the temperature range of 1550 - 1850°C and stresses of 110 to 220 MPa. This excellent creep resistance has been attributed to a high Peierls stress. At higher temperatures under the same stress conditions dislocation glide appears to become climb controlled. So it appears that for highly creep resistant applications single crystal alumina, silicon carbide, yttrium aluminum garnet, mullite and beryllia are desirable materials candidates.

6.0 REFERENCES

Ackermann, R. J. and Thorn, R. J. (1961) "Vaporization of Oxides." in Progress in Ceramic Science, (J. E. Burke, Ed.). Pergammon Press, 39.

Adewoye, O.O. (1981) "Anomalous Plastic Flow in α-SiC." Crystal Lattice Defects, 9, 107-111.

Amelinckx, S., Strumore, G. and Webb, W. W. (1960) "Dislocations in Silicon Carbide." J. Appl. Physics, 31, 1359.

Argon, A. S. (1970) "Internal Stresses Arising from the Interaction of Mobile Dislocations," Scripta Met., 4, 1001-1004.

Ashby, M. F. (1969) "On Interface-Reaction Control of Nabarro-Herring Creep and Sintering." Scripta Met., 3 [11] 837-842.

Ashby, M. F., Raj, R., and R. C. Gifkins (1970) "Diffusion-Controlled Sliding at a Serrated Grain Boundary." Scripta Met., 4 [9] 737-742.

Ashby, M. F. and Verrall, R. A. (1973) "Diffusion-Accommodated Flow and Superplasticity." Acta Metall., 21 [2] 149-163.

Aksay, I. A. and Pask, J. A. (1975) "Stable and Metastable Equilibria in the System SiO_2-Al_2O_3." J. Amer. Ceram. Soc., 58 [11-12] 507-512.

Austerman, S. B. (1964a) "Growth and Properties of Beryllium Oxide Single Crystals." J. Nuclear Mat., 14, 225.

Austerman, S. B. (1964b) "Self-Diffusion in Beryllium Oxide." J. Nuclear Mat., 14, 248.

Austerman, S. B. (1964c) "Diffusion and Creep in Beryllium Oxide." J. Nuclear Mat., 12, 337.

Baëta, R. D. and Ashbea, K. H. G. (1967) "Plastic Deformation and Fracture of Quartz at Atmosphere Pressure." Phil Mag., 15 [137] 931-938.

Barmore, W. L. and Vandervoort, R. R. (1965) "High-Temperature Plastic Deformation of Polycrystalline Beryllium Oxide." J. Amer. Ceram. Soc., 48, 499.

Barmore, W. L. and Vandervoort, R. R. (1967) "High-Temperature Creep and Dislocation Etch Pits in Polycrystalline Beryllium Oxide." J. Amer. Ceram. Soc., 50, [6] 316-320.

Batha, H. D. and Whitney, E. D. (1973) "Kinetics and Mechanism of the Thermal Decomposition of Si_3N_4." J. Amer. Ceram. Soc., 56 [7] 365-369.

Bayer, P. D., and Cooper, R. E. (1967) "A New Slip System in Sapphire." J. Matl. Sci., 2 [3] 301-302.

Becher, P. F. (1971) "Deformation Substructure in Polycrystalline Alumina." J. Materials Sci., 6, [4] 275-280.

Bell, R. L. and Cahn, R. W. (1957) "The Dynamics of Twinning and the Interrelation of Slip and Twinning in Zinc Crystals." Proc. Roy. Soc., London, A239, 494-521.

Bentle, G. G. and Kruefel, R. M. (1965) "Brittle and Plastic Behavior of Hot Pressed BeO." J. Amer. Ceram. Soc., 48, 570.

Bentle, G. G., and Miller, K. T. (1969) "Dislocations, Slip, and Fracture in BeO Single Crystals." J. Appl. Phys., 38 [11] 4248-4257.

Bertolotti, R. L. and Scott, W. D. (1971) "Compressive Creep of Al_2O_3 Single Crystals." J. Amer. Ceram. Soc., 54 [6] 286-291.

Bilde-Sorenson, J. B., Tholen, A. R., Gooch, D. J., and Groves, G. W. (1976) "Structure of the <01$\bar{1}$0> Dislocation in Sapphire." Phil Mag., 33 [6] 877-899.

Bowen, N. L. and Greig, J. W. (1924) "The System: $Al_2O_3 \cdot SiO_2$." J. Amer. Ceram. Soc., 7 [4] 238-254.

Bradt, R. C. (1967) "Cr_2O_3 Solid-Solution Hardening of Al_2O_3." J. Amer. Ceram. Soc., 50 [1] 54-55.

Bratton, R. J. (1969) "Initial Sintering Kinetics of $MgAl_2O_4$." J. Amer. Ceram. Soc., 52 [8] 417-419.

Bratton, R. J. (1971) "Precipitation and Hardening Behavior of Gzochralski Star Sapphire," J. Appl. Phys., 42 [1] 211-216.

Bretheau, T., Castaing, J., Rabier, J., and Veyssiere, P. (1979) "Movement des Dislocations à Haute Température des Oxydes Binaires et Ternaires." Adv. Phys., 28 [6] 835-1014.

Burton, B. (1972) "Interface Reaction Controlled Diffusional Creep: A Consideration of Grain Boundary Dislocation Climb Sources." Mater. Sci. Eng., 10 [1] 9-14.

Burton, B. (1973) "On the Mechanism of the Inhibition of Diffusional Creep by Second Phase Particles." Mater. Sci. Eng., 11, 337-343.

Busovne, B. J., Jr. (1981) "The Precipitation Hardening Behavior of Ti^{4+}-doped Sapphire." Ph.D. Thesis, The Pennsylvania State University.

Cadoz, J. and Pellisier, B. (1976) "Influence of Three-Fold Symmetry on Pyramidal Slip of Alumina Single Crystal." Scripta. Met., 10, [7] 597-600.

Cadoz, J. L. (1978) "Etude de la Deformation Plastique de L'alun$\bar{u}$ne α Suivant le Système de Glissement Prismatique." Ph.D. Thesis, Universite de Paris-Sud Paris.

Cadoz, J. L., Castaing, J. and Philibert, J. (1981) "Prismatic Slip in Al_2O_3 by Compression Tests." Rev. Phys. Appl., 16, 135-144.

Campbell, W. B., Hurst, V. J., and Moody, W. E. (1959) "Thorium Oxide and Uranium Oxide Cleavage." J. Amer. Ceram. Soc., 42 [5] 262.

Cannon, R. M. and Coble, R. L. (1974) "Review of Diffusional Creep of Al_2O_3," in Deformation of Ceramic Materials, (R. C. Bradt and R. E. Tressler, Eds.). Plenum Press, New York.

Cannon, W. R. and Sherby, O. D. (1973) Third Power Stress Dependence in Creep of Polycrystalline Nonmetals." J. Amer. Ceram. Soc., 56, 157-160.

Cannon, R. M., Rhodes, W. H., and Heuer, A. H. (1980) "Plastic Deformation of Fine-Grained Alumina (Al_2O_3): I, Interface - Controlled Diffusional Creep." J. Amer. Ceram. Soc., 63 [1-2] 46-53.

Carter, G. M. Henshall, J. L., and Hooper, R. M. (1988) "Indentation Creep in Single-Crystal Cubic Zirconia at Room Temperature." J. Amer. Ceram. Soc., 71 [5] C-270.

Carter, C. H., Davis, R. F., and Bentley, J. (1984) "Kinetics and Mechanisms of High Temperature Creep in Silicon Carbide: II, Chemically Vapor Deposited." J. Amer. Ceram. Soc., 67 [11] 732-740.

Castaing, J., Cadoz, J., and Kirby, S. H. (1981) "Prismatic Slip of Al_2O_3 Single Crystals Below 1000°C in Compression Under Hydrostatic Pressure." J. Amer. Ceram. Soc., 64 [9] 504-511.

Cawley, J. D. (1984) "Oxygen Diffusion in Alpha Alumina." Ph.D. Thesis, Case Western Reserve University, Cleveland, OH.

Chang, R. (1959) "High-Temperature Creep and Anelastic Phenomena in Polycrystalline Refractory Oxides." J. Nuclear Mat., 1, 174.

Chang, R. (1960) "Creep of Al_2O_3 Single Crystals." J. Appl. Phys., 31 [3] 484-487.

Chang, R. and Grooves, G. W. (1965) "Effect of Creep Deformation on the Conductivity of Undoped and Cr-doped Alumina Crystals." Brit. J. Appl. Pys., 16 [5] 715-719.

Chang, R., Bentle, G. G. and Ekstrom, F. E. (1963) "Materials Science and Technology Applications." (ed. D. R. Marsh) Prentice-Hall Englewood Cliffs, NJ, 533.

Chokshi, A. H. and Porter, J. R. (1985) "Creep Deformation of an Alumina Matrix Composite Reinforced with Silicon Carbide Whiskers." J. Amer. Ceram. Soc., 68 [6] C-144 - C-145.

Chokshi, A. H. and Porter, J. R. (1986) "High Temperature Mechanical Properties of Single Phase Alumina." J. of Matl. Sci., 21 [2] 705-710.

Chokshi, A. H. and Porter, J. R. (1986) "Analysis of Concurrent Grain Growth During Creep of Polycrystalline Alumina." J. Amer. Ceram. Soc., 69 [2] C-37.

Cline, C. F., Newkirk, H. W., Barmore, W. L. and Vandervoort, R. R. (1967) "Creep-Electrical Conductivity Correlations in Polycrystalline Beryllium Oxide." J. Amer. Ceram. Soc., 50, [4] 221-222.

Coble, R. L. (1958) Initial Sintering of Alumina and Hematite." J. Amer. Ceram. Soc., 41 [2] 55-62.

Coble, R. L. (1963) "A Model for Boundary Diffusion Controlled Creep in Polycrystalline Materials." J. Appl. Phys., 34 [6] 1679-1682.

Coble, R. L. and Guerard, Y. H. (1963) "Creep of Polycrystalline Aluminum Oxides." J. Amer. Ceram. Soc., 46 [7] 353-354.

Conrad, H. (1965) "Mechanical Behavior of Sapphire." J. Amer. Ceram. Soc., 48 [4] 195-201.

Conrad, H., Stone, G., and Janowski, K. (1965), "Yielding and Flow of Sapphire (Alpha - Al_2O_3 Crystals) in Tension and Compression." Trans. AIME, 233 [5] 889-897.

Copely, S. M., and Pask, J. A. (1966) "Deformation of Polycrystalline Ceramics," in Materials Science Research, (W. W. Knegel and H. Palmour III, Eds.). Plenum Press, New York, 3, 189-224.

Corman, G. S. (May 1989) "High-Temperature Creep of Yttria-Stabilized Zirconia Single Crystals." G. E. Research and Development, Technical Information Series, Ceramics Laboratory, #89CRD084.

Corman, G. S. (1990) "Creep of Oxide Single Crystals." Air Force Technical Report WRDC-TR-90-4049.

Cotton, F. A. and Wilkinson, G. (1980) in Advanced Inorganic Chemistry, J. Wiley and Sons, New York, p. 276.

Crosby, A. and Evans, P. E. (1973) "Creep in Pure and Two Phase Nickel-Doped Alumina." J. Mater. Sci., 8, 1573-1580.

Darroudi, T. (March 1986) "The Creep Testing of Refractories." St. Louis Refractories Symposium.

Davies, C. K. L. and SinhaRoy, S. K. (1970) "High Temperature Creep Deformation of Polycrystalline Alumina in Tension." Proc. Brit. Ceram. Soc., 15, 193-209.

Davis, R. F and Pask, J. A. (1971) in High Temperatrue Oxides, Part IV (ed. A. M. Alper) Academic Press, Inc., NY.

DeBruin, H. J. and Watson, G. M. (1964) "Self-Diffusion of Beryllium in Unirradiated Beryllium Oxide." J. Nuclear Mat., 14, 239.

deMeesler, B., Yin, C., Donner, M., and Conrad, H. (1973) in Rate Processes in Plastic Deformation, (J. C. M. Li and A. K. Mukherjeer, Eds.). ASM.

Dimos, D. and Kohlstedt, D. L. (1987) "Diffusional Creep and Kinetic Demixing in Yttria-Stabilized Zirconia." J. Amer. Ceram. Soc., 70 [8] 531-536.

Dominguez-Rodriguez, A., Lagerloff, K. P. D., and Heuer, A. H. (1986) "Plastic Deformation and Solid-Solution Hardening of Y_2O_3-Stabilized ZrO_2." J. Amer. Ceram. Soc., 69 [3] 281-284.

Dokko, P. C., Pask, J. A. and Mazdiyasni, K.S. (1977) "High-Temperature Mechanical Properties of Mullite Under Compression." J. Amer. Ceram. Soc., 60 [3-4] 150-155.

Donald, I. W. and McMillan, P. W. (1976) "Ceramic-Matrix Composites." J. of Matl. Sci., 11 949-972.

Donkhan, N., Duclos, R., and Escaig, B. (1973) Structural and Mechanical Study of Creep on Al_2O_4Mg Single Crystals." J. Physique Paris, 34 [11-12 C9] 379.

Dorn, J. E., Mote, J. D. (1963) in Proc. of the Third Symposium on Naval Structural Mechanics, (A. M. Freudenthal, Ed.). Pergammon Press, New York, 95-168.

Duclos, R., Doukhan, N., Escaig, B. (1978) "High Temperature Creep Behaviour of Nearly Stoichiometric Alumina Spinel." J. Matl. Sci., 13 [8] 1740-1748.

Duclos, R. (1981) "High Temperature Deformation of $MgO \cdot 1.8Al_2O_3$ Spinel Single Crystals of <111> Axial Orientation." J. Phys. Paris, 42, 49-57.

Edington, J. W. and Klein, M. J. (1966) "Slip and Fracture in Single Crystals of Thoria." J. Appl. Phys., 37, 3906-3908.

Evans, P. E. (1970) "Creep in Yttria- and Scandia-Stabilized Zirconia." J. Amer. Ceram. Soc, 53 [7] 365-369.

Evans, A. G. and Rawlings, R. D. (1969) "The Thermally Activated Deformation of Crystalline Materials." Phys. Stat. Sol., 34 9-31.

Farnsworth, P. L. and Coble, R. L. (1966) "Deformation Behavior of Dense Polycrystalline SiC." J. Amer. Ceram. Soc., 49 [5] 264-268.

Firestone, R. F., and Heuer, A. H. (1976) "Creep Deformation of 0° Sapphire." J. Amer. Ceram. Soc., 59 [1-2] 24-29.

Fisher, J. C. (1954) "On the Strength of Solid Solution Alloys." Acta. Met., 2 [1] 9-10.

Fleisher, R. L. (1963) "Substitutional Solution Hardening." Acta Met., 11 [3] 203-209.

Folweiler, R. C. (1961) "Creep Behavior of Pore-Free Polycrystalline Aluminum Oxide." J. Appl. Phys., 32 [5] 773-778.

Frantsevich, I. N., Kravets, V. A., Egorov, L. O. Nazarenko, K. V. and Smushkevich (1971) "High Temperature Deformation of α-SiC," Porosh. Metall., 3 [99] 74-77.

Frost, H. J., Ashby, M. F. (1982) in Deformation-Mechanism Maps, The Plasticity and Creep of Metals and Ceramics. Pergammon Press, Oxford.

Fryxell, R. E. and Chandler, B. A. (1964) "Creep, Strength, Expansion, and Elastic Moduli of Sintered BeO as a Function of Grain Size, Porosity and Grain Orientation." J. Amer. Ceram. Soc., 47, 283-291.

Ghate, B. B. (1972) "Synthesis and Pressure-Sintering Kinetics of High-Purity, Fine-Grained Mullite." Ph.D Dissertation, Lehigh University.

Gifkins, R. C. (1956) "Diffusional Creep Mechanisms." Acta. Met., 4, 98.

Gifkins, R. C. (1968) "Diffusional Creep Mechanisms." J. Amer. Ceram. Soc., 51 [2] 69-72.

Gilbert, A. (1965) "Deformation and Fracture of Thoria." Phil. Mag., 12 139-144.

Gilman, J. J. (1959) "Plastic Anisotropy of LiF and Other Rocksalt-Type Crystals." Acta Met., 7 [9] 608-613.

Gilman, J. J. (1966) "Monocrystals in Mechanical Technology." ASM Trans. Q., 59, 597-629.

Gooch, D. J. and Grooves, G. W. (1972) "Prismatic Slip in Sapphire." J. Amer. Ceram. Soc., 55 [2] 105.

Gooch, D. J. and Grooves, G. W. (1973a) "The Creep of Sapphire Filament with Orientations Close to the C-Axis." J. Matl. Sci., 8 [9] 1238-1246.

Gooch, D. J. and Grooves, G. W. (1973b) "Non-Basal Slip in Sapphire." Phil. Mag., 28 [3] 623-637.

Green II, H. W. (1970) "Diffusional Flow in Polycrystalline Materials." J. Appl. Phys., 41 [9] 3899-3902.

Greenwood, G. W. (1970) "Possible Effects on Diffusion Creep and Some Limitations of Grain Boundaries as Vacancy Sources or Sinks." Scr. Met., 4 [3] 171-174.

Haggerty, J. S. (1973) "Growth of Titanium and Chromium Strengthened Sapphire Fibers." Technical Report AFML-TR-73-2.

Haneda, H. Miyazawa, Y. and Shirasaki (1984) "Oxygen Diffusion in Single Crystal Yttrium Aluminum Garnet." J. Cryst. Growth, 68, 581-588.

Hawkins, R. J. and Alcock, C. B. (1968) "A Study of Cation Diffusion in UO_{2+x} and ThO_2 using α-Ray Spectrometry." J. Nuclear Matls., 26, 112-122.

Herring, C. (1950) "Diffusional Viscosity of Polycrystalline Solid." J. Appl. Phys., 21, 437-445.

Heuer, A. H., Cannon, R. M., and Tighe, N. J. (1970) in Ultrafine-Grain Ceramics. (J. J. Burke, N. L. Reid, and Voker Weiss, Eds.). Syracuse University Press, Syracuse, NY, pp. 339-365.

Heuer, A. H., Firestone, R. F., Snow, J. D., and Tullis, J. (1970) "Non-basal Slip in Alumina at High-Temperatures and Pressures." Proc. Conf. in Ceramics in Severe Environments, Raleigh, NC, pp. 331-340.

Heuer, A. H., Tighe, N. J.and Cannon, R. M. (1980) "Plastic Deformation of Fine-Grained Alumina (Al_2O_3): II, Basal Slip and Nonaccommodating Grain-Boundary Sliding." J. Amer. Ceram. Soc., 63 [1-2] 53-58.

Hewson, C. W. and Kingery, W. D. (1967) "Effect of MgO and $MgTiO_3$ Doping on Diffusion Controlled Creep of Polycrystalline Aluminum Oxide." J. Amer. Ceram. Soc., 50 [4] 218-219.

Hirthe, J. P. and Lothe, J. (1982) Theory of Dislocations, 2nd Ed. John Willey and Sons, Inc., New York.

Hockey, B. J. (1971) "Plastic Deformation of Aluminum Oxide by Indentation and Abrasion." J. Amer. Ceram. Soc., 54 [5] 223-231.

Hollenberg, G. W. and Gordon, R. S. (1973) "Origin of Anomalously High Activation Energies in Sintering and Creep of Impure Refractory Oxides." J. Amer. Ceram. Soc., 56 [2] 109-110.

Holt, J. B. (1964) "Self-Diffusion of Oxygen in Single Crystal Beryllium Oxide." J. Nuclear Mat., 11, 107.

Hornstra, J. (1960) "Dislocations, Stacking Faults, and Twins in the Spinel Structure." J. Phys. Chem. Solids, 15, 311.

Hou, L. D., Tiku, S. K., Wang, H. A., Kröger, F. A. (1979) "Conductivity and Creep in Acceptor-Dominated Polycrystalline Al_2O_3." J. Mater. Sci., 14, [8] 1877-1889.

Hsu, S. E., Kobes, W., and Fine, M. E. (1967) "Strengthening of Sapphire by Precipitates Containing Titanium." J. Amer. Ceram. Soc., 50 [3] 149-151.

Hulse, C. O. and Pask, J. A. (1966) "Analysis of Deformation of a Fineclay Refractory." J. Amer. Ceram. Soc., 49 [6] 312-318.

Hutchinson, Jr., C. A. and Malon, J. G. (1949) "The Volatilization of Beryllium Oxide in the Presence of Water." 71, 1338.

Hwang, L., Heuer, A. H., and Mitchell, T. E. (1975) "Slip Systems in Stoichiometric $MgAl_2O_4$ Spinel," in Deformation of Ceramic Materials, (R. C. Bradt and R. E. Tressler, Eds.). Plenum Press, NY, 257.

Ingel, R. P., Lewis, D., Bender, B. A., and Rice, R. W. (1982) "Temperature Dependence of Strength and Fracture Toughness of ZrO_2 Single Crystals." Comm. Amer. Ceram. Soc., C-150 - C-152.

Ikuma, Y. and Gordon, R. S. (1983) "Effect of Doping Simultaneously with Iron and Titanium on the Diffusional Creep of Polycrystalline Al_2O_3." J. Amer. Ceram. Soc., 66 [2] 139-147.

Kelly, A. B. and Nicholson, R. B. (1963) "Precipitation Hardening," in Prog. in Matl. Sci., 10, 149-391.

Kenesha, F. J. and Donglaos (1971) "Oxidation of Metals." 3, 1.

King, A. D. (1971) "Thorium Diffusion in Single Crystal ThO_2." J. Nuclear Matls., 38, 347-349.

Kingery, W. D., Pappis, J., Doty, M. E., and Hill, D. C.(1959) "Oxygen Ion Mobility in Cubic $Zr_{0.85}\,Ca_{0.15}\,O_{1.85}$." J. Amer. Ceram. Soc., 42 [8] 393-398.

Klassen-Neklyudova, M. V., Govorkov, V. G., Urusovskaya, A. A., Voinova, N. N. and Kozlovskaya, E. E. (1970) "Plastic Deformation of Corundum Single Crystals." Phys. Stat. Sol., 39 [2] 679-688.

Kotchick, D. M. (1978) "Deformation Dynamics of Doped and Undoped a-Axis and c-Axis Sapphire." Ph.D. Thesis Ceramic Science, The Pennsylvania State University.

Kotchick, D. M. and Tressler, R. E. (1980) "Deformation Behavior of Sapphire Via the Prismatic Slip System." J. Amer. Ceram. Soc., 63 [7-8] 429-434.

Kreglo, Jr., J. R. and Smothers, W. J. (1967) "Creep Characteristics of Selected High-Alumina Bricks." J. of Metals, 20, 20-22.

Kronberg, M. L. (1957) "Plastic Deformation of Single Crystals of Sapphire: Basal Slip and Twinning." Acta Met., 5 [9] 507-524.

Kronberg, M. L. (1962) "Dynamical Flaw Properties of Single Crystals of Sapphire, I." J. Amer. Ceram. Soc., 45 [6] 274-279.

Labush, R. (1970) "A Statistical Theory of Solid Solution Hardening." Phys. Stat. Sol., 41 [2] 659-669.

Lackey, W. J., D. P. Stinton, G. A. Cerny, L. L. Fahrenbacher, and A. C. Schaffhauser (1983) "Ceramic Coatings for Heat Engine Mateirals - Status and Future Needs." in Proc. of Int. Symposium on Ceramic Components for Heat Engines, Hakone, JAPAN.

Lagerlof, K. P. D., Mitcheel, T. E. And Heuer, A. H. "Lattice Diffusion Kinetics in Undoped and Impurity-Doped Sapphire [α-Al_2O_3]: A Dislocation Loop Annelaing Study, " J. Am. Ceram. Soc., 72 [11] 2154-71.

Lane, J. E., Carter, C. H. and Davis, R. F. (1988) "Kinetics and Mechanisms of High Temperature Creep in Silicon Carbide: III, Sintered α-Silicon Carbide." J. Amer. Ceram. Soc., 71 [4] 281-295.

Langdon, T. G. (1975) "Grain Boundary Deformation Processes," in Deformation of Ceramic Materials, (R. C. Bradt and R. E. Tressler, Eds.) Plenum Press, NY, 101-126.

Lankford, J. (1986) "Deformation and Fracture of Yttria-Stabilized Zirconia Single Crystals." J. Matl. Sci., 21 [6] 1981-1989.

Lesage, B., Huntz, A. M. and Petot-Ervas, G. (1983) "Transport Phenomena in Undoped and Cromium- or Yttrium-Doped Alumina." Radiat. Eff., 75, 283-99.

Lessing, P. A. and Gordon, R. S. (1975) "Impurity and Grain Size Effects on the Creep of Polycrystalline Magnesia and Alumina," in Deformation of Ceramic Materials, (R. C. Bradt and R. E. Tressler, Eds.). Plenum Press, NY.

Lessing, P. A.,and Gordon, R. S. (1977) "Creep of Polycrystalline Alumina, Pure and Doped with Transition Metal Impurities." J. Matl. Science, 12, 2291-2302.

Lessing, P. A., Gordon, R. S. and Mazdiyasni, K. S. (1975) "Creep of Polycrystalline Mullite." J. Amer. Ceram. Soc., 58 [3-4] 149.

Lifshits, I. M. (1963) "Theory of Diffusion-Viscous Flow of Polycrystalline Bodies." Soviet Phys., 17, [4] 909.

Long, G. and Fosler, L. M. (1961) "Aluminum Nitride Containers for Vacuum Evaporation of Aluminum." Amer. Ceram. Soc. Bull., 40 [7] 423-425.

Martin, J. W. (1968) Precipitation Hardening, Oxford Pergamon Press.

Martin, A. J. and Ellis, G. C. (1963) "The Ductility Problem in Beryllium," in The Metallurgy of Beryllium, The Institute of Metals, London: Chapman and Hall Ltd.

Mazdiyansni, K. S. and Brown, L. M. (1972) "Synthesis and Mechanical Properties of Stoichiometric Aluminum Silicate (Mullite)." J. Amer. Ceram. Soc., 55 [11] 548-552.

McClintock, F. A. (1966) "Creep," in Mechanical Behavior of Materials, 625-656, (F. A. McClintock and A. S. Argon, Eds.). Addison-Wesley Publishing Co., Inc., Reading, MA.

McKee, W. D., Jr. and Aleshin, E. (1963) "Aluminum Oxide-Titanium Oxide Solid Solution." J. Amer. Ceram. Soc., 46, [1] 54-58.

Mecartney, M. L., Donlon, W. T., and Heuer, A. H. (1980) "Plastic Deformation in CaO-Stabilized ZrO_2 (CSZ)." J. Matl. Sci., 15 [4] 1063-1065.

McLean, D. (1966) "The Physics of High Temperature Creep in Metals." Report on Progress in Physics, 29, 1-33.

McLean, M. (September 1982) "Creep Behavior of High-Temperature Metal Matrix Composites," in Fatigue and Creep of Composite Materials. (H. Lilholt and R. Talreja, Eds.). Proc. 3rd Riso International Symosium on Metallurgy and Materials Science, pp. 6-10.

Michael, D. J. and Tressler, R. E. (1974) "Deformation Dynamics of Pore Free Ti^{4+}-Doped and Pure c-Axis Sapphire Crystals." J. Matl. Sci., 9 [11] 1781-1788.

Minford, W. J. (1977) "Microstructure, Crystallography, and Creep of Directionally Solidified Oxide Eutectics." Ph.D. Thesis in Ceramic Science, The Pennsylvania State University.

Mitchell, T. E., Hwang, L., Heuer, A. H. (1976) "Deformation in Spinel." J. Mater. Sci., 211 [2] 264.

Mitchell, T. E. (1979) "Application of Transmission Electron Microscopy to the Study of Deformation in Ceramic Oxides," J. Amer. Ceram. Soc., 62 [5-6] 254-267.

Mocellin, A. and Kingery, W. D. (1971) "Creep Deformation in MgO-Saturated Large-Grain-Size Al_2O_3." J. Amer. Ceram. Soc., 54 [7] 339-341.

Mohapatra, S. K. and Kröger, F. A. (1977) "Defect Structure of α-Al_2O_3 Doped with Magnesium." J. Amer. Ceram. Soc., 60 [3-4] 141-148.

Monkman and Grant (1956).

Morgan, C. S. and Hall, L. L. (1966), Proc. Brit. Ceram. Soc. 49, 410.

Mott, N. F. and Nabarro, F. R. N. (1948) Conference on the Strength of Solids, Physical Society, London.

Nabarro, F. R. N. (1948) "Deformation of Crystals by the Motion of Single Ions," Report of a Conference on the Strength of Solids (Bristol). The Physical Society, London pp. 75-90.

Nabarro, F. R. N., Basinski, Z. S., and Holt, D. B. (1964) "Work Hardening of Ceramics and Metals." Adv. Phys., 13, 193.

Nabarro, F. R. N. (1967) "Steady State Diffusional Creep." Philos. Mag., 16 [140] 231-237.

Newey, C. W. A.and Radford, K. C. (1968) "Plastic Deformation of Magnesium Aluminate Single Crystals," in Anisotropy in Single-Crystal Refractory Compounds, 2. Plenum Press, New York, NY, p. 321.

Newkirk, H. W. and Smith, D. K. (1964) "Studies of the Formation of Crystalline Synthetic Bromellite, I Microcrystals." U.S. Atomic Energy Commission, Contact No. W-7405-eng-48.

Newkirk, H. W. and Smith, D. K. (1965) "Studies on this Formation of Crystalline Synthetic Bromellite, II Macrocrystals." Amer. Mineralogist, 50, 44.

Oishi, Y. Ando, K. and Kabota, Y. (1980) "Self-Diffusion of Oxygen in Single Crystal Alumina,." J. Chem. Phys., 73 [3] 1410-1412.

Oishi, Y., Ando, K., Suga, N. and Kingery, W. D. "Effect of Surface Condition on Oxygen Self-Diffusio Coefficients for Single Crystal Al_2O_3." J. Am. Ceram. Soc., 66 [8] C-130-131.

Oishi, Y. H. and Kingery, W. D. (1960) "Self-Diffusion of Oxygen in Single Crystal and Polycrystalline Aluminum Oxide." J. Chem Phys., 33 [2] 480-486.

Oishi, Y., Ando, K. and Matsuhiro (1977) "Self-Diffusion Coefficient of Oxygen in Vapor-Grown Single Crystal Alumina." Yogyu Kyokai Shi, 85 [10], 522-524.

Orowan, E. (1940) "Problems of Plastic Gliding." Proc. Phys. Soc., 52, 8-22.

Paladino, A. E. and Kingery W. D. (1962) "Aluminum-Ion Diffusion in Aluminum Oxide." J. Chem. Phys., 37 [5] 957-962.

Paladino, A. E. and Coble, R. L. (1963) "Effect of Grain Boundaries on Diffusion-Controlled Processes in Aluminum Oxide." J. Amer. Ceram. Soc., 46 [3] 133-136.

Palmour, H., III (1966) "Multiple Slip Processes in Magnesium Aluminate at High-Temperatures." Proc. Brit. Ceram. Soc., 6, 209.

Parratt, N. J. (1972) Fiber-Reinforced Materials Technology, Van Nostrand Reinheld Co., London.

Partridge, P. G. (1967) "The Crystallography and Deformation Modes of HCP Metals." Met. Review, 118, 169-194.

Passmore, E. M. and Vasilos, T. (1966) "Creep of Dense, Pure, Fine-Grained Aluminum Oxide." J. Amer. Ceram. Soc., 49 [3] 166-168.

Penty, R. A. and Hasselman, D. P. H. (1972) "Creep Kinetics of High-Purity Ultrafine Grain Polycrystalline Mullite." Mater. Res. Bull., 7 [10] 1117-1124.

Philips, D. S., Mitchell, T. E., and Heuer, A. H. (1977) "Identification of the Precipitates in Star Sapphire," presented at the American Ceramic Society Basic Science and Nuclear Divs. Fall Meeting.

Pletka, B. J., Mitchell, T. E. and Heuer, A. H. (1972) "Precipitation in Titania-Doped Sapphire" in The Society of Materials Science, Japan, Volume IV, Tokyo, pp. 413-421.

Pletka, B. J., Mitchell, T. E., and Heuer, A. H. (1974) "Dislocation Structures in Sapphire Deformed by Basal Slip." J. Amer. Ceram. Soc., 57 [9] 388-393.

Pletka, B. J. (1975a) Ph.D. Thesis, Dept. of Metallurgy and Materials Science, Case Western Reserve University.

Pletka, B. J., Mitchell, T. E., and Heuer, A. H. (1975b) "Strengthening Mechanisms in Sapphire," in Deformation of Ceramic Materials. (R. C. Bradt and R. E. Tressler, Eds.). Plenum Press, NY.

Pletka, B. J., Heuer, A. H., and Mitchell, T. E. (1977) "Work-Hardening in Sapphire (α-Al_2O_3)." Acta Met., 25 [1] 25-33.

Poirier, J. P. (1978) "Is Power-Low Creep Diffusion Controlled?" Acta Met., 26, 629-637.

Pollock, J. T. A. (1972) "Filamentary Sapphire, Part I; Growth and Microstructural Characterization." J. Matl. Sci., 7, 631-648.

Poteat, L. E. and Yust, C. S. (1966) "Creep of Polycrystalline Thorium Dioxide." J. Amer. Ceram. Soc., 49 [8] 410-414.

Poteat, L. E. and Yust, C. S. (1968) "Ceramic Microstructures." (ed. R. M. Fulrath and J. A. Pask) Wiley, New York, 646.

Price, P. B. (1963) in Electron Microscopy and Strength of Crystals. (G. Thomas and J. Washburn, Eds.). Interscience, New York, p. 41.

Pysher, D. J. (1989) "High-Temperature Strength, Creep and Creep Rupture of Ceramic Fibers." M.S. Thesis in Ceramic Science, The Pennsylvania State University.

Radford, K. C. and Terwilliger, G. R. (1974) "High-Temperature Deformation of Ceramics: II, Specific Behavior." J. Amer. Ceram. Soc., 53 [6] 465-472.

Raj, R. and Ashby, M. F. (1971) "On Grain Boundary Sliding and Diffusional Creep." Met. Trans., 2 1113.

Rasmussen, J. R., Stringfellow, G. B., Cutler, I. B, and Brown, S. D. (1965) "Effect of Impurities on the Strength of Polycrystalline Magnesia and Alumina." J. Amer. Ceram. Soc., 48 [3] 146-150.

Reed, D. J. and Wuensch, B. J. (1980) "Ion-Probe Measurement of Oxygen Self-Diffusion in Single-Crystal Al_2O_3." J. Amer. Ceram. Soc., 63 [1-2] 88-92.

Reedy, K. P. R. and Cooper, A. R. (1981) "Oxygen Diffusion in Magnesium Aluminate Spinel." J. Amer. Ceram. Soc., 64 [6] 368-371.

Reedy, K. P. R. and Cooper, A. R. (1982) "Oxygen Diffusion in Sapphire." J. Amer. Ceram. Soc., 65 [12] 634-638.

Rhodes, W. H., Sellers, D. J., Vasilos, T., Heuer, A. H., Duff, R., and Burnett, P. (1965) Summary Report 3-25-65, AVCO Corp., Navy Contract, NOW-65-034-P.

Rhodes, W. H. and Carter, R. E. (1966) "Catatonic Self-Diffusion in Calcia-Stabilized Zirconia." J. Amer. Ceram. Soc., 49 [5] 244-249.

Rosenthal, D. (1964) Introduction to Properties of Materials, Von Nostrand, Princeton, NJ, p. 92.

Roz, S. K. and Coble, R. L. (1968) "Solubilities of Magnesia, Titania, and Magnesium Titanate in Aluminum Oxide." J. Amer. Ceram. Soc., 57 [1] 1-6.

Schouplein, R. and Gibbs, P. (1960) "Surface Structure in Corundum: I, Etching of Dislocations." J. Amer. Ceram. Soc., 43 [9] 458-472.

Schick, H. L. (1960) "A Thermodynamic Analysis of the High Temperature Vaporization Properties of Silica." Chem. Rev., 331.

Seeger, A., Krommüller, H., Mader, S., and Träuble, H. (1961) "Work-hardening of Hexagonal Close-Packed Crystals and in the Easy Glide Region of Face-Centered Cubic Crystals." Phil. Mag., 7 [65] 639-655.

Seltzer, M. S. (1968) "Correlation Between Activation Energies for Steady-State Creep and Self-Diffusion in Beryllium-Oxide." J. Nuclear Mater., 26, 232.

Seltzer, M. S., and Talty, P. K. (1975) "High-Temperature Creep of Y_2O_3-Stabilized ZrO_2." J. Amer. Ceram. Soc., 58 [3-4] 124-130.

Shahinian, P. (1971) "High-Temperature Strength of Sapphire Filament." J. Amer. Ceram. Soc., 54 [1] 67-68.

Simpson, L. A. and Carter, R. E. (1966) "Oxygen Exchange and Diffusion in Calcia-Stabilized Zirconia." J. Amer. Ceram. Soc., 49 [3] 139-144.

Smith, D. K., Cline, C. F., and Austerman, S. B.(1964) "The Crystal Structure of Beta-Beryllia." J. of Nuclear Mat., 14, 237.

Stavrolakis, J. A. and Norton, T. H. (1950) "Measurement of the Torsion Properties of Alumina and Zirconia at Elevated Temperatures." J. Amer. Ceram. Soc., 33 [9] 263-268.

Stephens, J. R. and Nathal, M. V. (September 18-22, 1988) Status and Prognosis for Alternative Engine Materials, NASA Tech. Memo. 10093, 6th International Symposium on Superalloys, TMS-AIME.

St.-Jacques, R. G. and Angers, R. (1972) "Creep of CaO-Stabilized ZrO_2." J. Amer. Ceram. Soc., 55 [11] 571-574.

Stokes, R. J., Johnson, T. L., and Li, C. H. (1959) "Effects of Surface Condition on Initiation of Plastic Flow in Magnesium Oxide." Trans. AIME, 215 [6] 437-444.

Storms, E. K. (1967) The Refractory Carbides, 2, Academic Press.

Strife, J. R. and Sheehan, J. E. (1988) "Ceramic Coatings for Carbon-Carbon Composites." Ceramic Bulletin, 67 [2] 369-374.

Sugita, T. and Pask, J. A. (1970) "Creep of Doped Polycrystalline Al_2O_3." J. Amer. Ceram. Soc., 53 [11] 609-613.

Suzuki, H. (1957) The Yield Strength of Binary Alloys," in Dislocations and Mechanical Properties of Crystals, (J. C. Fisher, Ed.), New York, John Wiley and Sons, Ltd.

Tressler, R. E. and Barber, D. J. (1974) "Yielding and Flow of c-Axis Sapphire Filaments." J. Amer. Ceram. Soc., 57 [1] 13-19.

Tressler, R. E. and Michael, D. J. (1975) ":Dynamics of Flow of c-Axis Sapphire," in Deformation of Ceramic Materials. (R. C. Bradt and R. E. Tressler, Eds.). Plenum Press, New York, 195.

Vandervoort, R. R. and Barmore, W. L. (1963) "Compressive Creep of Polycrystalline Beryllium Oxide." J. Amer. Ceram. Soc., 46 [4] 180-184.

Wachtman, J. B., Jr. and Maxwell, L. H. (1954) "Plastic Deformation of Ceramic-Oxide Single-Crystals." J. Amer. Ceram. Soc., 37 [7] 291-299.

Wachtman, J. B., Jr. and Maxwell, L. H. (1957) "Plastic Deformation of Ceramic-Oxide Single Crystals, II." J. Amer. Ceram. Soc., 40 [11] 377-385.

Walker, D. G., Rotsey, W. B. and Wood, B. R. A. (1971) J. Mater. Sci., 587.

Warshaw, S. I., and Norton, F. H. (1962) "Deformation Behavior of Polycrystalline Aluminum Oxide." J. Amer. Ceram. Soc., 45 [10] 479-486.

Weertman, J. (1955) "Theory of Steady-State Creep Based on Dislocation Climb." J. Appl. Phys., 26 [10] 1213-1217.

Weertman, J. (1957a) "Steady-State Creep Through Dislocation Climb." J. Appl. Phys., 28 [3] 362-364.

Weertman, J. (1957b) "Steady-State Creep of Crystals." J. App.. Phys., 28 [10] 1185-1189.

Weertman, J. (1960) "Creep of Indium, Lead and Some of Their Alloys with Various Metals." Trans. AIME, 207-218.

Weertman, J. (1968) "Dislocation Climb Theory of Steady-State Creep." ASM Trans. Q., 61, 681-694.

Wiederhorn, S. M. (1969) "Fracture of Sapphire." J. Amer. Ceram. Soc., vol. 52, no. 9, pp. 485-451.

Wilcox, B. A. and Clauer, A. H. (1972) "Role of Grain Size and Shape in Strengthening of Dispersion-Hardened Nickel Alloys." Acta. Metall. 20 [5] 743-757.

Winkler, E. R., Sarver, J. F., and Cutler, I. B. (1966) "Solid Solution of Titanium Dioxide in Aluminum Oxide." J. Amer. Ceram. Soc., 49 [12] 634-637.

NASA

Report Documentation Page

1. Report No.	2. Government Accession No.	3. Recipient's Catalog No.
NASA CR-187060		

4. Title and Subtitle	5. Report Date
The High Temperature Creep Behavior of Oxides and Oxide Fibers	January 1991
	6. Performing Organization Code

7. Author(s)	8. Performing Organization Report No.
Linda E. Jones and Richard E. Tressler	CAM-9009
	10. Work Unit No. 510-01-50

9. Performing Organization Name and Address	11. Contract or Grant No.
Center for Advanced Materials The Pennsylvania State University 410 Walker Building University Park, Pennsylvania 16802	NAGW-1381
	13. Type of Report and Period Covered Contractor Report Topical
12. Sponsoring Agency Name and Address	14. Sponsoring Agency Code
National Aeronautics and Space Administration Lewis Research Center Cleveland, Ohio 44135-3191	

15. Supplementary Notes

Project Manager, Brian F. Quigley, Materials Division, Engine Materials Office, NASA Lewis Research Center, (216) 433-8358.

16. Abstract

A thorough review of the literature has been conducted on the high-temperature creep behavior of single and polycrystalline oxides which potentially could serve as fiber reinforcements in ceramic or metal matrix applications. Sapphire when oriented with the basal plane perpendicular to the fiber axis (C-axis oriented) is highly creep resistant at temperatures in excess of 1600 °C and applied loads of 100 MPa and higher. Pyramidal slip is preferentially activated in sapphire under these conditions and steady-state creep rates in the range of $10^{-7} - 10^{-8}$ s^{-1} have been reported. Data on the creep resistance of polycrystalline beryllia suggest that C-axis oriented single crystal beryllia may be a viable candidate as a fiber reinforcement material; however, the issue of fabricability and moisture sensitivity must be addressed for this material. Yttrium aluminum garnet (YAG) also appears to be a fiber candidate material having a high resistance to creep which is due to it's complex crystal structure and high Peierl's resistance. The high creep resistance of garnet suggests that there may be other complex ternary oxides such as single crystal mullite which may also be candidate materials for fiber reinforcements. Finally, CVD and single crystal SiC, although not oxides, do possess a high resistance to creep in the temperature range between 1550 and 1850 °C and under stresses of 110 to 220 MPa. From a review of the literature, it appears that for high creep resistant applications sapphire, silicon carbide, yttrium aluminum garnet, mullite and beryllia are desirable candidate materials which require further investigation.

17. Key Words (Suggested by Author(s))	18. Distribution Statement
High temperature fibers; Oxides; Oxide fibers; Single crystal fibers; Creep; Composites	Unclassified – Unlimited Subject Category 24, 27

19. Security Classif. (of this report)	20. Security Classif. (of this page)	21. No. of pages	22. Price
Unclassified	Unclassified	115	A06

*For sale by the National Technical Information Service, Springfield, Virginia 22161

☆U.S. GOVERNMENT PRINTING OFFICE: 1991 - 548-186/20312